15

THE LIBERATION CHARACTERISTICS OF GREENSIDE No 2 SEAM COAL

A thesis submitted to the
UNIVERSITY OF CAPE TOWN
in fulfilment of the requirements
for the degree of
MASTER OF SCIENCE IN ENGINEERING

by

MARTIN COLQUHOUN HARRIS B.Sc (Chem. Eng.) (Cape Town)

Department of Chemical Engineering
University of Cape Town
Rondebosch, Cape
South Africa

October, 1987

SYNOPSIS

In South Africa, ever increasing quantities of fine (-0,5 mm) coal are being produced as a result of the increased use of mechanised mining methods. Very few mines beneficiate the fines; in most cases they are discarded. However the fine size of this material suggests that it should be well liberated, with the potential to produce a low ash product.

This thesis forms part of an ongoing research program examining the use of flotation to beneficiate coal fines to produce a low ash product. Coal is a highly heterogeneous material, consisting of a number of both organic (maceral) and inorganic (mineral) components with different physical and technological properties. Therefore in order to evaluate and interpret flotation results, an understanding of the liberation characteristics of both the organic and inoganic components is required.

This thesis presents a liberation study on fine coal from the Greenside Colliery, a typical colliery in the Witbank Coalfield which is the most important source of South African low ash coal. The study was performed by milling a run of mine coal sample to varying degrees of fineness (from 30 % finer than 150 micron to 90 % finer than 150 micron), screening, and assessing the liberation of each size fraction. These results were compared to those obtained from a sample of naturally arising fines (thickener underflow). Liberation was assessed by float and sink analysis, and for this purpose a new technique was developed that enables rapid and accurate float and sink analysis of coal down to a few micron in size. Petrographic analyses were performed to determine the liberation of the organic coal components.

It was found that an increase in the milling time resulted in an increase in liberation of the milled samples, but that the change was quite small. Even the finest sample contained a relatively high proportion of middling material, indicating that significant liberation would require extremely fine grinding. In the size fractions of the samples, the distribution of the various organic and inorganic components was similar, except in the finest size fraction. This fraction (-25 micron) contained a high proportion of fine but unliberated inertinite particles, and was in all cases it was found to be the least liberated size fraction. The maceral liberation of all the size fractions was high. In all respects, the thickener underflow exhibited similar characteristics to the milled samples.

ACKNOWLEDGEMENTS

The author would like to extend his sincere thanks to

Dr J-P. Franzidis for his assistance and encouragement in directing this study

the Foundation for Research Development of the CSIR for funding the research, and particularly Mr Dieter Krueger, coordinator of the Coal Research Program

the Council for Mineral Technology (MINTEK) for the preparation of the coal samples

Dr R.M.S. Falcon of Falcon Research Laboratories for the petrographic analysis of the samples

Professor R. P. King of the Department of Metallurgy at the University of the Witwatersrand for providing the samples used for testing the new float and sink device, along with the results of float and sink analyses performed in his laboratory

Mr A. M. Barker, Chief Technical Officer in the Department of Chemical Engineering at the University of Cape Town for manufacturing the new float and sink apparatus

Mr D.W. Horsfall of the Anglo American Corporation and Mr R.C. Dunne formerly of MINTEK for many helpful discussions

colleagues and staff at the Department of Chemical Engineering at the University of Cape Town for their interest and willing assistance.

CONTENTS

APPENDICES

A. Partition curve data for the comparison of the two float and sink techniques.

B. Size distribution data.

C. Density Distribution Data.

D. Washability Data.

E. Petrographic Analysis Data of the Size Fractions.

F. Petrographic Washability Analysis Data.

G. Derivation of the Ash versus Inverse Relative Density Correlation.

H. "A new method for the rapid float-sink analysis of coal fines" by J-P. Franzidis and M.C. Harris. Reprint of a paper appearing in the J. S. Afr. Inst. Min. Metall., vol. 86, No 10, pp 409 - 414, Oct. 1986.

LIST OF TABLES

LIST OF FIGURES

CHAPTER 1

INTRODUCTION

1.1. Background

Due to the increased use of mechanised mining methods, the South African coal industry is producing ever increasing quantities of fine coal. This coal is nominally -500 micron in size, but in practice the top size is more like 1 mm. It has been estimated that the proportion of run-of-mine coal reporting to the fines fraction may be as high as 16 % (Anon, 1985).

The size distribution of this fine material suggests that it should be well-liberated, with the potential to produce low ash coal (L.A.C.). As early as 1976, a plea was made for an urgent program of research into the upgrading of the fines from the Witbank No 2 seam to obtain a low ash product (Horsfall, 1976). Since then, a few of the mines have taken steps to recover and upgrade the fines to thermal quality: one plant utilises water-only cyclones, another flotation, and two have recently installed spiral plants. At the Greenside Colliery alone, 1 mm by 0,1 mm fines are treated in a dense medium circuit, to produce low ash coal (Fourie et al, 1980).

Thus fines cleaning circuits are still comparatively rare. The majority of South African coal fines are not beneficiated, but are discarded by being pumped underground or into ponds. A recent survey (DMEA, 1987) has put the quantity of bituminous fines slurry being discarded by South African collieries annually at nearly 4 MT. A small proportion of the fines are dewatered and added to the middling material for use as thermal coal. This alternative is false economy, as it usually necessitates overwashing the coarser fractions to accomodate the higher natural ash content of the fines. This constitutes a serious waste of a valuable national resource.

In an attempt to redress this problem, a program of work was started in 1983 in the Department of Chemical Engineering at the University of Cape Town to investigate flotation as a means of beneficiating South African coal fines. Flotation was chosen as it is a well proven method for coal fines beneficiation overseas. However the same technology applied to South African coals, with the exception of the Natal coking coals, had previously proved unsuccessful.

A preliminary investigation was carried out using factorially designed experiments to determine the effect of basic factors such as particle size, aeration rate, impeller speed, pulp density, collector concentration, and frother concentration on the flotation of four South African coals (Fickling, 1986). The most notable feature of the results was that any change in the recovery or rate of flotation of coal was generally accompanied by a corresponding change in the recovery or rate of the flotation of the ash. It was argued that this might be the result of insufficient liberation at the particle sizes being considered, the finest being 95 % passing 300 micron.

Liberation is an important factor in flotation, as it is in all processes that exploit differences in surface properties to effect a separation. It is more important than in processes that exploit differences in bulk properties, such as dense medium separation. It is relatively easy, for example, in an efficient dense medium process, to separate coal particles which differ in ash content by as little as 1 %. Flotation is much more sensitive to the presence of middling material, as the surface characteristics of the coal particles will be very similar for a wide range of particle ash contents. Separation therefore becomes extremely difficult.

However, below a particle size of 100 micron the efficiency of density separation processes drops off rapidly for coal particles because of viscous and drag forces. It is for washing material below this size that separation on the basis of surface properties become obligatory.

Now in order to evaluate and interpret flotation results of very fine material, a knowledge of the liberation characteristics is required. However, information regarding the liberation characteristics of South African coal fines is scant: this is due in part to the absence of a suitable method for evaluating the liberation of very fine particles. Panopoulos et al (1983, 1986) have shown that Witbank No 2 seam coals are not significantly liberated even down to 75 micron: there is a need to continue this investigation down to a few micron in size by a suitable method.

Coal is a highly heterogeneous material, consisting of different organic components (or macerals) as well as the inorganic (or mineral) impurities that form ash during combustion. As the different coal macerals are regarded to have an important influence on flotation performance, and possess different technological properties, an understanding of the liberation characteristics of both the organic and inorganic components of a coal is required.

Thus a study should be performed to determine the extent and nature of the liberation of the different coal components down to as small a particle size as is possible. This can be performed by milling the coal to varying degrees of fineness, screening, and assessing the liberation of each size fraction by a suitable method.

1.2. Aim

The aim of this thesis is to determine the liberation characteristics of a Witbank No 2 seam coal, as this is the most important source of South African thermal and low ash coal for export. The aim of the liberation study is to establish the liberation characteristics during size reduction of the different coal components, and the ash (or mineral) components from the coal.

In order to perform the liberation study, it was necessary to first establish a technique and method for the liberation analysis of fine coal.

In the next chapter, this thesis outlines the nature of coal, and the differences between an investigation of the liberation of coal and that of metalliferous ores. Various methods for evaluating coal liberation are presented, and the findings of other researchers are discussed.

Chapter 3 deals with the analytical techniques used in this study and presents in detail the development and evaluation of a new float and sink technique for liberation studies on fine coal.

Chapter 4 describes the choice and preparation of samples and equipment, and outlines details of the experimental program.

In chapter 5 the results of the liberation study are presented along with a discussion of the findings. The conclusions of the investigation are summarised in chapter 6.

CHAPTER 2

LITERATURE SURVEY

When beneficiation of a mineral is being assessed or considered, the liberation characteristics of the mineral are of significant importance. For metalliferous ores, liberation is normally assessed according to the definition of Gaudin (1939), in which the degree of liberation of a mineral is defined as the percentage of that mineral occurring as free particles in relation to the total of that mineral occurring in free and locked forms. However, assessing the liberation of coal is considerably more complex, as coal consists of a large number of both organic (maceral) and inorganic (mineral) species. It is not sufficient to consider only the liberation of the organic combustible components from the inorganic ash forming components, as the former exhibit different technological and beneficiation properties. Therefore, before going into detail about coal liberation theory, it is necessary first to describe the constituents of coal and their properties, and some of the characteristics of South African coal.

2.1. Coal as a Mineral

Coal is derived from a layered mass of plant material by chemical and physical alteration, and modification during and after deposition. It is a heterogeneous combustible material consisting of a variety of carbonaceous and inorganic mineral substances. Thus the physical and chemical properties of coal, and their influence on its technological behaviour are much more difficult to characterize than is the case with most other minerals or mineral complexes.

Most of the chemical, physical and technological properties of a coal will be determined by its grade, type and rank. Grade, type and rank are the result of the deposition, biochemical degradation and metamorphosis of the original plant constituents. Determination of these properties involves the microscopic study, identification and classification of the various carbon remnants and is known as coal petrology.

2.1.1. Coal Type or Petrographic Composition

The coal type is determined by the nature of the dominant, original plant material that was deposited in the swamps prior to peatification, and by the mode and extent of the subsequent biochemical degradation.

The end products of the conversion consist of a number of distinct organic materials, known as macerals. These can be divided into three broad groups that each exhibit similar physical, chemical and technological properties. The three groups are:

(a) vitrinite
(b) exinite
(c) inertinite

Table 2.1 shows some of the relative properties of the different maceral groups.

Characteristic associations of macerals exhibiting a band width greater than 50 micron are called microlithotypes. Figure 2.1 shows the most common microlithotypes and their component macerals.

TABLE 2.1

Physical and chemical properties of the different coal macerals (Falcon (a), (b), 1978).

	Vitrinite	Exinite	Inertinite
Origin	Woody plants. Anaerobic decomposition	Chemically resistant parts of a plant	Woody plants. Aerobic decomposition
Reactivity	Very Reactive	Reactive	Inert except for reactive semi-fusinite and macrinite
Volatile Composition	High: important coke component	Very High	Inert in the range of coking coals
Ease of Oxidation	Easily oxidised	Less easily oxidised	Very difficult to oxidise
Breakability	Brittle	Stronger: Impart strength to the microlithotypes in which they occur	
Chemical Composition	Oxygen rich	Hydrogen rich	Carbon rich
Relative Density (low rank)	1,2 - 1,3	1,1	1,4 -1,6

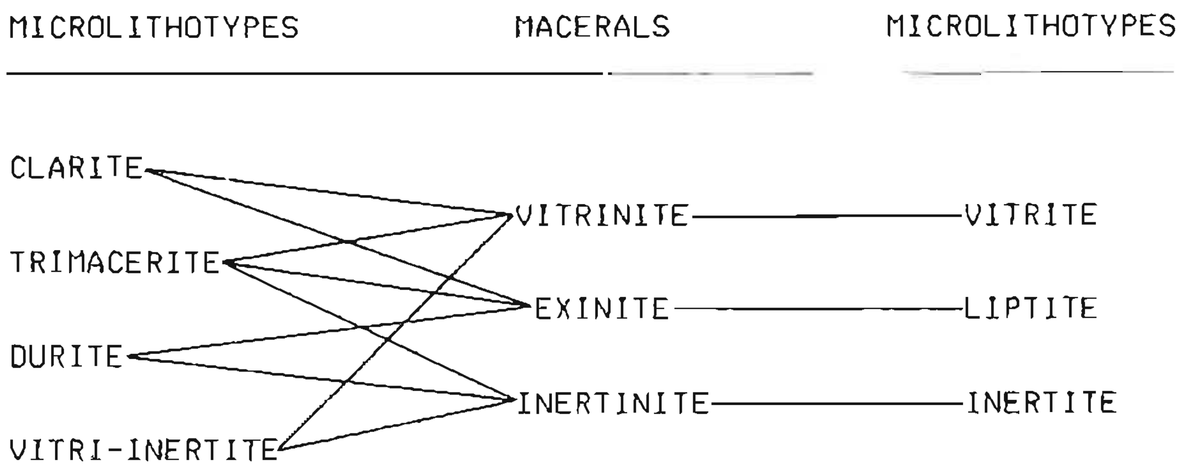

Fig. 2.1 The characteristic associations of the macerals to form microlithotypes.

2.1.2. Coal Rank

Rank or degree of coalification is determined by the extent of metamorphosis of the coal as a result of temperature and pressure. As the rank of a coal changes, the physical and chemical properties of the macerals are altered.

Rank determinations are carried out by reflectance measurements of vitrinite. Vitrinite is used as a reference material because it is the most homogeneous petrographic component and its characteristics change continuously and linearly with rank.

2.1.3. Grade or Mineral Associations

Mineral associations with coal can be divided into two groups:

(a) Syngenetic minerals - these are intimately intergrown with the coal, and were either formed or accumulated in coal swamps up to the time of peatification. These minerals are extremely difficult to liberate during any beneficiation process.

(b) Epigenetic minerals - these were deposited in cleats and fissures after solidification of the coal seam. Although they are often microscopic in size, they are much more easily liberated during a beneficiation process.

The relative proportions of minerals occurring in either of these two forms will determine the liberation potential of a particular coal.

2.2. Characteristics of South African Coal

2.2.1. Petrographic Composition

The average maceral composition of South African coals differs widely from that which is found in many of the major coal producing regions overseas, such as Europe. These differences are summarised in Table 2.2.

As can be seen, South African coals tend to be inertinite enriched, which makes them generally less reactive than the equivalent European coals (except for Natal coals).

South African coals tend to be chemically rather than physically changed because not only are the pressure effects smaller (shallower burial depth) but temperature effects associated with widespread igneous intrusions are more significant.

TABLE 2.2

The average relative proportions of coal constituents in South African and European Coals (Falcon, 1978 (a)).

	Average Relative Proportions (%)	
	South Africa	Europe
Vitrinite	40	70
Exinite	0 - 5	15
Inertinite	60 (± 20)	15
Syngenetic Mineral	14	3

2.2.2. Rank

The rank of South African coals tends to increase steadily from west to east. The western sector of the main Karroo Basin produces very low rank coals. An increase in rank is observed in the Transvaal, while in some parts of Natal very high ranks are attained from contact metamorphism due to igneous intrusions.

2.2.3. Mineral Associations

The main mineral groups that are associated with South African coals, along with their main occurrence and relative density, are presented in Table 2.3.

The clay minerals account for 60 to 70 % of mineral intergrowth, with the major components being kaolinite, illite and chlorite; the relative proportions of each depends on the rank of the coal in which they occur.

They are typically extremely fine and widely disseminated throughout the coal matrix. They are associated with all the maceral groups and are therefore the most difficult to liberate.

TABLE 2.3

The main mineral groups found in South African coals and their occurrence (Falcon, 1978(a)).

Mineral or Group	Main Occurrence	Av. Relative Density
Clay minerals	Syngenetic	2,3 - 2,6
Carbonates	Epigenetic	2,7 - 3,8
Sulphides	Epigenetic	5
Quartz	Both	2,65

The carbonate minerals include siderite, ankerite, dolomite and calcite. South African coals are relatively poor in syngenetic carbonates, probably due to the high redox potential in the formation environment.

The sulphide minerals are extremely important owing to the harmful effects of sulphur in coke or boiler coal. Syngenetic sulphides are rare, except for small concretions of pyrite occurring predominantly in vitrinite. Epigenetic sulphides do occur, but generally South African coals contain a relatively low concentration of these minerals.

Quartz occurs in South African coals in both syngetic and epigenetic forms. Syngenetic quartz can occur either as coarse wind or water deposited material, or as fine material intimately associated with the clay during coal formation.

As can be seen in Table 2.2, South African coals on average contain much higher proportions of syngenetic material than is the case overseas. This fact constitutes the main problem in the beneficiation of most South African coals.

2.3. Coal Liberation

2.3.1. Liberation Theory

One of the most important aspects of assessing the beneficiation potential of a material are its liberation characteristics. Most of the work that has been published on liberation has dealt with the liberation of metalliferous ores, in which the desired mineral constitutes a very small proportion of the ore body. Before the desired mineral, or minerals, can be separated from the associated gangue, the ore must be reduced in size to obtain sufficient release or liberation of the desired material. Optimisation of the degree of comminution is required to ensure cost efficiency, and this requires understanding and measurement of the degree of liberation.

Liberation is normally assessed according to the definition proposed by Gaudin (1939), in which the degree of liberation of a certain mineral was defined as the percentage of that mineral occurring as free particles in relation to the total of that mineral occurring in free and locked forms. Various models (Gaudin, 1939; Wiegel and Li, 1967; King, 1975; Klimpel, 1983) have been proposed to correlate the degree of liberation with decreasing particle size distribution for a substance "A" occluded in a bulk material "B", and some of these have been used with considerable success to describe various metalliferous ore systems.

However application of traditional liberation theory to coal presents considerable difficulties. Even when milled to extremely fine sizes, the degree of liberation of most South African coals would be zero if the definition of Gaudin was used. Also coal is extremely heterogeneous; simple assessment of the liberation of coal as a two component system (ie. coal and ash) does not take into account the different technological properties of the different coal components, and their distribution during size reduction.

The aim of coal beneficiation is to turn out a product of a saleable grade. Since coal forms the abundant phase of the "ore", it is often possible to achieve sufficient liberation at relatively coarse sizes. As this is possible despite the fact that there is no liberation according to Gaudin's definition, it is necessary to assess the liberation of coal on a different basis to that used for most metalliferous ores.

2.3.2. The Need for the Study of Coal Liberation

Coal is generally only crushed prior to beneficiation (if any beneficiation is practised) to obtain the size required for sale in the marketplace, and not for the purposes of increasing liberation. The degree of liberation that is achieved at these coarse sizes generally defines the type of product that a particular mine produces. Typical product grades and sizes of South African coals are summarised in Table 2.4.

TABLE 2.4

Typical grades and sizes of South African domestic and export coals (Horsfall, 1980).

		Product and Size (mm)		Ash Content (%)
General		Rounds	+31,5	10 - 18
General		Cobbles	100 - 31,5	10 - 18
General		Nuts	40 - 22,4	11 - 20
General		Peas	25 - 6,3	11 - 20
General	E.S.C.O.M.	Smalls	-25	12 - 21
General	E.S.C.O.M.	Duff	-6,3	12 - 23
Captive power station			-25	20 - 27
Power station (export)			Usu. -32	10 - 16
Blend coking coal			Usu. -32	10 - 13
Straight coking coal			Usu. -32	10 - 14
Low ash export coal			Usu. -32	7 - 7,5
Liquid fuel (Sasol)			Usu. -38	+30

There are, however, two main areas in which the study of coal liberation is of considerable importance:

a) Increased use of mechanised mining methods by the coal industry has resulted in the production of ever increasing quantities of coal fines (usually nominally -500 micron).

Due to the high ash content of this material, in most cases it is either accumulated or discarded, without beneficiation. However the fine size of this material suggests that this fraction should contain a large proportion of high grade material. There is therefore a considerable cost incentive to the beneficiation of this material. However in order to evaluate the efficiency of a beneficiation process for the fines, the liberation characteristics of the material must be evaluated.

b) There is a considerable price incentive for the production of low ash coal (approx. 7 % ash). The production of super low ash coal (< 4 % ash) for specialised applications could become important in the future. The proportion of syngenetic material present in most South African coals would require very fine grinding before coal of this grade could be produced at reasonable yields. The degree of size reduction that is necessary to produce high quality products requires a thorough understanding of the liberation characteristics of the coal, particularly at very fine sizes.

2.3.3. Methods of Assessing Degree of Coal Liberation

The liberation of a sample of material can be assessed either by examination, i.e. optical (e.g. using a microscope) or X-ray (e.g. microprobe), or by segregation of the material on the basis of different physical characteristics of the components that constitute the material. The fractions obtained by the latter method can then be analysed to give the distribution of the different components.

Visual assessment of the degree of liberation of coal can be obtained by point counting of polished sections of the material under a microscope. However, while this method is invaluable in ascertaining the proportions of the different petrographic constituents in a particular coal sample, assessment of the degree of liberation by this method is extremely difficult, due to the complex heterogeneous nature of coal and the very large number of grains that would have to be examined to ensure accurate results. Thus for this method to be practical, the examination, either optical or otherwise, would have to be automated.

While considerable success has been obtained on assessing the degree of liberation of various metalliferous ores using automated point count techniques (King, 1979), it has not so far been possible to apply this technique to coal. This is due to the difficulty of programming a computer to distinguish between the various components present in the coal, a task for which a human operator requires considerable training and experience. However the development of such a technique would be a considerable advance in the study of coal liberation.

It is usually possible to separate the different components of an ore by differences in physical properties. Coal consists of components of different characteristic relative density (see Tables 2.1 and 2.3), so the most usual method of assessing coal liberation is segregation of the material on the basis of relative density, or float and sink analysis.

The sample is separated into a series of fractions by successive immersion into liquids of increasing relative density, starting at the relative density of the lightest component, up to the relative density of the heaviest component. After each immersion, the float material, i.e. the material with a relative density lower than that of the liquid, is removed. The analysis can also be performed in the reverse order, i.e. from the highest relative density to the lowest, in which case the sink fraction is removed after each immersion, or the sample can be split into subsamples, and a separate subsample used at each relative density.

The fractions can then be analysed to obtain the distribution of the different components as a function of relative density.

There are a number of ways in which the liberation characteristics of a coal can be assessed by float and sink analysis, and these are described in detail below.

2.3.3.1. Density Distribution

The density distribution of a coal sample presented in the form of a frequency histogram can be a useful aid to visual assessment of the degree of liberation of the coal. Since the relative density of pure coal is normally below 1,6, and the relative density of the associated mineral components is greater than 2, a perfectly liberated sample would contain little or no material in the relative density range 1,6 to 2,0. The density distribution below 1,6 R.D. depends on the relative proportions of the organic or maceral constituents in the coal, as these have different characteristic relative densities, as shown in Table 2.1.

2.3.3.2. Washability Analysis

The relationship between yield, relative density and ash content define the washability characteristics of a coal sample. Where a beneficiation process is required to produce a product of a specific grade, the washability of the feed will define the maximum or theoretical yield of the required quality that can be obtained from the material.

2.3.3.3. Petrographic Washability Analysis

Petrographic washability analysis shows the distribution of the organic constituents with relative density, and indicates the degree of liberation of the coal macerals and microlithotypes.

2.3.3.4. The M-Curve

As discussed in section 2.3.1., quantifying the liberation of coal using the definition of Gaudin would have little or no meaning. However a number of methods have been proposed to quantify the degree of liberation, or liberation efficiency, of coal.

A method proposed by Birtek (1980) relies on presenting the washability data in the form of M-curves, where cumulative percent yield is plotted against the cumulative product of percentage ash and yield, this latter being termed "ash per 100 units of feed" by Dell (1957).

A typical M-curve plot is presented in Fig. 2.2. In this diagram, line AC represents the feed line, line AB the pure coal line, and line BC the pure ash line. The graph is for a coal consisting of 20 % ash, and ADC is a typical M-curve. It is obvious that all the data must fall within the triangle ABC. Thus for a coal that is totally unliberated, the data would lie along the line AC, whereas for a coal that is completely liberated the data would lie along the line ABC.

A number of ways of assessing liberation efficiency from data presented in this form have been proposed. In the method proposed by Birtek and used by Birtek and King (1984, 1986), the liberation efficiency is measured by the

FIGURE 2.2 The characteristics of a typical M-Curve.

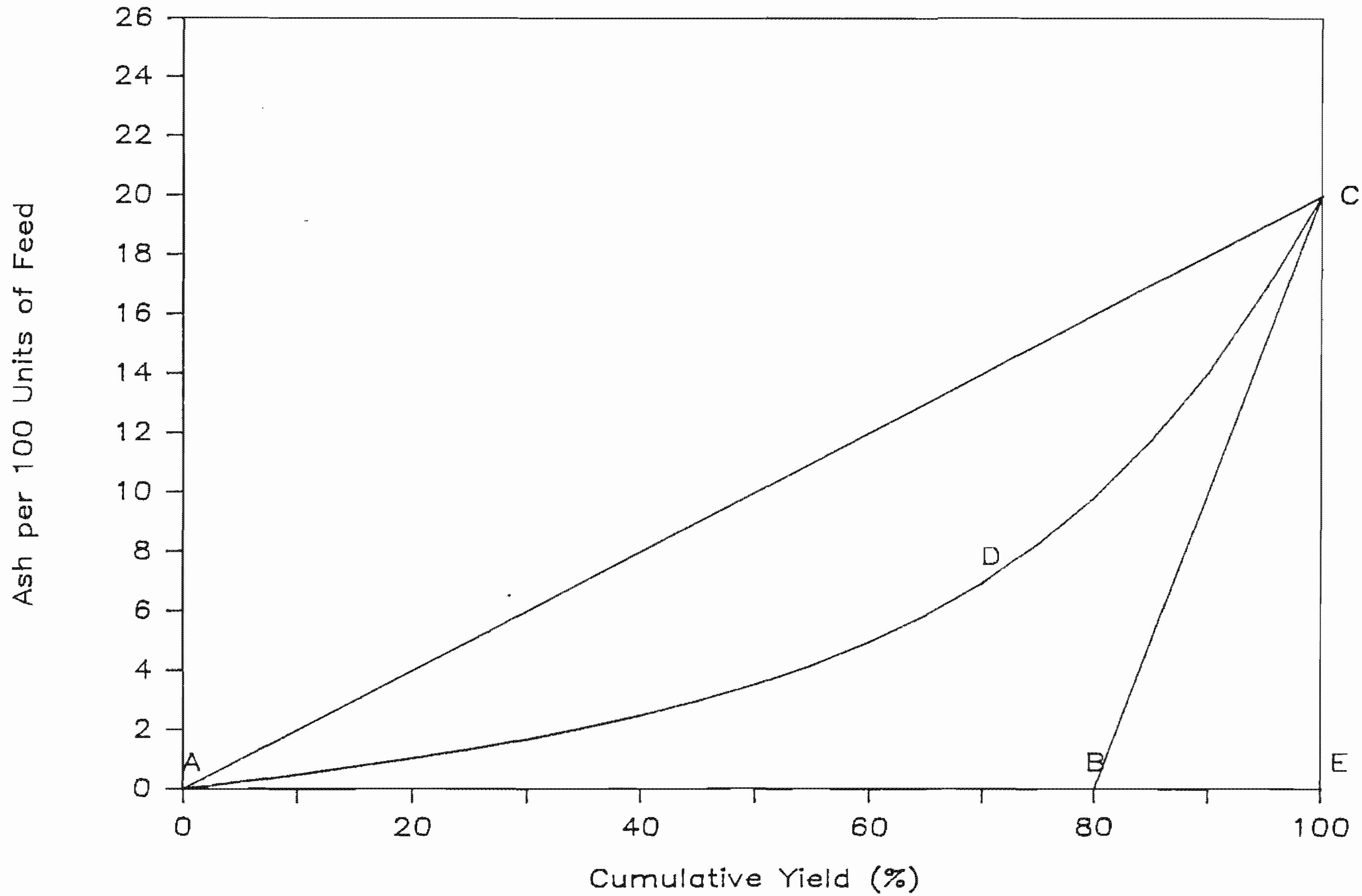

discrepancy of the actual curve from the ideal curve. Referring to Fig. 2.2, liberation efficiency L is given by:

$$L = \frac{\text{Area ADCA}}{\text{Area ABCA}} * 100$$

2.3.3.5. Ash Content as a Function of Relative Density

It has been shown (King, 1982) that if a coal particle was considered to consist of only two components, i.e. coal and ash, the following relation would hold:

$$Ash(\%) = \frac{(100/Sg) - (100/Sg_c)}{(1/Sg_a) - (1/Sg_c)} \qquad (2.1)$$

Where: Sg = relative density of a particle
Sg_c = relative density of coal
Sg_a = relative density of ash

Equation (2.1) can be simplified to give (see Appendix G):

$$Ash(\%) = P*Sg^{-1} + Q \qquad (2.2)$$

Where: P,Q = function parameters (by linear regression).

Equation (2.2) shows that if coal is considered to consist of a single coal component and an ash component, the relationship between ash content and the inverse of relative density is linear.

By manipulation, equation (2.2) can be used to predict the relative density of the coal and ash components (see Appendix G):

$$Sg_c = P.(Q-100)/100.Q - P/100 \qquad (2.3)$$

and:

$$Sg_a = Q.Sg_c/(Q-100) \qquad (2.4)$$

It has been reported (Panopoulos and King, 1983; Birtek and King, 1984, 1986) that South African coals typically exhibit a relationship between ash and relative density that is best fitted by two straight lines. This is best explained by considering the coal particle as a three component system, consisting of one ash component and two coal components of different characteristic relative densities. This can be accounted for by the presence of significant amounts of both vitrinite and inertinite in most South African coals.

Since two straight lines, a high ash line and a low ash line, may be fitted to each set of data, equation (2.3) can be used to obtain the predicted relative density of the light coal component (Sg_{lc}) from the low ash line, and equations (2.3) and (2.4) can be used to obtain the predicted relative densities of the heavy coal component (Sg_{hc}) and the ash component (Sg_a) from the high ash line.

Equation 2.4 gives a prediction of the relative density of the ash component. However in a study of the liberation of ash, one is really concerned with the liberation of mineral matter. The relationship between the ash content and the actual mineral matter content of a particular coal is complex. The distinct mineral phases in coal mainly comprise quartz, clay minerals, carbonate minerals and sulphides. All these minerals, with the exception of quartz, are decomposed during high temperature combustion.

A number of authors have studied mineral matter content of South African coals with respect to ash analysis. Savage (1967) compared acid extraction and low temperature oxidation as methods of obtaining the mineral matter content of a number of coals. The values of the mineral matter to ash ratio obtained varied between 1,07 and 1,24. A value of 1,16 was obtained for a sample of Greenside No 2 seam coal. Gaigher (1980), by means of low temperature radio-frequency ashing techniques, found that the ratio between the mineral matter and ash contents of 35 product samples from South African collieries varied from 1,08 to 1,25. Values for the Greenside No 2 seam varied between 1,15 for a 10 % ash sample and 1,22 for a 20 % ash sample.

If the mineral matter to ash ratio is known, this can be incorporated into equation (2.4) to predict the relative density of the mineral matter:

$$Sg_m = \alpha . Q . Sg_c / (\alpha . Q - 100) \qquad (2.5)$$

Where: Sg_m = Relative density of the mineral matter
α = Mineral matter to ash ratio

2.3.4. Liberation Characteristics of South African Coal

Very little published data exists on the liberation characteristics of South African coals. Horsfall (1977) presented curves for a Witbank No 2 seam coal showing the increase in yield that occurs at a particular product grade with decreasing particle size. This data is presented in Fig. 2.3.

Sanders and Brookes (1986) presented similar data for coals from the Witbank No 2 seam and from the Ermelo coalfield, as part of a comparison of the washability characteristics of coals from Europe, Australia, Botswana, India, Brazil and South Africa. However both these studies were confined to coal larger than 0,5 mm in size. In both cases it was shown

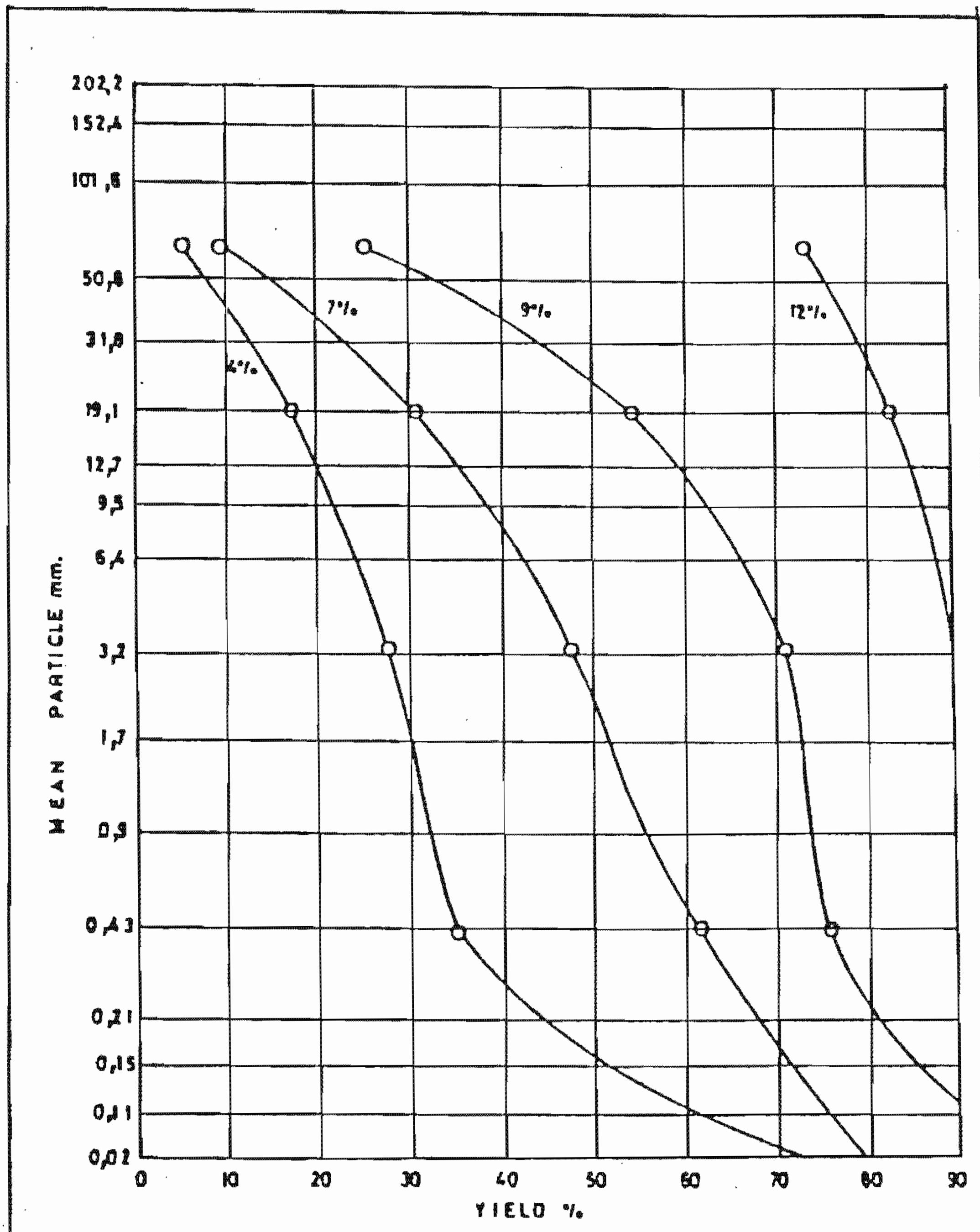

FIGURE 2.3 Liberation curves of a Witbank No 2 seam coal showing ash versus yield at different particle sizes (from Horsfall, 1977).

that while the washability characteristics were improved in the finer size fractions, the yield of low ash material remained poor. Marked improvement in the yield of low ash coal would require a significantly finer feedstock, indicating the need to investigate the liberation of coal at sizes finer than 0,5 mm.

Panopoulos et al (1983, 1986) presented density distribution data for a sample of coal fines from the Landau Colliery near Witbank. The sample was split into three size fractions between 500 and 125 micron. Little or no increase in liberation was observed as the size fraction became finer, the finest fraction (-150+125 micron) remaining substantially unliberated.

At the time when the work presented in this thesis was initiated, a similar investigation into the liberation characteristics of a number of South African coals was undertaken at the Department of Metallurgy of the University of the Witwatersrand. In the first part of the investigation, coal fines from several South African collieries, including Greenside, were investigated. In the second part of the investigation, samples of coarse coal were selected from different seams of six of the major South African coal deposits. The coarse samples were crushed to -1 mm in size. Both the fines and the milled samples were split into size fractions, and the liberation of each size fraction was assessed by float and sink analysis. The effect on the liberation characteristics of further milling the coals was not investigated. The results for the -25 micron fraction, which could not be obtained by float and sink analysis, were calculated from the composition of the coarser size fractions.

The preliminary findings of this work can be summarised as follows (Birtek and King, 1984, 1986):

a) Vitrinite tends to accumulate in the coarser sizes while inertinite accumulates in the finer sizes.

b) The -25 micron size fraction is invariably richer in mineral matter, either as a result of liberation of fine mineral matter or an accumulation of mineral matter rich inertinite.

c) Down to 25 micron there is no liberation of mineral matter from coal within the definition of Gaudin (1939).

In particular, the calculated liberation efficiencies of the size fractions of a sample of Greenside coal showed a marked decrease in the liberation efficiency of the finest fraction (-38 micron) compared to that of all the other size fractions. The liberation efficiency of the size fractions above 38 micron varied from 54,4 to 64 %, while the liberation efficiency of the -38 micron fraction was only 38,7 %.

Falcon and Falcon (1982, 1984) investigated a number of coals from the Witbank coalfield with respect to the liberation of the different organic and inorganic constituents, as part of a study on selective maceral and microlithotype concentration by flotation. Their investigation was conducted on coal between 500 and 150 micron in size. Good liberation of the organic constituents at this size was observed, although separation by flotation was largely unsuccessful.

2.4. Summary

The heterogeneous structure of coal indicates that a study of coal liberation should include both the maceral and mineral components. Because of the high syngenetic clay content of South African coals, liberation will occur at very fine sizes, therefore the liberation characteristics of very fine coal must be evaluated. This will require milling the coal to varying degrees of fineness, and evaluating the liberation of the coal by a suitable method. The method used should be float and sink analysis, but the technique must be extended to enable analysis of very fine sizes (< 38 micron).

The results can be interpreted using density distribution histograms, washability analysis and petrographic washability analysis. The M-Curve can be used to quantify liberation efficiency. The relationship between ash content and inverse of relative density can be used to calculate the relative densities of the predominant components of the coal, and their distribution during size reduction.

CHAPTER 3

ANALYTICAL TECHNIQUES

3.1. Float and Sink Analysis of Fine Coal

Float and sink analysis was selected as the method of assessing the degree of coal liberation. As the investigation required assessing the liberation of coal samples milled to progressively finer sizes, a float and sink technique was required that was suitable for analysing very fine material. This section describes the evaluation of existing methods for carrying out float and sink analysis of coal fines, and then outlines the development of a method for extending the float and sink analysis to ultrafine sizes.

3.1.1. Evaluation of Existing Methods

The most common method for the float and sink analysis of coal fines involves the use of separating funnels, in which particles separate under gravity in a suitable heavy liquid. While this method presents little difficulty for coal samples consisting of particles larger than 500 micron, the technique becomes extremely time consuming for samples containing very fine particles, or a high proportion of material close to the specific gravity of separation, as very long separating times are required. For practical purposes, this method is unsatisfactory for samples containing particles finer than 75 micron.

Alternative methods aimed at speeding up the process rely on the use of a centrifuge. In the method recommended by the International Organization for Standardization (I.S.O., 1981), a sample of coal (20 to 60 gram) is placed in a centrifuge tube with liquid of the lowest density. After spinning, the floats are collected from the surface with a scoop, liquid of the next highest density is added to the sinks and the process is repeated until the highest density is reached. A disadvantage of this method is the initial high loading of the tubes which can result in a significant amount of entrained and thus misplaced material; moreover, it is difficult in practice to scoop all the floats from the surface accurately, without leaving some material behind or causing some mixing with the sinks. The sequential treatment of a single sample can also lead to significant cumulative error as the quantity being treated becomes smaller.

A second centrifugal method is that of Hall (1934), in which a fine gauze tray is fitted inside the centrifuge tube, suspended between the floats and the sinks by wires hung over the edge of the tube. This gauze is used to pull out the solid plug of floats after centrifugation. Problems with this method are that the gauze tends to trap some sink material during centrifugation, which will report to the floats; and that on removal of the gauze some float material is invariably left behind, and is difficult to recover.

3.1.2. Development of a New Method

Due to the unsatisfactory nature of the methods discussed above, it was decided to develop new apparatus and method. The fineness of the material under investigation necessitated the use of a centrifugal technique.

The apparatus, shown in Figs. 3.1 and 3.2, was designed to fit into a standard 100 ml Polytetrafluoroethylene (PTFE)

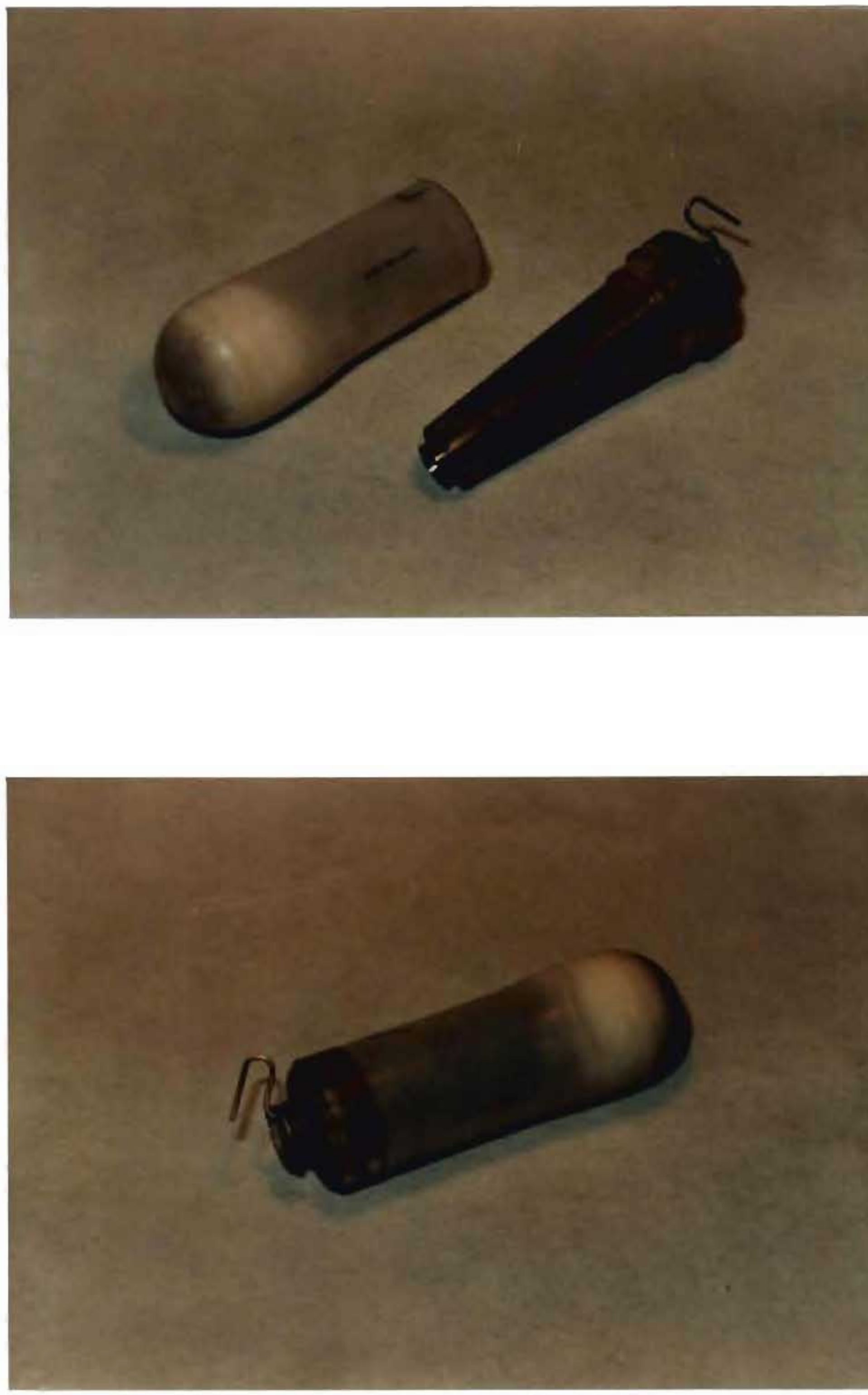

FIGURE 3.1 The new float and sink apparatus.

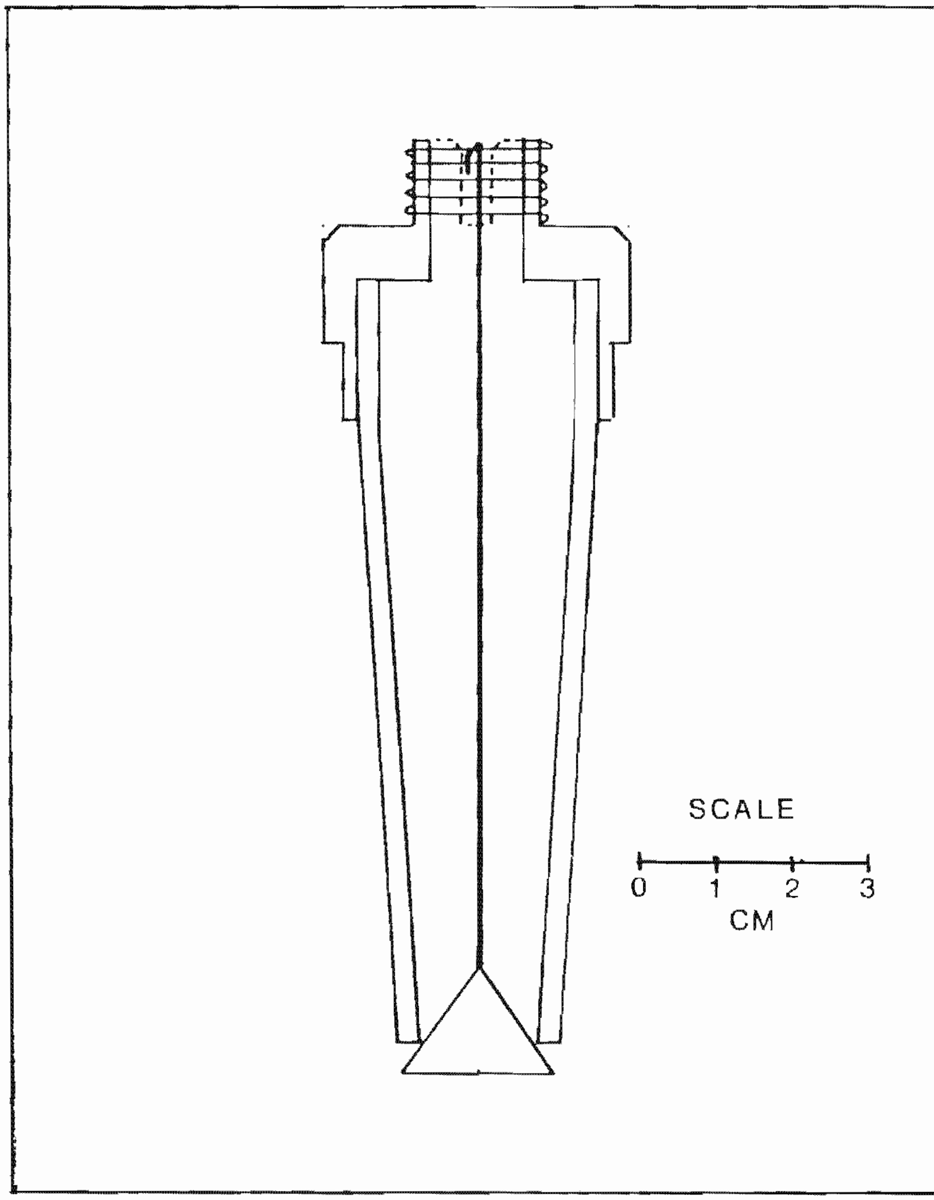

FIGURE 3.2 A schematic diagram of the new float and sink apparatus.

centrifuge tube. It consists of a tapered tube, with the bottom sealed by a conical plug. This plug is connected via a rod to a spring at the top of the device. When sufficient downward force acts on the plug (as occurs during centrifugation), the spring is compressed, and the bottom of the tube opens. When the downward force on the plug ceases, the spring is relaxed, and the bottom of the tube is sealed again.

The device was manufactured out of perspex. This material has the advantage of being both transparent and sufficiently tough to withstand the high stresses of centrifugation. A disadvantage is that perspex is soluble in most organic liquids, so that if heavy liquids such as bromoform, tetrabromoethane (TBE), or Certigrav (a commercial organic liquid mixture used for float and sink determinations) were required to be used, the device would have to be manufactured out of a different material. The most appropriate materials of construction would be PTFE or stainless steel. The device was initially manufactured out of glass, but this material proved too prone to breaking in the centrifuge.

The heavy liquid used with the apparatus in this work was zinc chloride solution. Advantages of this heavy liquid are that it is very cheap and does not give off toxic vapours, like the more commonly used organic liquids such as bromoform or TBE. A limitation is that the highest specific gravity that can be obtained is 1,8.

The use of the new apparatus is illustrated in Fig. 3.3. Unlike the I.O.S. method, which uses sequential treatment of a single sample, the new method uses a different sample at each specific gravity. In this way cumulative data are obtained directly.

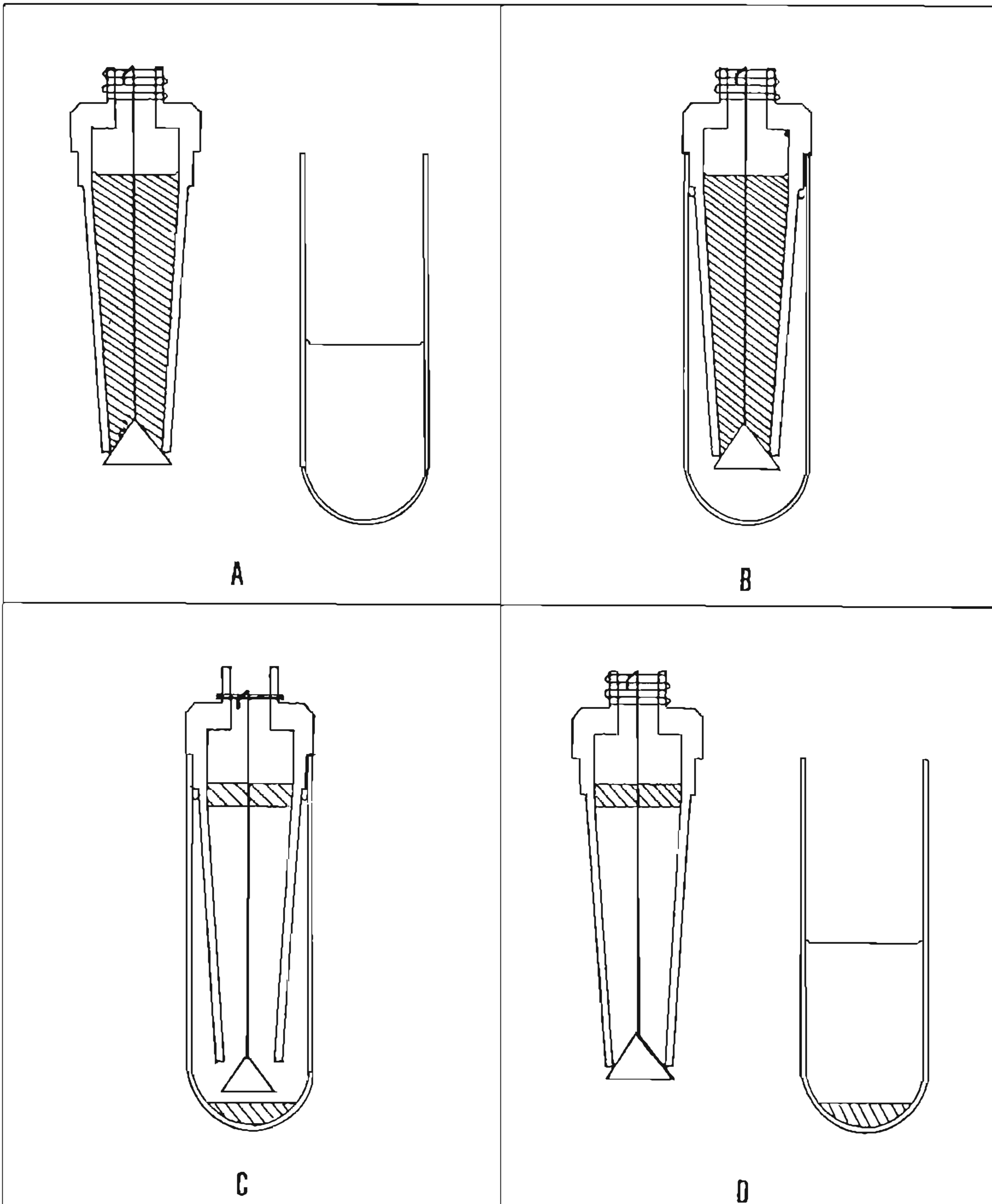

FIGURE 3.3 The use of the new float and sink apparatus.

The procedure can be broken down into four stages:

A) Approximately 2 g of dry coal is dispersed in zinc chloride solution of the required specific gravity, and transferred into the separating device. The separating device is then filled to the required level with zinc chloride solution, as is the centrifuge tube.

B) The device is inserted into the centrifuge tube, although the contents of the two remain isolated from each other.

C) The tube is then spun in a centrifuge. During spinning, centrifugal force on the conical plug pulls it down, compressing the spring. This links the fluid in the separating device with that in the centrifuge tube, and enables sink material to enter the tube.

D) When the centrifuge is stopped, the spring causes the conical plug to seal the device again, isolating the float material from the sink material. Thus the two fractions are separated merely by removing the device from the centrifuge tube. The separation is achieved with none of the problems associated with the existing methods discussed above (section 3.1.1.).

For this work a Beckman TJ 6 centrifuge with a TH 4 swing arm rotor was used. It is important that a centrifuge with a swing arm rotor is used, so that the line of force acts down the centre of the tube. With the centrifuge spinning at 4000 rpm, about 15 minutes are required for samples of +25 micron material; samples of -25 micron material usually require between 1 and 2 hours of spinning time.

If material less than 53 micron in size is being analysed, the conical plug may be locked closed during initial centrifugation, resulting in a provisional separation in the device. If this were not done the fine coal slurry in the device would behave like a liquid with a higher specific gravity than the clear zinc chloride solution in the centrifuge tube. Thus when the conical plug opened, mixing would result, causing some float material to report to the sinks. After a provisional separation has been obtained with the plug locked, the spring is released, enabling the conical plug to open, and the tube is re-centrifuged to obtain the final separation.

3.1.3. Experimental Procedure

Before carrying out a series of float and sink analyses, a stock solution of zinc chloride is prepared with a specific gravity of approximately 1,8. Zinc chloride crystals are dissolved in water, and the solution is filtered to remove any insoluble impurities. A range of relative densities between 1,0 and 1,8 can then be obtained by adding water to the stock solution.

In this study Industrial Grade zinc chloride crystals were used, and the relative density of solutions was measured with a hydrometer.

The following experimental procedure was developed for use with the new apparatus:

a) Zinc chloride solution of the required density is prepared.

b) Approximately 2 g of dry coal is accurately weighed into a 25 ml sample bottle. The sample bottle has a conical bottom leading into a 4 mm diameter glass tube, which is connected to a short piece of rubber tubing. The rubber tubing is clamped shut.

Approximately 5 ml of zinc chloride solution is added to the bottle, along with a few microlitres of chemical dispersant Tween 20 (polyoxyethylene sorbitan monolaurate). The bottle is sealed and shaken until the coal is thoroughly wetted.

The bottle is then placed in an ultrasonic bath for 5 minutes to further aid dispersion. The lid of the sample bottle is removed, and any adhering coal is washed into the bottle with a few millilitres of zinc chloride solution.

The rubber tube of the sample bottle is then inserted into the top of the separating device, and the clamp is removed. A syringe is used to wash any remaining coal particles from the sample bottle into the device. The separating device is then filled to the required level with zinc chloride solution, as is the centrifuge tube. The device is then inserted into the centrifuge tube.

c) Steps (a) and (b) are repeated for the other tubes.

d) The conical seal spring on all the tubes is locked (For samples consisting of particles larger than 53 micron this step, and steps (g) and (h), can be omitted).

e) The tubes are balanced, and then placed in the centrifuge.

f) The tubes are spun until the solids have separated into float and sink fractions, with clear liquid in between.

g) The centrifuge is stopped, and the conical seal springs on all the tubes are released.

h) The tubes are spun for the time required to achieve the final separation.

i) The separation devices are removed from the centrifuge tubes, and the float and sink fractions are filtered using a Buchner funnel containing preweighed glass fibre filter paper (GF/B). Ordinary filter paper cannot be used as zinc chloride solution destroys it. Each coal fraction is washed with three successive aliquots of water. It was ascertained that this resulted in no measurable zinc chloride retention in the coal. Finally the coal is washed with a few millilitres of ethanol to facilitate removal of the coal and the filter paper from the funnel. The float and sink coal fractions are then dried overnight in an oven at 105 °C.

3.1.4. Experimental Evaluation of the New Method

3.1.4.1. Repeatability Experiments

In order to establish the precision of the method a number of replicate experiments were performed on different size fractions of a sample consisting of a synthetic mixture of washed and waste coal from the Greenside Colliery near Witbank. The float and sink analyses were carried out at relative densities of 1,4 , 1,5 and 1,6. The results are presented in Table 3.1. As can be seen, the method is extremely precise for the size ranges examined. The maximum standard deviation observed from four replicates was only 0,6 %. Also a mass balance of the floats and the sinks shows acceptably small and relatively constant mass losses.

TABLE 3.1

The results of repeatability experiments using the new float and sink technique.

Size Fraction (micron)	Relative Density	Number of Replicates	Mean Yield of Floats (%)	Standard deviation	Average mass loss(%)
-300+106	1,6	4	56,3	0,2	0,9
-106+ 75	1,6	2	59,1	0,3	2,8
- 75+ 38	1,6	4	59,9	0,3	2,5
- 38+ 20	1,5	4	49,8	0,6	2,1
-300+106	1,4	4	34,5	0,4	2,4
-106+ 75	1,4	2	34,8	0,2	2,4
- 75+ 38	1,4	4	31,1	0,5	2,5

3.1.4.2. Reproducibility Experiments

To investigate the accuracy of the method, comparative experiments were performed on three samples of Greenside No 2 seam coal obtained from Professor R.P. King of the Department of Metallurgy at the University of the Witwatersrand. The samples were of dense medium cyclone underflow and overflow, taken during the operation of a pilot rig in which dense medium separation of fines was being investigated (King and Juckes, 1983). The new method was used to obtain the float and sink curves for the -90+75 micron fraction of the underflow and overflow samples. These results were then used to obtain a partition curve for the cyclone for each of the samples examined.

The partition curves that were obtained were compared with those of Professor King's research group, which were obtained using a double column gravitational separating technique, illustrated in Fig 3.4. This method is very accurate but extremely time consuming. The top column acts as a "rougher" and the lower column as a "cleaner". For the work in question, Professor King's group used a sequential

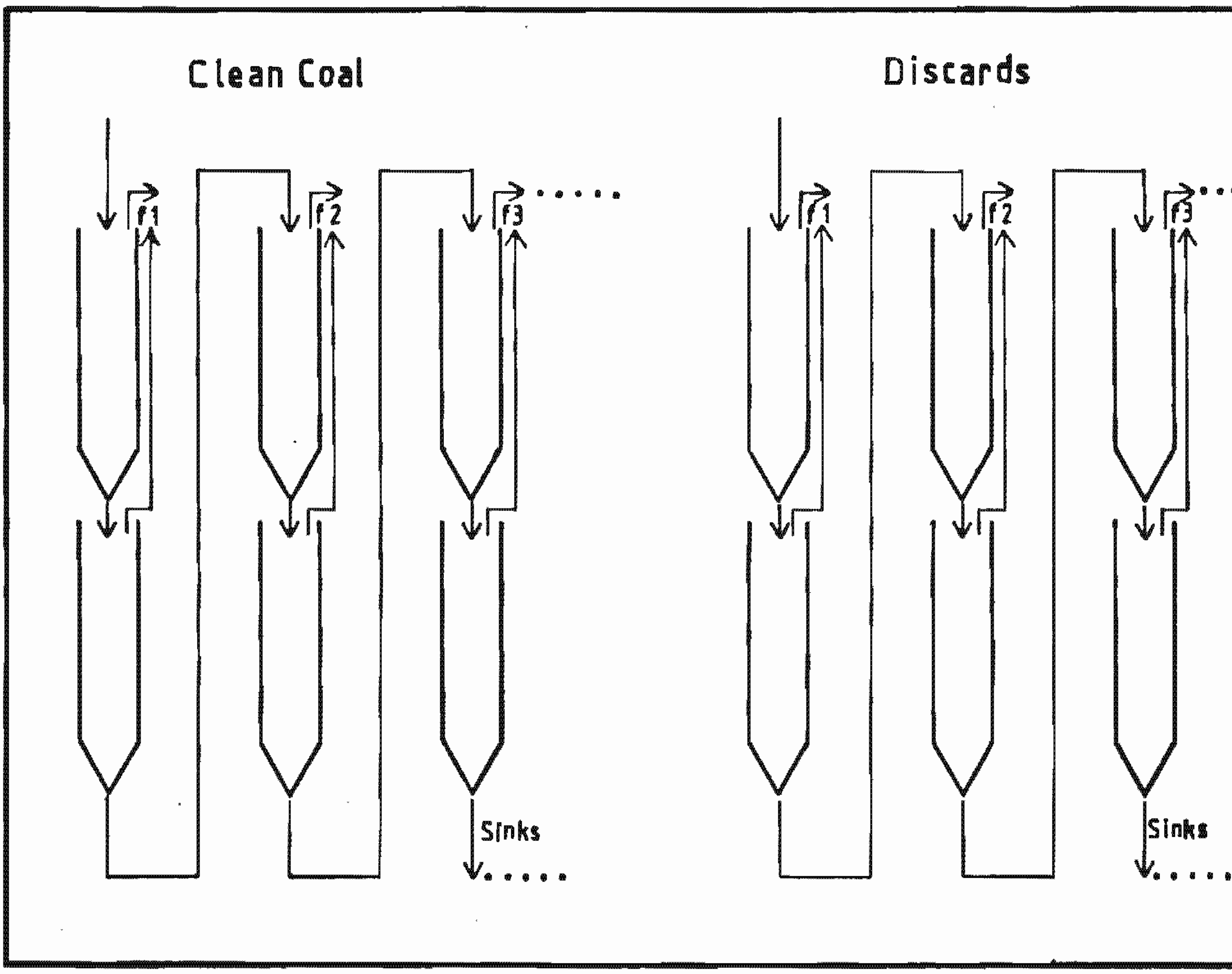

FIGURE 3.4 Double column method of float and sink analysis (from King and Juckes, 1983).

treatment of a single sample, with Certigrav as the heavy liquid. Since a gravitational technique was used, it was not possible to compare reproducibility for samples of finer sizes.

The detailed results of the comparative experiments are presented in Appendix A. Partition curves comparing the two sets of results are presented in Figs. 3.5 to 3.7.

The following partition function used by King and Juckes (1983) has been fitted to the results:

$$R(x) = b_3 + (b_4 - b_3) * \frac{\exp(b_2 x) - 1}{\exp(b_2 x) + \exp(b_2) - 2}$$

Where: x = normalised specific gravity, S/S_c
S = specific gravity of the particle
S_c = cut point S.G. (S at partition factor = 0,5)
R = partition factor
b_2, b_3, and b_4 are function parameters

Least squares best estimates of the parameters S_c, b_2, b_3, and b_4 were obtained by nonlinear regression analysis of the experimental data.

For each sample, curves were fitted to the combined set of data, and to each set of data obtained by the two different methods. Table 3.2 presents parameters from the least squares fit for each curve and the cut point. As a different number of points has been used to obtain each curve, the sum of error squared divided by the number of points has been included for purposes of comparison.

A very good agreement between the two sets of data can be seen in Fig. 3.5 and Fig. 3.6. The poor fit apparent in Fig. 3.7 can be explained by the fact that there was

FIGURE 3.5 Comparison of the results obtained using the new method and the double column method, sample 1.

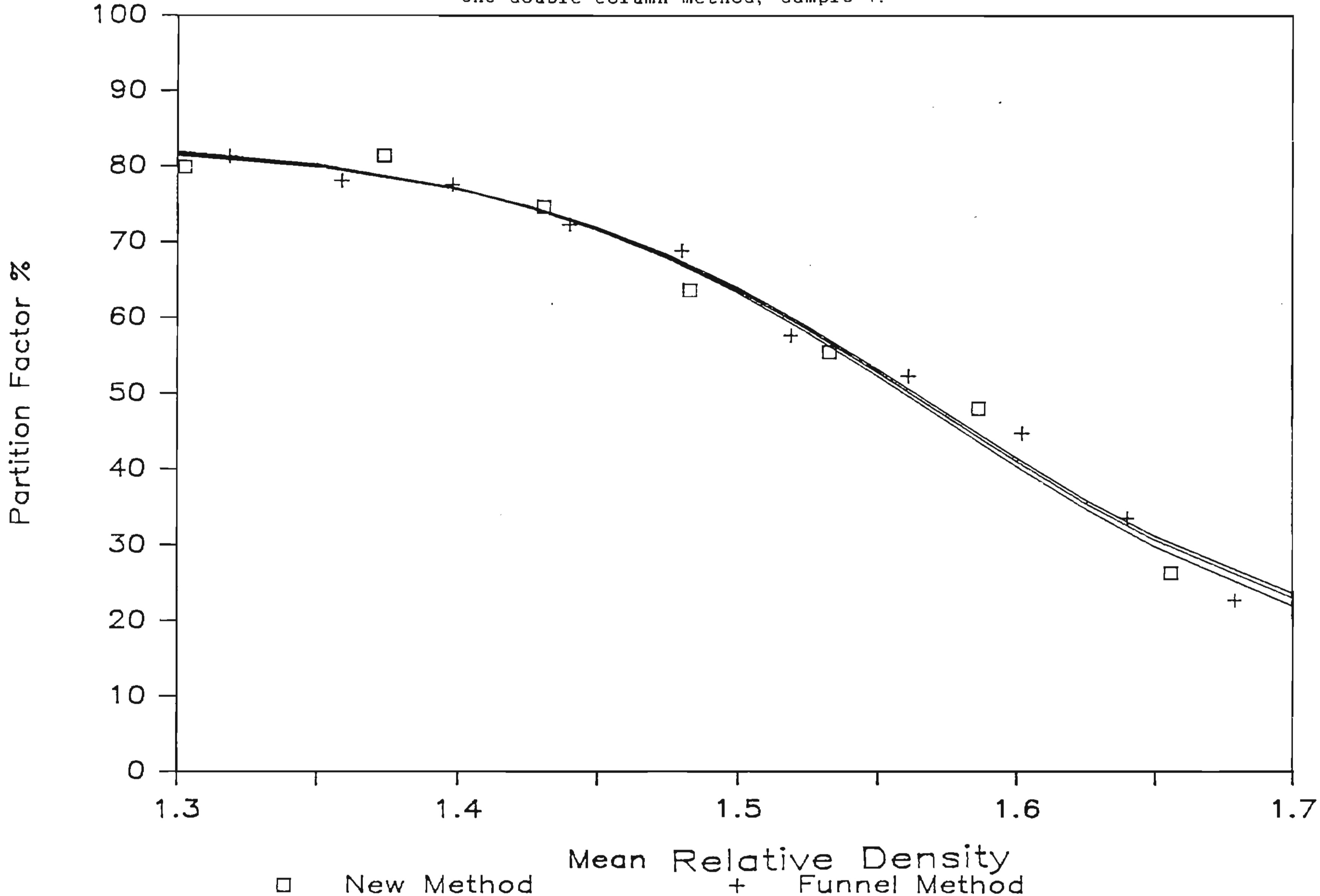

FIGURE 3.6 Comparison of the results obtained using the new method and the double column method, sample 2.

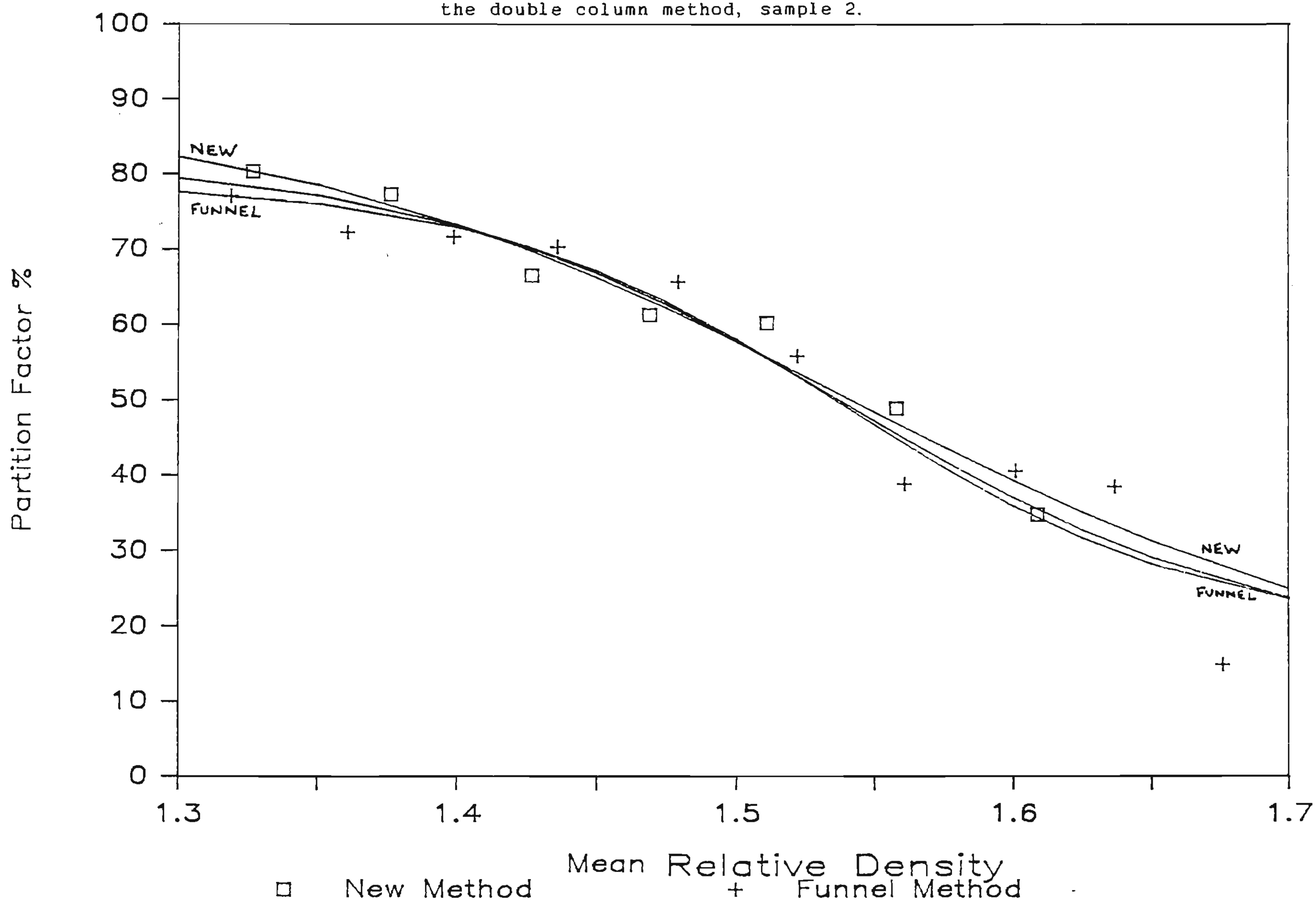

FIGURE 3.7 Comparison of the results obtained using the new method and the double column method, sample 3.

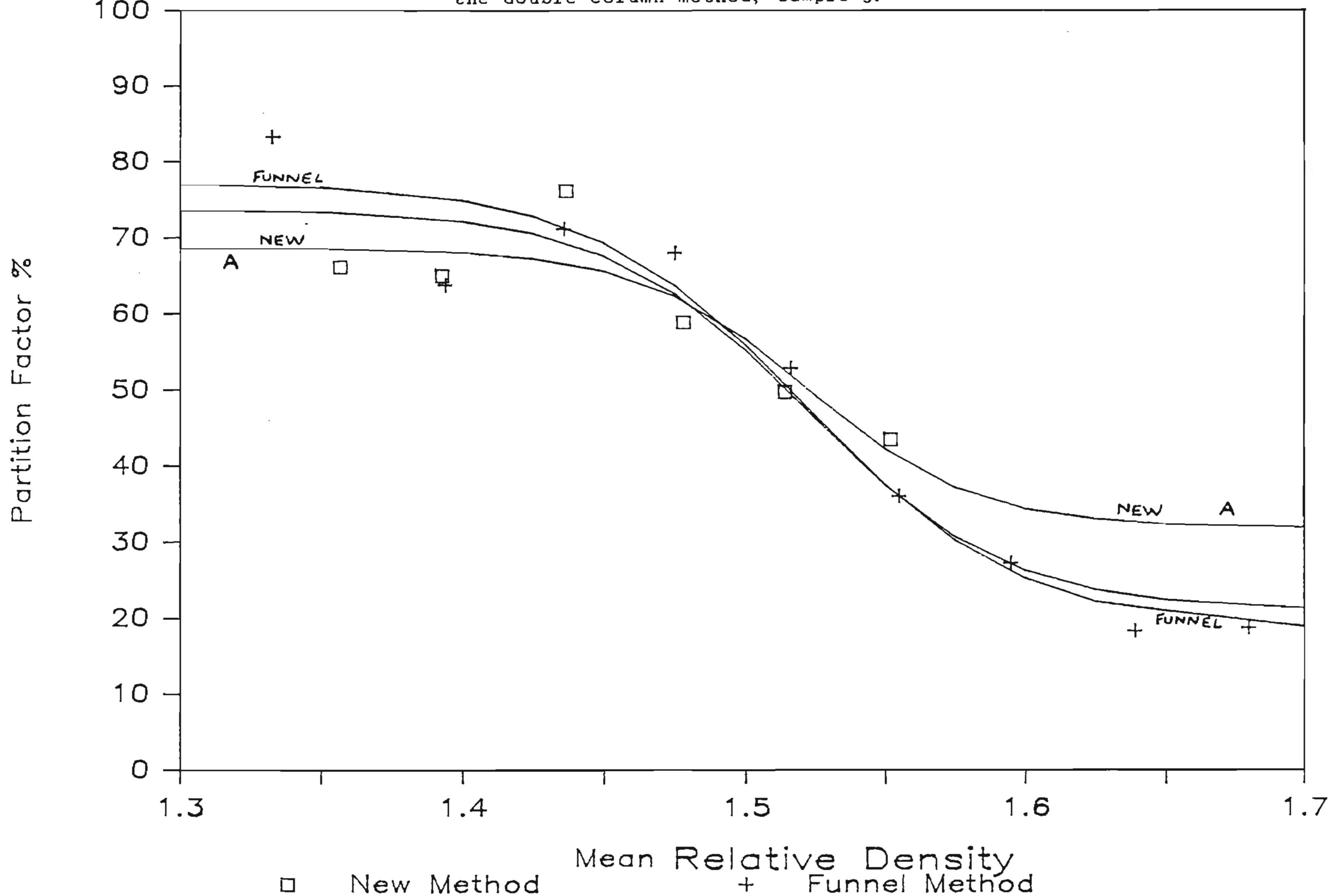

insufficient material to obtain more points in the higher specific gravity range of the graph (see Fig. 3.7, graph A). Thus the first two points have an exaggerated effect on the shape of the curve. Both sets of data exhibit a high degree of scatter, indicating possible inconsistencies in the coal sample, rather than problems in either of the float and sink methods. The high degree of scatter requires a large number of points to obtain a satisfactory curve fit. When the graph using the combined data is compared with the separating funnel method data, a much better agreement is apparent.

TABLE 3.2

A comparison of the function curve fit parameters of the two float and sink methods for the partition curves presented in Figs. 3.5, 3.6 and 3.7.

Method	S_c	(Sum of Error)^2	(Sum of Error)^2 / No of Points
		Figure 3.5	
New method	1,563	42,30	6,04
Funnel method	1,570	21,32	2,13
Combined data	1,570	73,56	4,33
		Figure 3.6	
New method	1,546	34,46	4,96
Funnel method	1,553	198,48	19,85
Combined data	1,550	247,55	14,56
		Figure 3.7	
New method	1,519	121,09	20,18
Funnel method	1,523	187,17	20,78
Combined data	1,523	386,43	25,76

3.1.4.3. Conclusions

It was decided on the basis of the results presented in the previous sections that float and sink analyses could be carried out with the new method both precisely and accurately, with none of the problems associated with the other methods.

Details of the development and evaluation of the new float and sink technique have been published in the Journal of the South African Institute of Mining and Metallurgy (Franzidis and Harris, 1986). A reprint of the paper is presented in Appendix H.

3.2 Petrographic Analyses

The petrographic analyses reported in this thesis were performed by Falcon Research Laboratories (Pty) Limited. The analyses were obtained by microscopic examination using reflected light on relief-polished surfaces under oil immersion, to enhance reflectivity differences. A Leitz MPV2 ore microscope was used, with a photomultiplier and digital read-out.

Preparation of the samples involved mixing with epoxy resin and moulding into a particulate block under pressure for 8 hours, after which the surface of each block was ground and polished to the required level for petrographic analysis.

The petrographic analysis consisted of group maceral analysis, microlithotype analysis, and the measurement of rank by means of vitrinite reflectance. The group maceral analyses were based upon a count of 500 points, whilst for microlithotypes 300 points were counted.

3.3. Ash Determinations

Ash determinations were performed using a muffle furnace according to SABS Standard Method 926.

CHAPTER 4

EXPERIMENTAL PROGRAM

4.1. Sample Selection

For the purposes of this study it was decided to investigate the liberation characteristics of coal from the No 2 seam from the Witbank coalfield, as this is the most important source of South African export coal. Samples were obtained from the Greenside Colliery near Witbank (Fig. 4.1). Greenside produces for export both low ash coal and power station smalls, and can be considered typical of the export collieries in the region.

It was decided to obtain two different samples of Greenside No 2 seam coal for investigation:

a) A sample of coarse, unwashed coal in a narrow size range, which could be milled to varying degrees of fineness in the laboratory, so that the relative liberation of the organic and inorganic components of the coal during size reduction could be evaluated.

b) A sample of the washing plant thickener underflow. This consists of the ultrafines, usually nominally -106 micron, that are produced during mining and any subsequent grinding, and are removed during the washing process and discarded to the slimes dam.

Two different sample sources were chosen to allow the comparison of the liberation characteristics of the fines produced by milling an artificially prepared coarse coal sample with those of the fines actually produced during the mining and washing process.

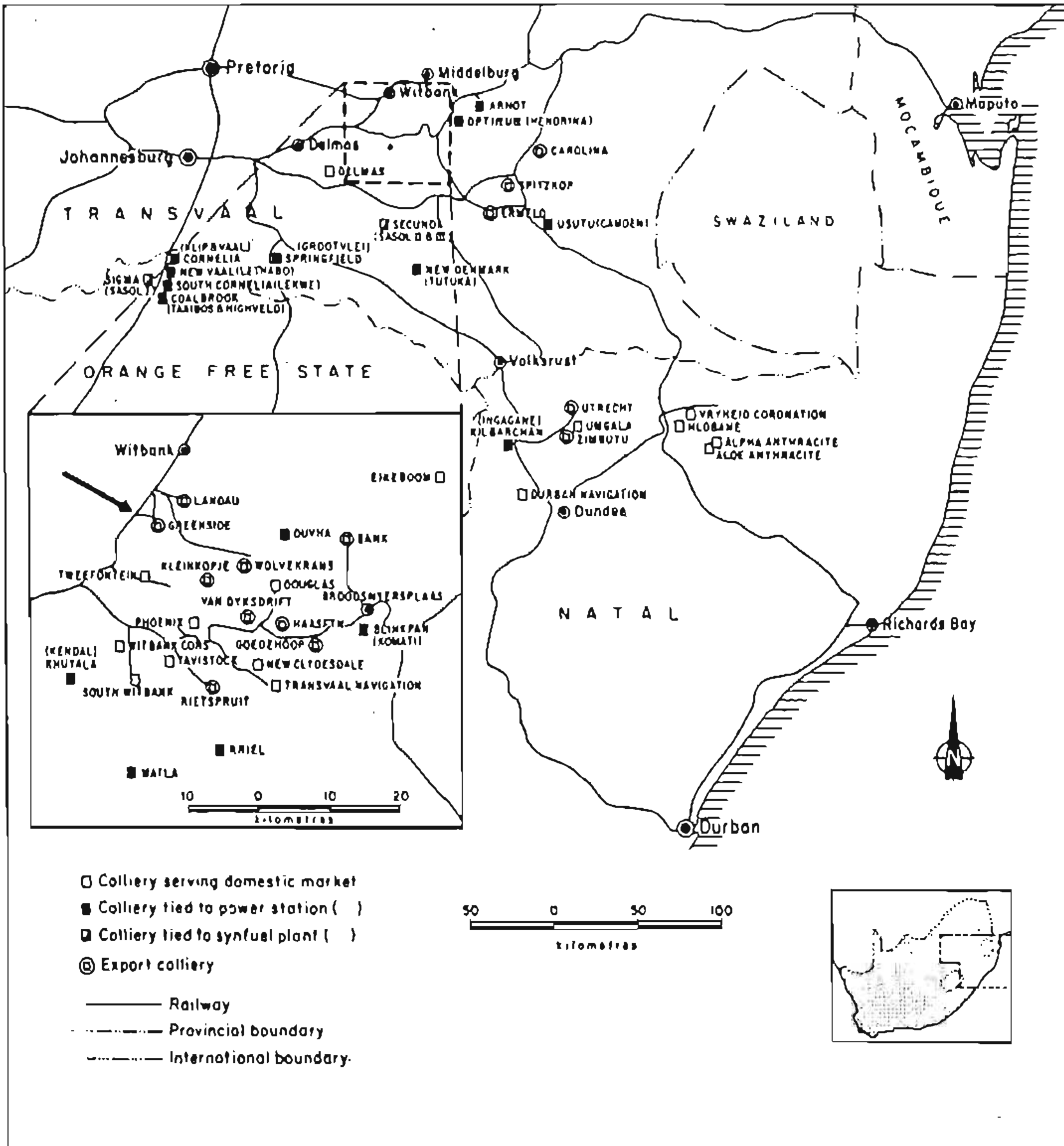

FIGURE 4.1 A map indicating the location of the major coal mines in South Africa. The enlarged section represents the Witbank Coalfield, and the arrow indicates the location of the Greenside Colliery (from Mehliss, 1985).

4.2. Sample Description

Two samples of No 2 seam coal were obtained from the Greenside Colliery. The first was of run-of-mine (r.o.m.) unwashed coal, and the second of thickener underflow. Both samples were prepared by the Ore Dressing Division of the Council for Mineral Technology (MINTEK), as described below, prior to delivery to U.C.T.

4.2.1. Run of Mine Sample

The preparation of the r.o.m. sample is illustrated in Fig. 4.2. The -10+6 mm fraction obtained from the original r.o.m. sample was blended and packed into 1 kg bags. The -6 mm material was discarded.

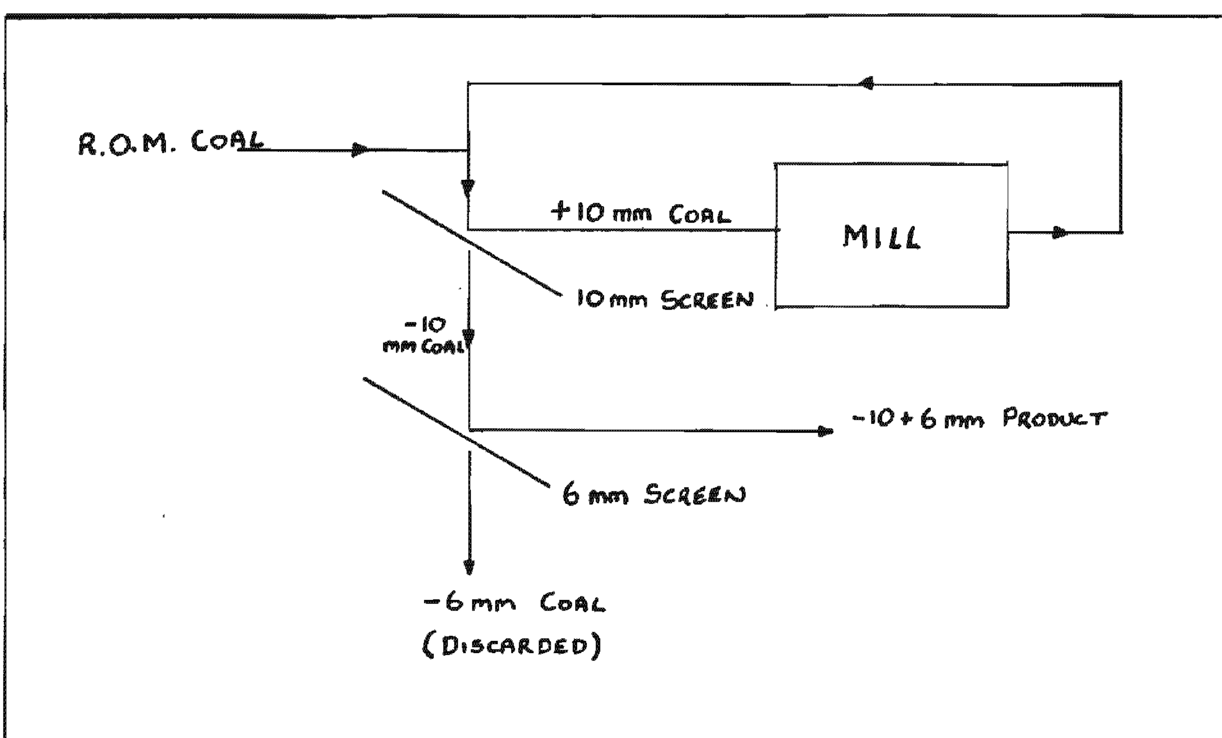

Fig 4.2 Sample preparation of r.o.m. coal as performed by MINTEK.

4.2.2. Thickener Underflow Sample

The thickener underflow sample was filtered on a pressure filter to remove most of the water, and dried in the sun. The sample was then blended, and packed into 300 g bags.

4.3. Sample Preparation

4.3.1. Milling

Three subsamples of the -10+6 mm coal were milled to varying degrees of fineness. The first sample was milled until 30 % was finer than 150 micron, which corresponds approximately to the size distribution of the material classified as "fines" in the washing plant (usually nominally -500 micron material). The second sample was milled until 90 % was finer than 150 micron, which corresponds approximately to the size distribution of the thickener underflow from the washing plant. The third sample was milled until 60 % was finer than 150 micron as an intermediate distribution between the two extreme distributions.

A stainless steel rod mill with a diameter of 31,6 cm was used. The mill was operated with 14 rods, and 1,5 kg of coal. The critical speed of the mill was calculated from the Chemical Engineers Handbook (Perry and Chilton, 1973):

$$N_c = \frac{76{,}6}{D^{1/2}} \qquad (4.1)$$

Where: N_c = Critical speed (rpm)

D = Diameter (feet)

For a mill diameter of 31,6 cm (1,04 ft) the formula gives a critical speed of 75,2 rpm. The mill was operated at 0,9 N_c (67 rpm) which is the region of optimum efficiency.

The milling curve of the -10+6 mm coal is presented in Fig. 4.3, which shows the proportion of the sample that is finer than 150 micron after a particular milling time. It can be seen that the curve is relatively linear over most of the range of milling times that were used. The milling times needed to produce the required samples were obtained by interpolation and are listed in Table 4.1.

TABLE 4.1

The time required to mill -10+6 mm Greenside coal until 30 %, 60 % and 90 % of the sample is finer than 150 micron.

Sample	Milling Time (min)
30 % -150 μm	17
60 % -150 μm	63
90 % -150 μm	99

4.3.2. Screening

All screening was performed wet using an Endecott Test Sieve Shaker with 200 mm diameter stainless steel laboratory test sieves. The sieve series used was as follows (all in micron): 250, 150, 106, 75, 53, 38 and 25.

FIGURE 4.3 The milling curve of the -10+6 mm coal sample.

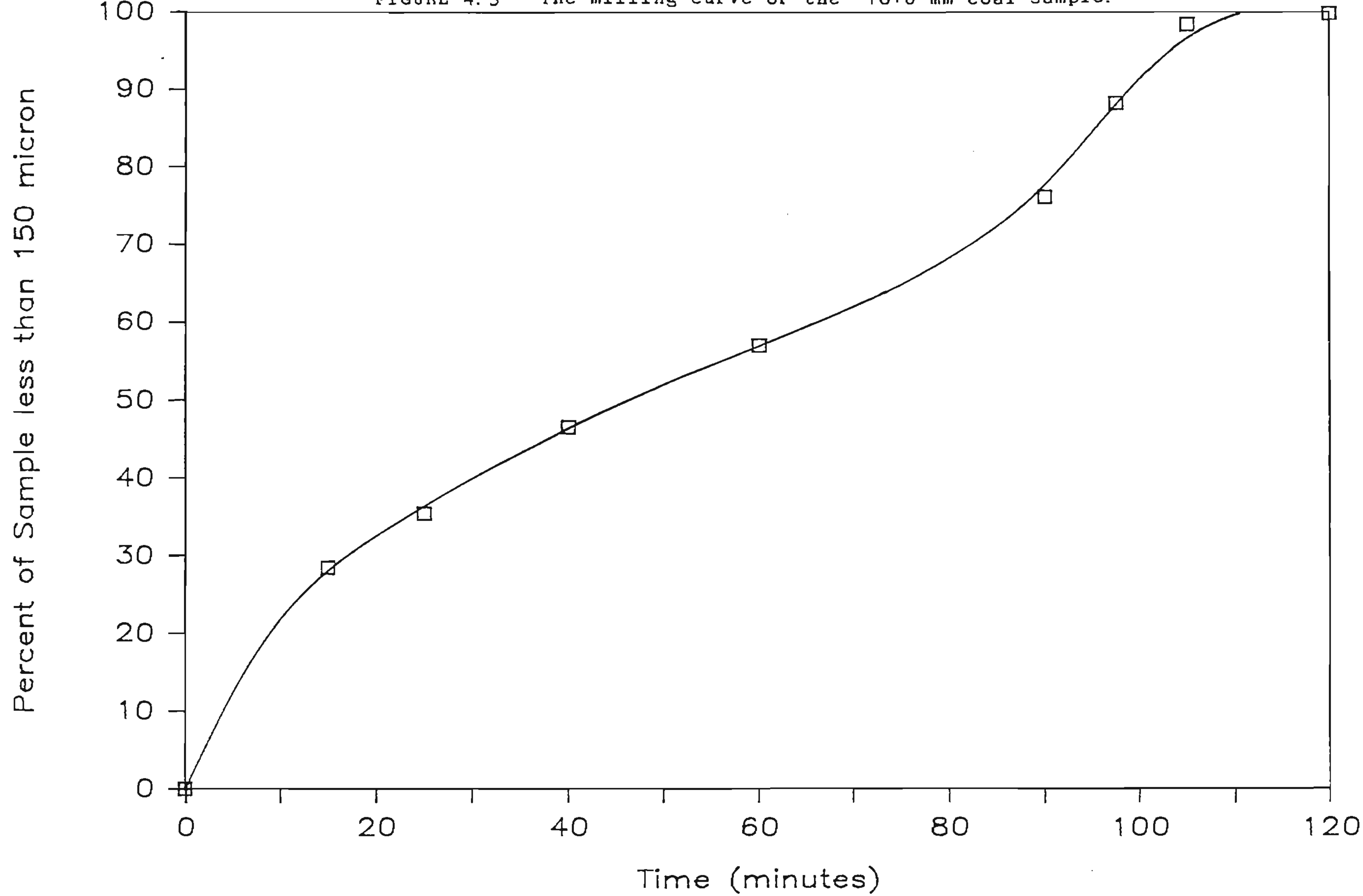

4.3.3. Other Equipment

Representative subsamples were obtained using a rotary splitter.

Wet samples were filtered using a Buchner funnel, and dried at 105 °C in an oven for at least 12 hours.

4.4. Liberation Study

The analyses performed in the liberation study are presented in Tables 4.2, 4.3, 4.4 and 4.5. These consisted of: size distribution (S.D.), ash content of the size fractions (Ash vs S.F.), float and sink analysis (Yield vs R.D.), washability analysis, i.e. ash content of the relative density fractions (Ash vs R.D.), petrographic analysis of the size fractions (P.A. vs S.F.) and petrographic washability analysis, i.e. petrographic analysis of the relative density fractions (P.A. vs R.D.). Table 4.2 presents the work performed on the -10+6 mm sample milled to 30 % finer than 150 micron. Table 4.3 presents the work performed on the -10+6 mm sample milled to 60 % finer than 150 micron. Table 4.4 presents the work performed on the -10+6 mm sample milled to 90 % less than 150 micron. Table 4.5 presents the work performed on the thickener underflow sample. Each table shows the various size fractions (in microns) that were used for the indicated analyses.

TABLE 4.2

Liberation study: The analyses performed on the size fractions of the sample milled to 30 % finer than 150 micron (all values in micron). (P.A. = Petrographic Analysis; S.F. = Size Fraction; S.D. = Size Distribution; R.D. = Relative Density).

S.D.	%Ash vs S.F.	Yield vs R.D.	%Ash vs R.D.	P.A. vs S.F.	P.A. vs R.D.
+250	+250	+150	+150	+150	-150+106
-250+150	-250+150	-150+106	-150+25	-150+106	-106+ 53
-150+106	-150+106	-106+ 75	-25	-106+ 53	- 53+ 25
-106+ 75	-106+ 75	- 75+ 53		- 53+ 25	-25
- 75+ 53	- 75+ 53	- 53+ 38		-25	
- 53+ 38	- 53+ 38	- 38+ 25			
- 38+ 25	- 38+ 25	-25			
-25	-25				

TABLE 4.3

Liberation study: The analyses performed on the size fractions of the sample milled to 60 % finer than 150 micron (all values in micron). (P.A. = Petrographic Analysis; S.F. = Size Fraction; S.D. = Size Distribution; R.D. = Relative Density).

S.D.	%Ash vs S.F.	Yield vs R.D.
+250	+250	+150
-250+150	-250+150	-150+106
-150+106	-150+106	-106+ 75
-106+ 75	-106+ 75	- 75+ 53
- 75+ 53	- 75+ 53	- 53+ 38
- 53+ 38	- 53+ 38	- 38+ 25
- 38+ 25	- 38+ 25	-25
-25	-25	

TABLE 4.4

Liberation study: The analyses performed on the size fractions of the sample milled to 90 % finer than 150 micron (all values in micron). (P.A. = Petrographic Analysis; S.F. = Size Fraction; S.D. = Size Distribution; R.D. = Relative Density).

S.D.	%Ash vs S.F.	Yield vs R.D.	%Ash vs R.D.	P.A. vs S.F.	P.A. vs R.D.
+250	+250	+150	+150	+150	-150+106
-250+150	-250+150	-150+106	-150+25	-150+106	-106+ 53
-150+106	-150+106	-106+ 75	-25	-106+ 53	- 53+ 25
-106+ 75	-106+ 75	- 75+ 53		- 53+ 25	-25
- 75+ 53	- 75+ 53	- 53+ 38		-25	
- 53+ 38	- 53+ 38	- 38+ 25			
- 38+ 25	- 38+ 25	-25			
-25	-25				

TABLE 4.5

Liberation study: The analyses performed on the size fractions of thickener underflow sample (all values in micron). (P.A. = Petrographic Analysis; S.F. = Size Fraction; S.D. = Size Distribution; R.D. = Relative Density).

S.D.	%Ash vs S.F.	Yield vs R.D.	%Ash vs R.D.	P.A. vs S.F.	P.A. vs R.D.
+250	+250	+106	+106	+106	+106
-250+150	-250+150	-106+25	-106+ 25	-106+ 25	-106+ 25
-150+106	-150+106	-25	-25	-25	-25
-106+ 75	-106+ 75				
- 75+ 53	- 75+ 53				
- 53+ 38	- 53+ 38				
- 38+ 25	- 38+ 25				
-25	-25				

CHAPTER 5

RESULTS AND DISCUSSION

This chapter presents the results of the experimental work carried out on the thickener underflow and the samples milled to 30, 60 and 90 % finer than 150 micron. The samples are analysed by size distribution, ash content of the size fractions, relative density distribution and washability (by the new float and sink technique), and petrographic analysis. Detailed results are presented in the appendices. An assessment of the liberation of the samples using the M-curve is presented, and the ash versus inverse of relative density data is calculated.

5.1. Size Distribution

The size distribution data of the thickener underflow and of the samples milled to 30 %, 60 % and 90 % finer than 150 micron are presented in Table B.1 in Appendix B. This shows the cumulative mass of material finer than a particular screen size. The data is presented graphically in Fig. 5.1 using logarithmic scales for both axes. Each of the four sets of data in Fig. 5.1 can be well represented by a straight line, indicating that the fine material that is produced during breakage of this particular coal has a particle size distribution that can be well approximated by the Gates-Gaudin-Schumann size distribution function (Perry and Chilton, 1973):

FIGURE 5.1 The size distribution of the four samples.

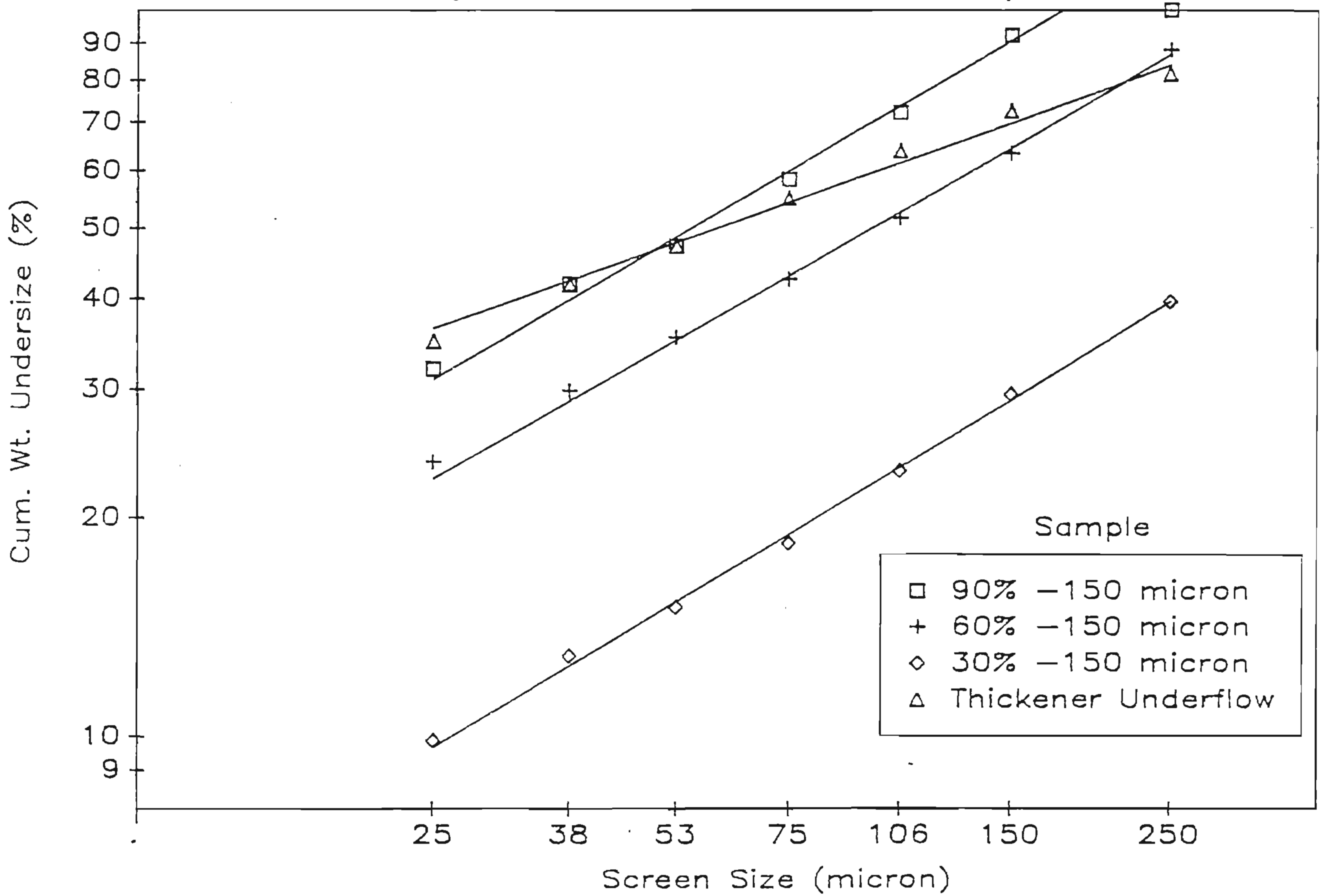

$$Y = (X/k)^m \qquad (5.1)$$

where: Y = Cumulative mass of material finer than a particular size (%).
X = Screen size (micron).
m,k = Function parameters.

When plotted on logarithmic axes, equation (5.1) represents a straight line of slope m. The Y intercept, or the cumulative mass of material in the sample less than 1 micron (i.e. Log(X) = 0), can be calculated from the function parameter k, where:

$$Y_{intercept} = m.Log(1/k) \qquad (5.2)$$

The values of m and k for the four samples are presented in Table 5.1.

TABLE 5.1

The Gates-Gaudin-Schumann function parameters for the four samples.

Sample	m	k
30 % -150 µm	0,61	0,62
60 % -150 µm	0,58	0,12
90 % -150 µm	0,60	0,081
Thickener Underflow	0,36	0,0013

5.1.1. Milled Samples

An examination of Fig 5.1 and Table 5.1 shows that the slopes of the size distribution functions of the three milled samples are practically equal, with the values of m in equation (5.1) ranging from 0,58 to 0,61. Thus m appears to be a constant for this coal under the particular conditions of comminution used in the preparation of the material.

5.1.2. Thickener Underflow

The slope of the size ditribution function of the thickener underflow, or the naturally arising fines, is considerably lower than that of the milled samples, indicating that this sample contains relatively larger proportions of both "ultrafine" (-25 micron) and "coarse" (+250 micron) material. The material present in this sample larger than 106 micron can essentially be considered misplaced as the stream sent to the thickener on the plant is the overflow of a classifying cyclone which has a cut point of 106 micron. Thus the presence of this material is a result of the imperfect operation of the cyclone.

5.1.3. Discussion

The difference in slope between the milled samples and the thickener underflow could be ascribed to the considerable difference between the natural production of fine material during mining and processing and that of comminution in a rod mill. However a significant contributory factor to this difference is the fact that the thickener underflow has passed through a classifying cyclone on the plant, which would imperfectly remove the coarser fractions. Thus if the cyclone were operating perfectly, the slope of the thickener underflow size distribution would probably be similar to that of the milled samples. The higher proportion of -25 micron material indicates that this material would have a smaller mean particle size than the sample milled to 90 % finer than 150 micron.

5.2. Ash Content of the Size Fractions

The ash content of the size fractions of the thickener underflow and of the samples milled to 30 %, 60 % and 90 % finer than 150 micron is presented in Fig. 5.2 and in Table B.2, in Appendix B.

5.2.1. Milled Samples

Fig. 5.2 shows that the ash content of the three milled samples follows the same trend with decreasing particle size. The ash content decreases, initially quite sharply, with decrease in particle size, but then increases sharply in the -25 micron fraction.

5.2.2. Thickener Underflow

The ash distribution of the size fractions of the thickener underflow follows a very different trend to that of the milled samples. As may be seen from Fig. 5.2, the thickener underflow sample shows a steady increase in ash content as particle size decreases, from 16.3 % in the coarsest fraction to 26 % in the finest fraction.

5.2.3. Discussion

For both the milled samples and the thickener underflow, it is clear that there is a concentration of ash in the -25 micron fraction during size reduction. This is due to the extremely fine size of a significant proportion of the mineral, mainly clay, present in the coal matrix. When liberated, this clay material reports to the ultrafine fraction.

FIGURE 5.2 The ash content of the four samples by size fraction.

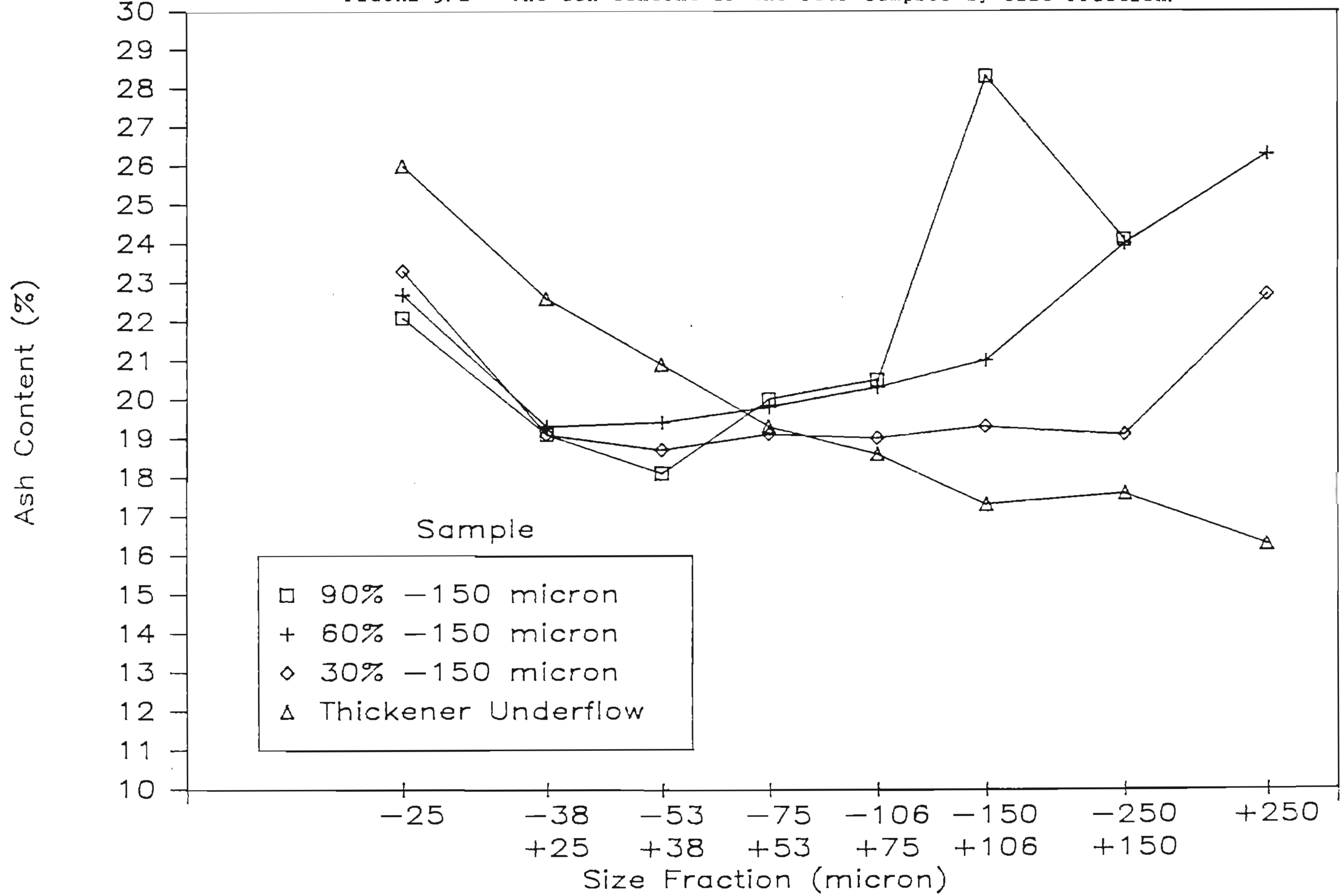

The high ash content of the coarse fraction of the milled samples is probably due to the presence of coarser and harder mineral components such as quartz or carbonate minerals in this fraction. As the coal is milled finer, the proportion of this material in the coarse fraction would tend to increase, which is consistent with the trend in Fig. 5.2. Thus the distribution of the ash in the size fractions of the milled samples suggests that there is a bimodal size distribution of the mineral components in this coal, such as that reported by Dawson (1983) in a study of coal fines from the Platberg Colliery, near Newcastle in Natal.

The lower ash content of the coarser fractions of the thickener underflow, compared to the milled samples, can be explained by the operation of the classifying cyclone on the washing plant. This would preferentially remove coarse particles with a higher ash content, and therefore higher relative density, since these particle are more likely to report to the cyclone underflow than relatively clean coal particles of the same diameter.

5.3. Density Distribution of the Size Fractions

5.3.1. Milled Samples

Fig. 5.3 shows normalised frequency histograms of the relative density of each of the size fractions of the sample milled to 30 % finer than 150 micron. Each column represents the proportion of material in a particular size fraction that reported to the floats in the indicated specific gravity range during float and sink analysis. Fig. 5.4 and Fig. 5.5 present the same information for the samples milled to 60 % and 90 % finer than 150 micron respectively.

FIGURE 5.3 The density distribution of the sample milled to 30 % finer than 150 micron by size fraction.

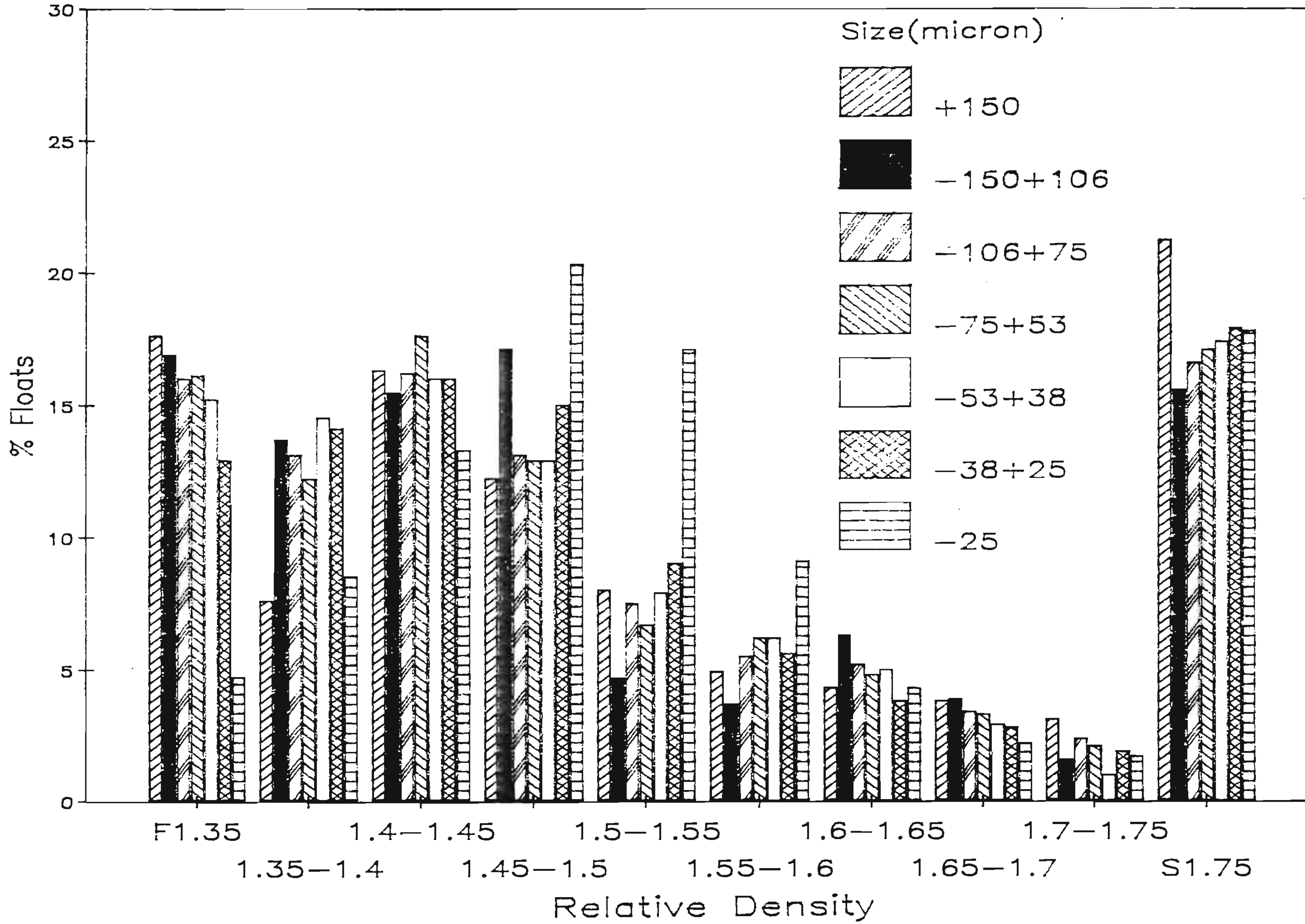

FIGURE 5.4 The density distribution of the sample milled to 60 % finer than 150 micron by size fraction.

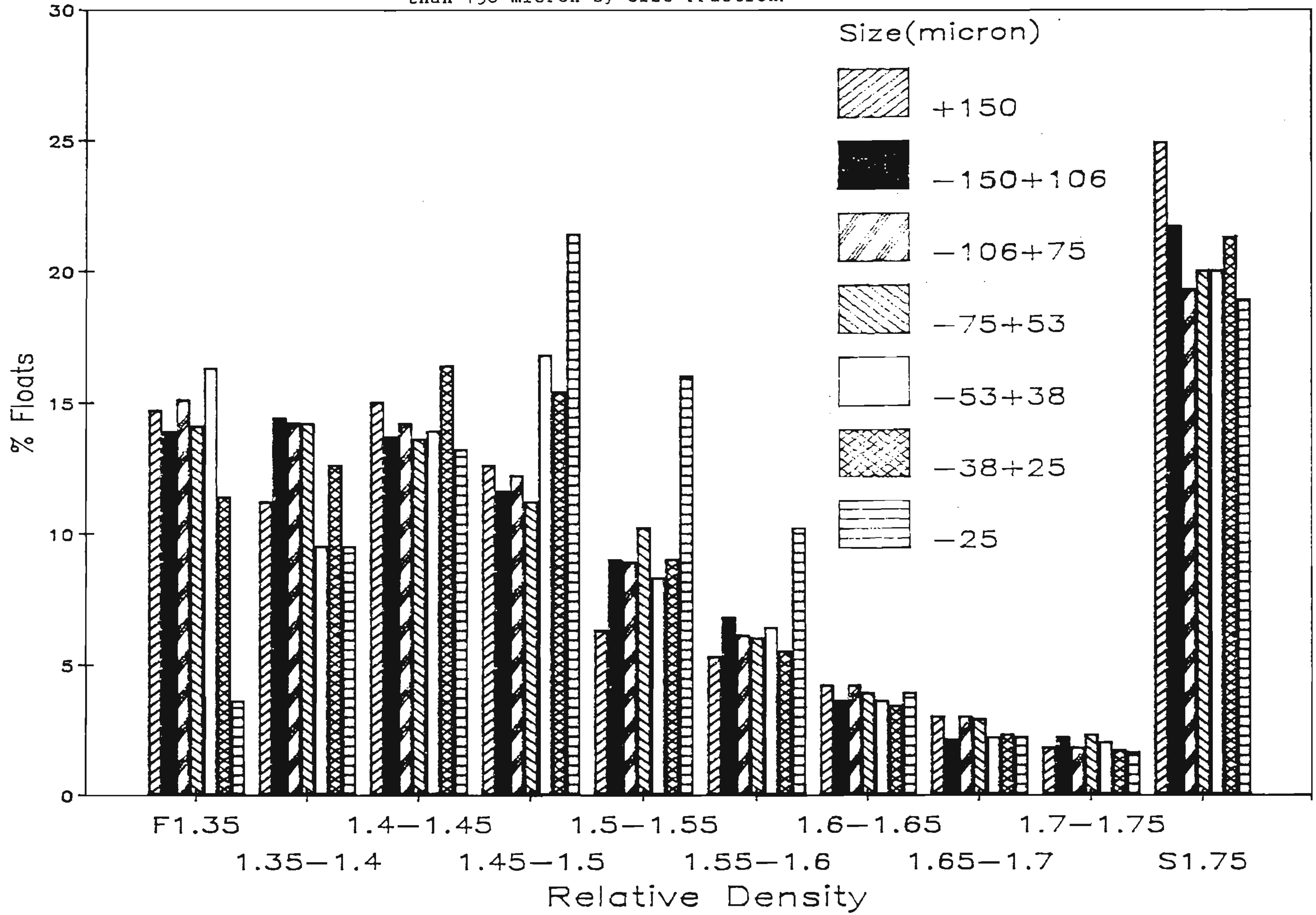

FIGURE 5.5 The density distribution of the sample milled to 90 % finer than 150 micron by size fraction.

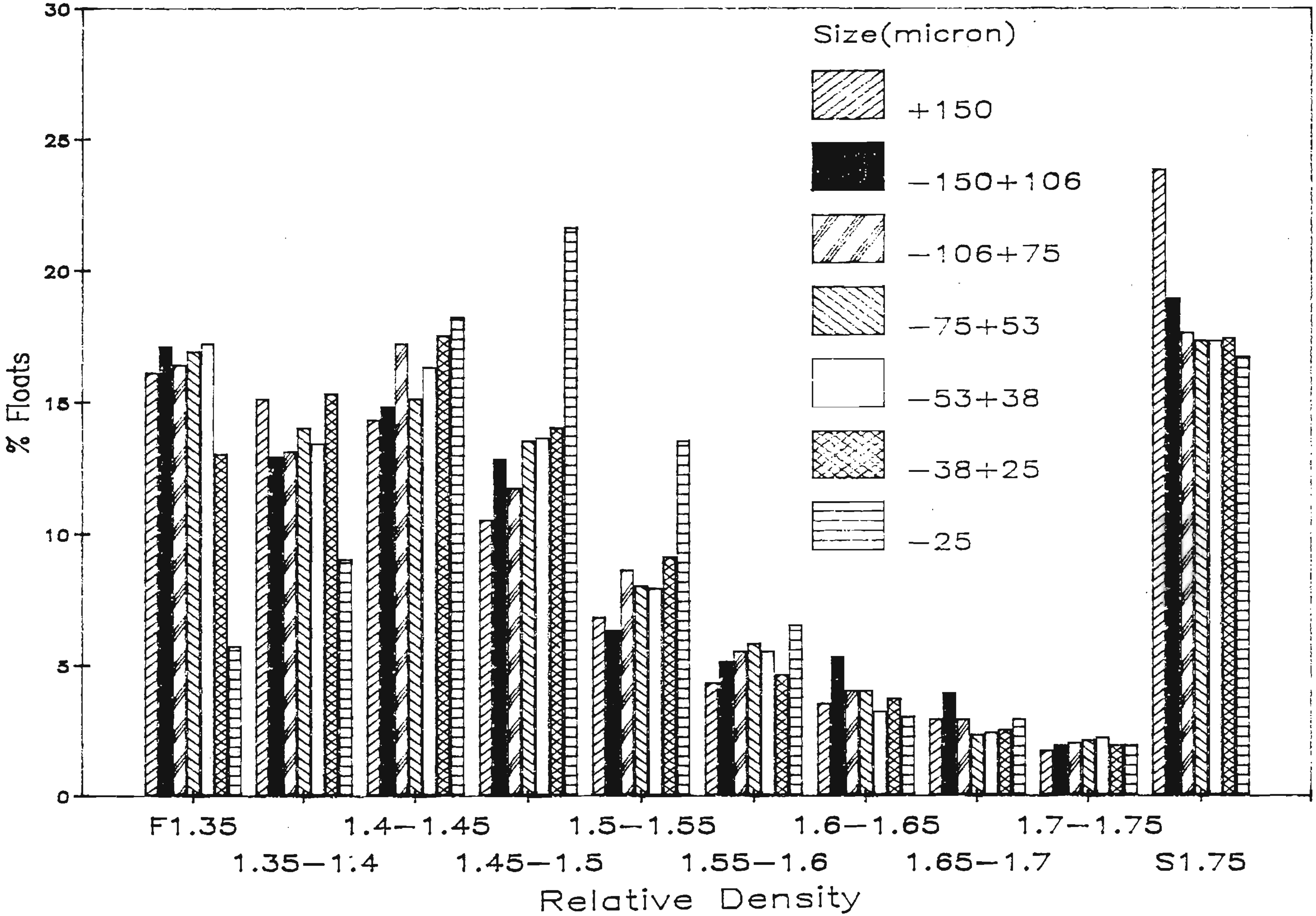

The density distribution data of each of the samples was normalised into relative density intervals of 0,05 for purposes of comparison. This was done by interpolation of a smooth curve drawn through the cumulative floats versus relative density data. The detailed data presented in Figs. 5.3 to 5.5 are listed in Tables C.1 to C.3 in Appendix C.

The relative density distributions of the three milled samples are best considered in two parts. The results for the size fractions above 25 micron will be discussed first, and then the -25 micron fraction will be considered on its own.

a) The Size Fractions Above 25 micron

Figs. 5.3 to 5.5 can each be divided into three relative density intervals: the interval below 1,6 which mainly consists of organic material, the interval from 1,6 to 1,75 which contains the middling material, and the interval above 1,75 which contains predominantly inorganic or mineral material.

In the interval below 1,6 none of the samples shows any apparent trend as the particle size becomes smaller. A comparison between the three samples similarly shows no apparent trend on grinding to varying degrees of fineness. Each sample exhibits a fairly similar distribution, with a significant amount of material in the relative density range 1,4 to 1,6. This corresponds to the relative density of the maceral inertinite, which is the predominant organic constituent of this coal.

In the interval between 1,6 and 1,75 the trend in all three samples is towards a small decrease in the amount of middling material as the size fraction becomes smaller. This indicates that the degree of liberation has been increased in the smaller size fractions, although only to a small extent. Considering the fineness of the size fractions examined in this investigation and the relatively small decrease in the amount of material in this relative density interval, complete eradication of this material would require extremely fine grinding.

The material with a relative density above 1,75 consists predominantly of mineral or ash forming components. For each of the samples the trend that can be observed corresponds to the distribution of ash by size fraction shown in Fig. 5.2, i.e. the amount of material of relative density > 1,75 tends to decrease with decrease in particle size, and then increase sharply in the -25 micron fraction.

b) The -25 micron Size Fraction

In Figs. 5.3, 5.4 and 5.5 it can be seen that the relative density distribution of the -25 micron size fraction of all three samples is significantly different to that of the other size fractions. In the -25 micron size fraction, there is a very large concentration of material in the 1,45 to 1,6 relative density range, with much less material below relative density 1,4 than in the other size fractions. In the density range 1,6 to 1,75 the -25 micron fraction is generally consistent with the trend exhibited by the other size fractions.

5.3.2. Thickener Underflow

The thickener underflow sample was split into only three size fractions: +106, -106+25 and -25 micron. This was a consequence of the absence of any significant trends in the density distributions of the size fractions above 25 micron in the milled samples. The relative density distribution of each of the size fractions of the thickener underflow sample is presented in Fig. 5.6. The normalised data can be found in Table C.4 in Appendix C.

It can be seen in Fig. 5.6 that the thickener underflow exhibits density distribution characteristics similar to those of the milled samples. Once again the most obvious feature is the very high proportion of material in the 1,45 to 1,6 relative density interval for the -25 micron size fraction, with correspondingly less material with relative density below 1,4 compared to the other size fractions.

5.3.3. Composite Samples

Fig. 5.7 presents a comparison of the relative density distributions of the four composite samples. These ditributions were obtained by mathematically reconstituting the size distribution data in Appendix B with the density distribution data in Appendix C for each of the four samples.

It is apparent from Fig. 5.7 that the density distributions of the four samples are fairly similar. As expected there is a small decrease in the amount of middling material as the sample becomes finer. In this regard the thickener underflow can be considered to be as fine or perhaps finer than the sample milled to 90 % finer than 150 micron.

5.3.4. Discussion

The comparatively small apparent increase in liberation with decreasing particle size in even the sample milled to 90 % finer than 150 micron must be ascribed to the extremely fine size of the clay minerals which form a significant portion of the mineral content of this coal. These clay

FIGURE 5.6 The density distribution of the thickener underflow sample by size fraction.

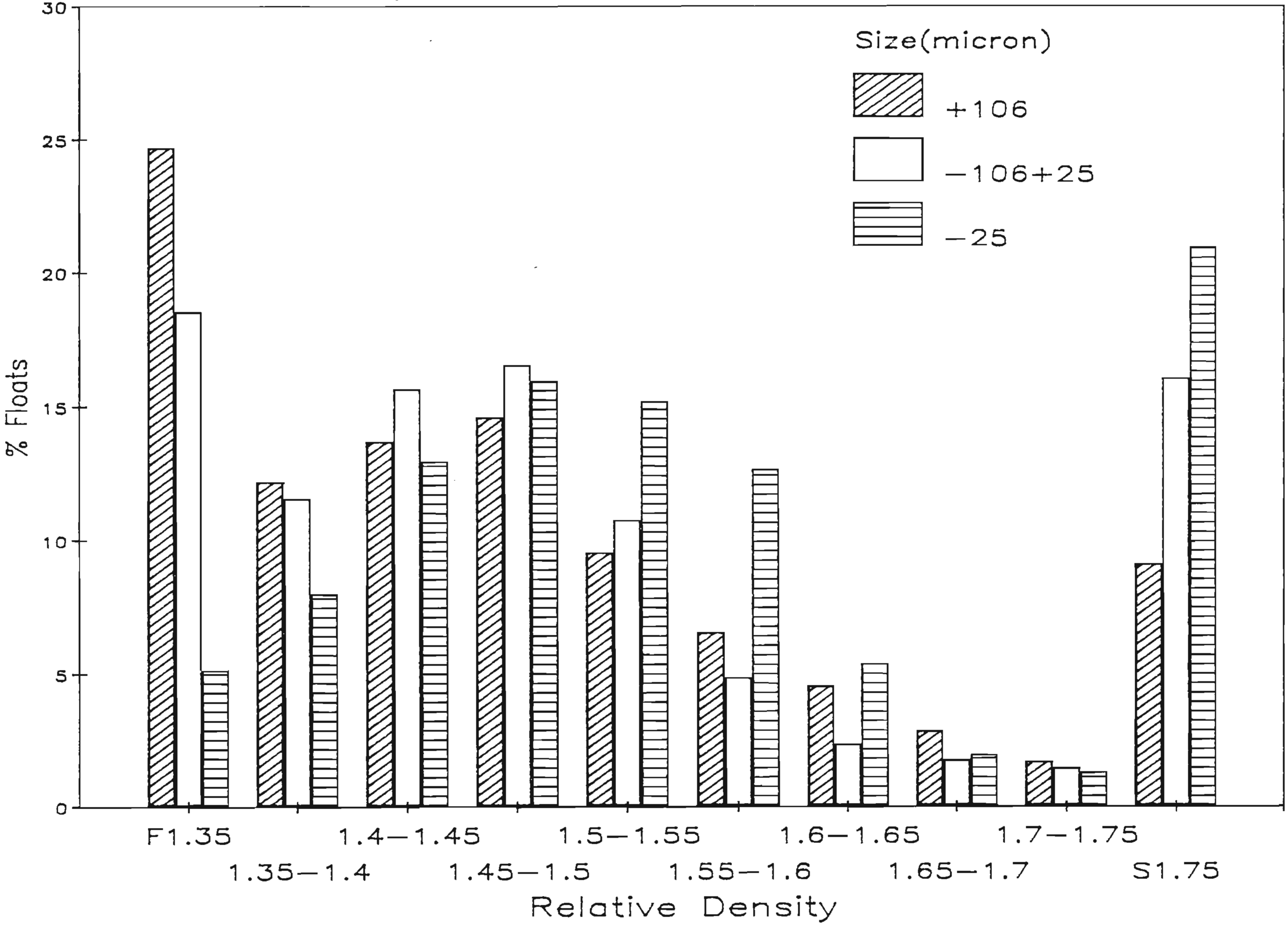

FIGURE 5.7 The density distribution of the four composite samples.

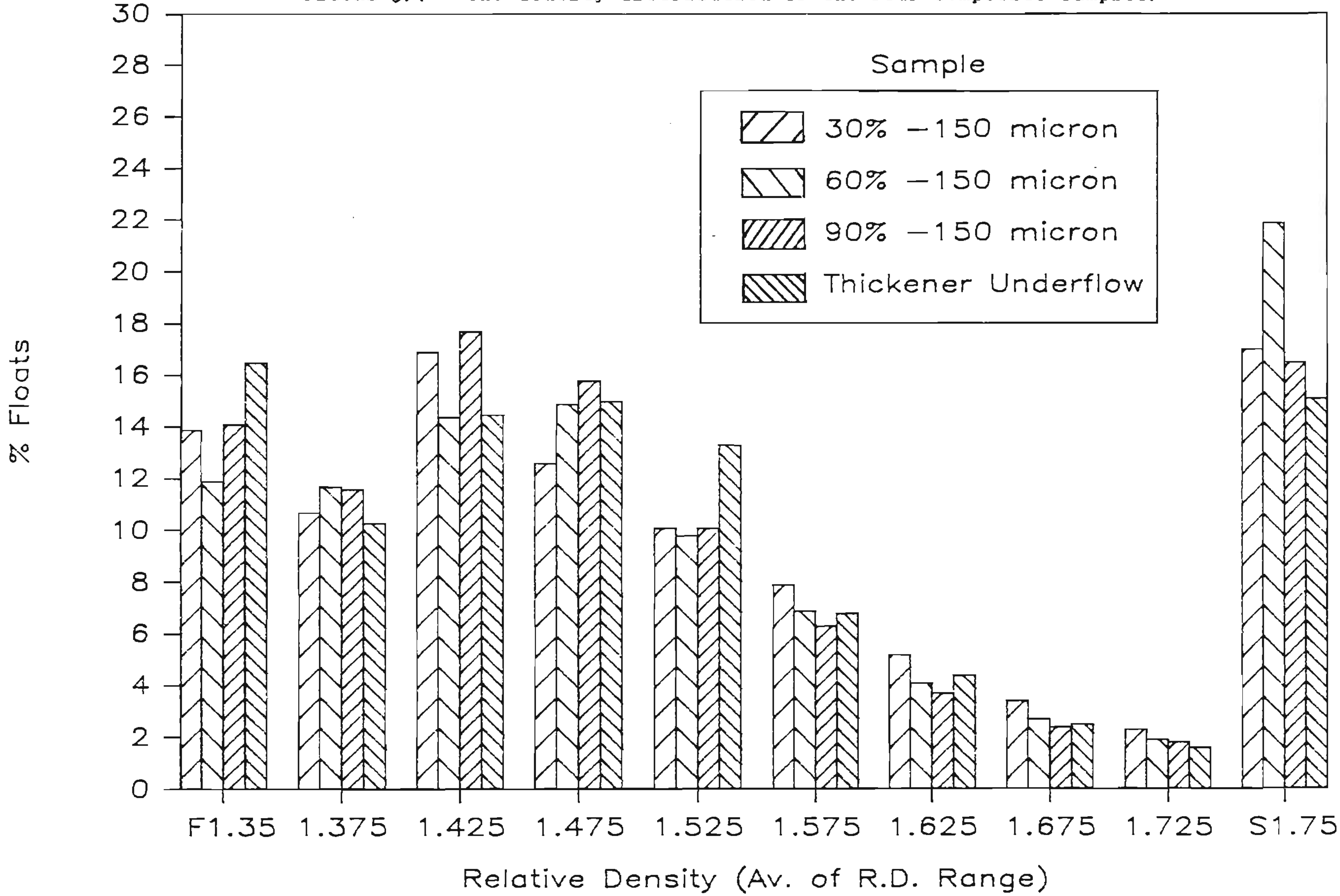

minerals are syngenetic in origin and are thus intimately intergrown with the coal matrix; extremely fine grinding would be required to achieve liberation.

Less easy to explain is the marked concentration of the -25 micron fraction of all the samples into the intermediate density range, and the comparatively small proportion of material in this size fraction in the lower density range. There are two possible explanations of this phenomenon:

a) A heavier organic component of the coal is concentrated into this size fraction during size reduction. The peak in the histograms of the -25 micron fraction corresponds closely to the relative density range of the maceral inertinite, suggesting that this maceral is preferentially liberated into the ultrafine fraction during size reduction.

b) The -25 micron fraction contains a high proportion of light middlings (as opposed to heavy middlings in the range 1,6 to 1,75 R.D.). This would imply that during size reduction light middling particles tend to be concentrated in the ultrafine fraction. This fraction is therefore less liberated than the other size fractions in that it contains relatively fewer clean liberated coal particles.

Both of these possibilities will be examined in subsequent sections (5.4.4. and 5.5.2.), after the washability and petrographic washability characteristics have been described.

5.4. Washability Characteristics of the Size Fractions

Because of the similarity of the density distributions of the +25 micron size fractions of the milled samples it was decided to reduce the number of size fractions investigated in subsequent analysis of these samples to three, namely +150, -150+25 and -25 micron. Also the sample milled to 60 % finer than 150 micron was not further investigated due to the relatively small changes in the density distribution that occur when the size distribution is changed from 30 % finer than 150 micron to 90 % finer than 150 micron.

Tables containing the detailed washability data of the samples milled to 30 % and 90 % finer than 150 micron and the thickener underflow are presented in Appendix D.

Tables D.1 to D.3 list the actual data obtained from the float and sink analysis of the +150, -150+25, and -25 micron size fractions of the sample milled to 30 % finer than 150 micron. Table D.4 contains the washability of the entire sample, reconstituted from the size fraction data. Fig 5.8 plots the cumulative yield versus cumulative ash content of the various size fractions and of the composite sample.

Similarly, Tables D.5 to D.8 list the data for the sample milled to 90 % finer than 150 micron, and Table D.9 to D.12 contains the data for the thickener underflow sample (note that the thickener underflow was screened at 106 micron). These data are plotted in Figs. 5.9 and 5.10 respectively.

Fig. 5.11 presents a comparison of the washability curves of the three composite samples.

5.4.1. Milled Samples

It may be seen from Figs. 5.8 and 5.9 that the -150+25 micron size fraction exhibits the best washability characteristics over almost the entire range of product grades for the samples milled to 30 % and 90 % finer than 150 micron. In each case the washability curve of the -25

FIGURE 5.8 Washability curves of the sample milled to 30 % finer than 150 micron by size fraction.

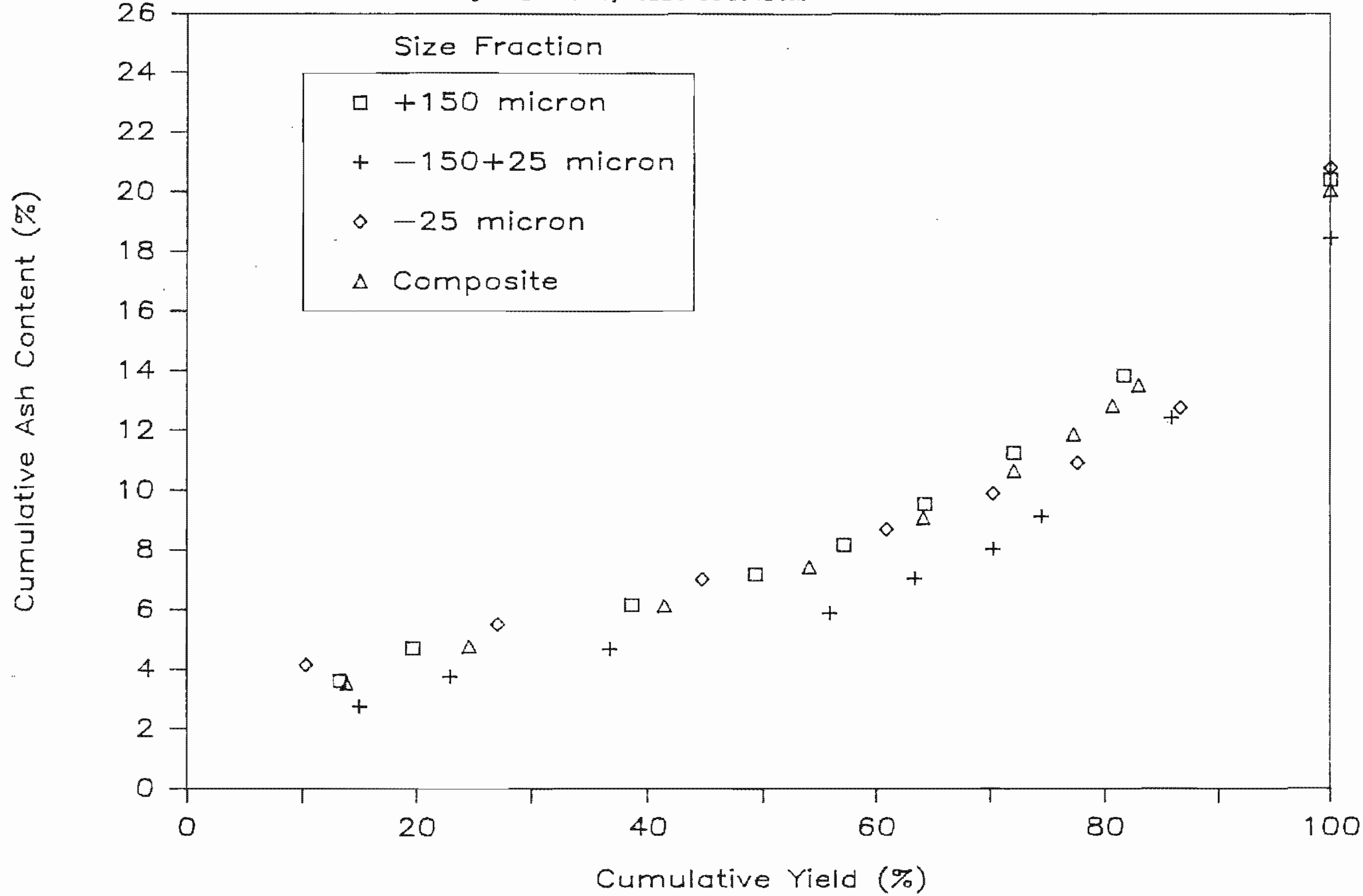

FIGURE 5.9 Washability curves of the sample milled to 90 % finer than 150 micron by size fraction.

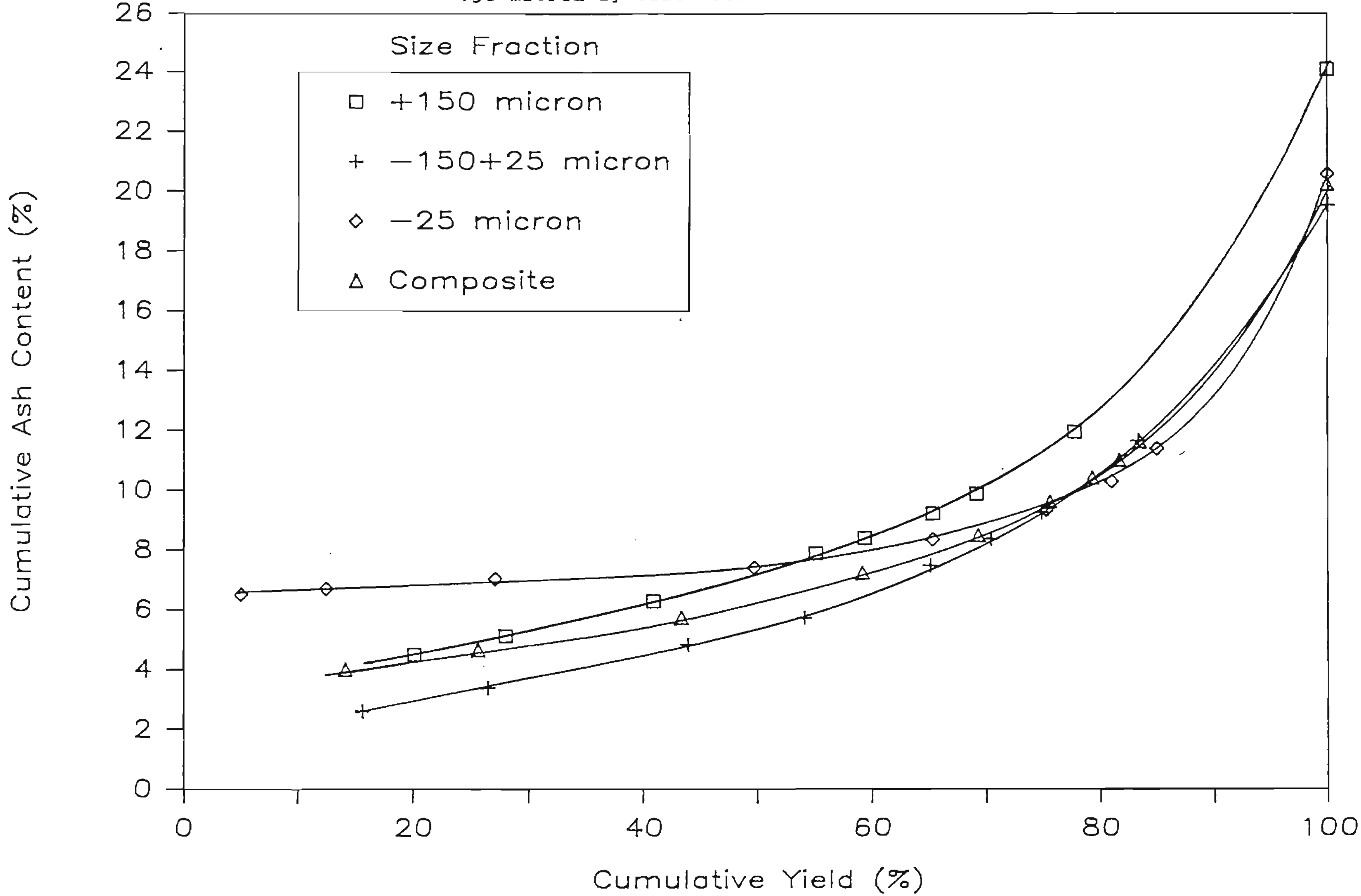

FIGURE 5.10 Washability curves of the thickener underflow sample by size fraction.

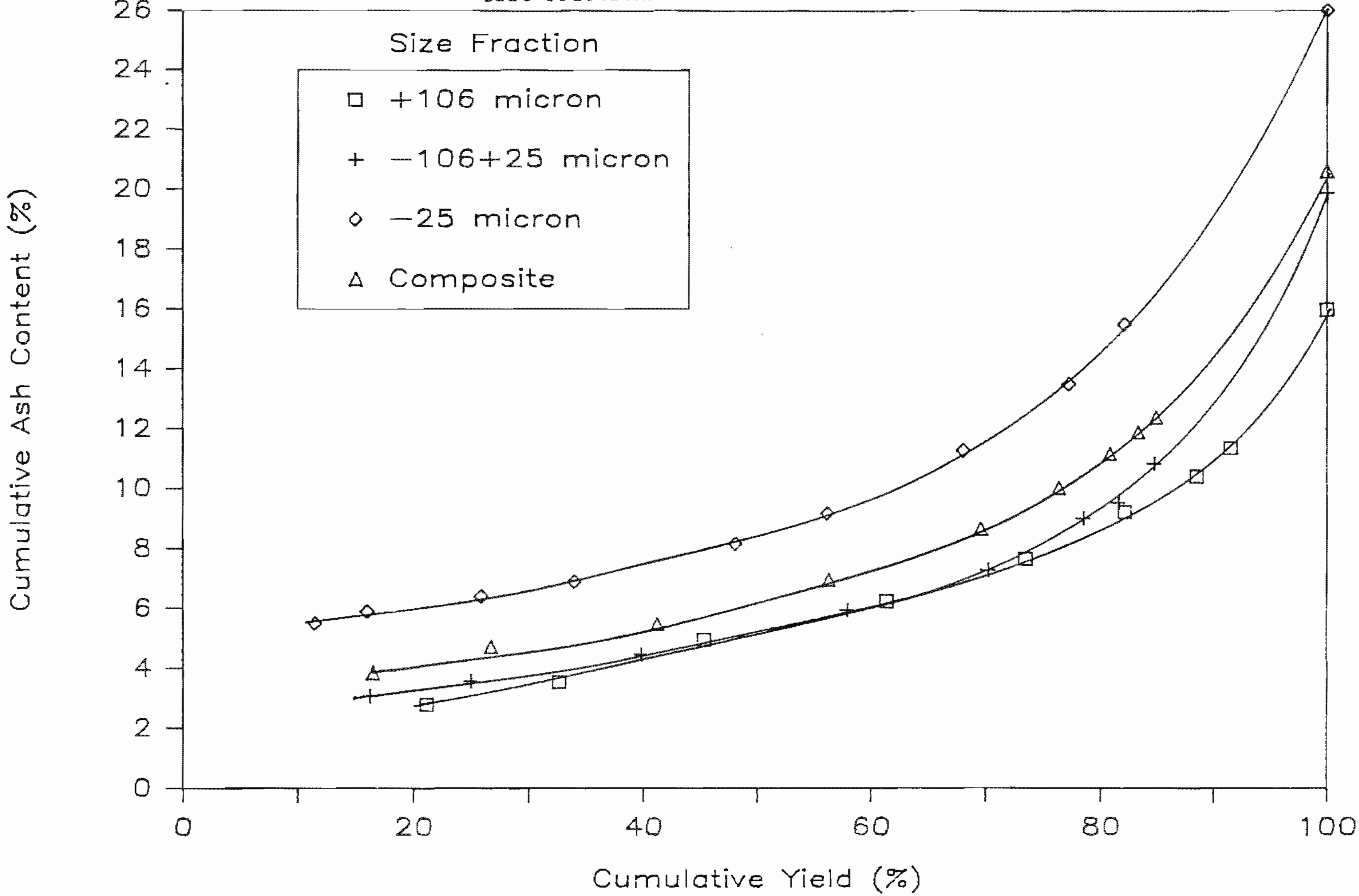

FIGURE 5.11 Comparison of the washability curves of the three composite samples.

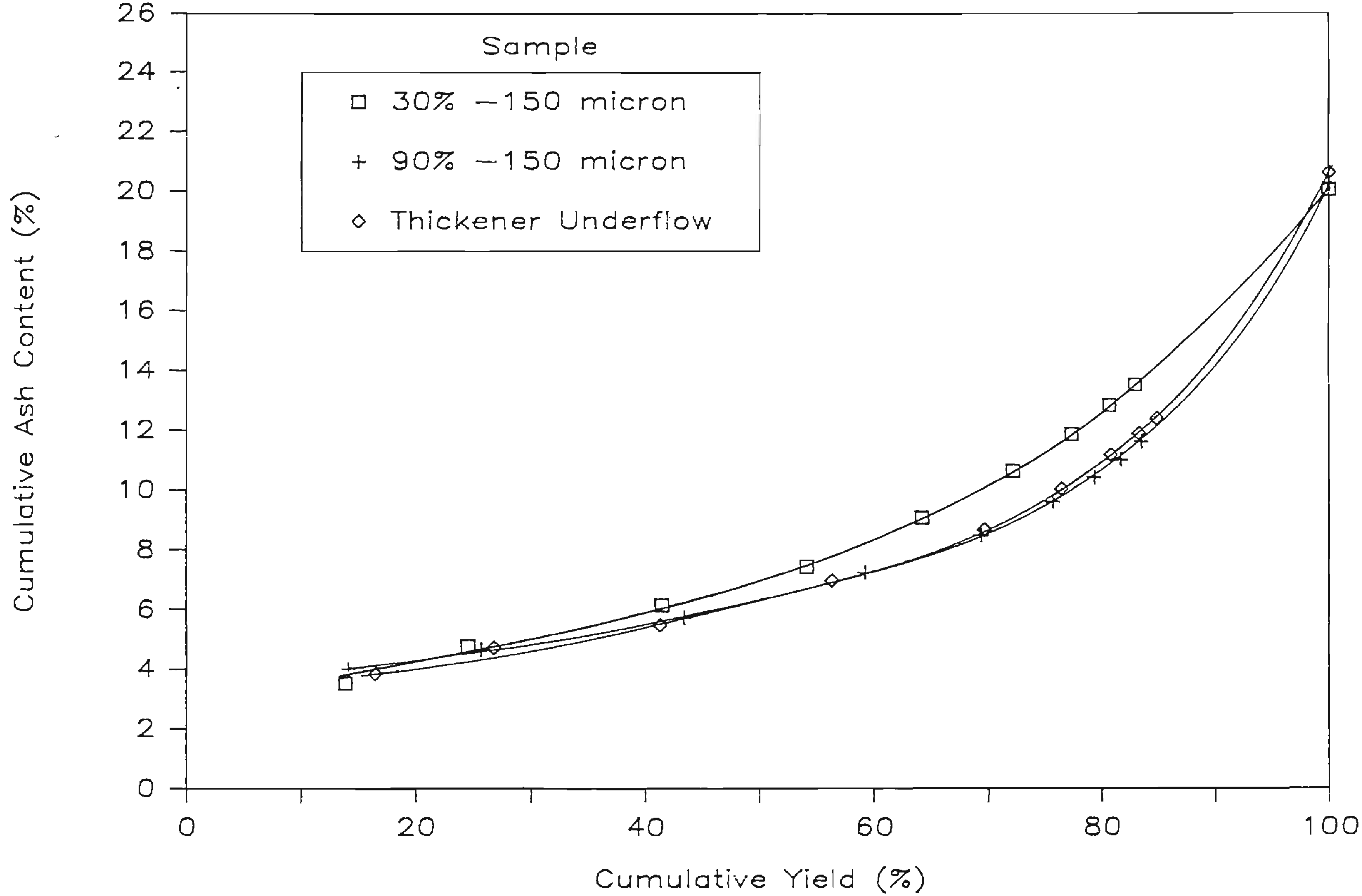

micron fraction lies above the curves of the other fractions and that of the composite sample, for an ash content below approximately 8 %. This implies that a lower yield will be obtained from the -25 micron fraction of a product with a particular ash content less than 8 %, than from any of the coarser size fractions. It is only for a product grade greater than approximately 12 % ash that the -25 micron fraction exhibits better washability characteristics than the other fractions.

The washability curves can be compared most easily by comparing the yields of coal of a particular grade that can be obtained from each size fraction. The predicted yields of coal of 7,4 % ash and 12,5 % ash for each of the samples are presented by size fraction in Table 5.2. An ash content of 7,4 % is a typical grade for low ash coal, while 12,5 % ash was chosen as a convenient point in the high yield region of the washability curves.

TABLE 5.2

The coal yield at 7,4 % ash and 12,5 % ash for the three samples by size fraction.

Sample	Size Fraction(μm)	Yield(%)	
		7,4 % Ash	12,5 % Ash
30 % -150 micron	Composite	53,2	79,7
	+150	50,6	77,4
	-150+ 25	65,8	86,4
	- 25	47,6	84,3
90 % -150 micron	Composite	63,0	85,7
	+150	51,1	78,7
	-150+ 25	64,3	85,4
	- 25	49,5	88,0
Thickener Underflow	Composite	62,5	84,8
	+106	71,5	93,4
	-106+ 25	70,3	88,6
	- 25	41,8	73,9

From Table 5.2 it can be seen that the milled samples show the same relationship between yield and size fraction for a particular grade of coal.

In the case of the low ash coal, the yield from the -150+25 micron size fraction is significantly higher than from the +150 micron fraction. This is consistent with the expectation of an increase in liberation with a decrease in particle size. However the yield from the -25 micron fraction is sharply lower, even lower than from the +150 micron fraction, which is contrary to expectation. This fraction, being the finest fraction, would be expected to be the most liberated, producing the highest yield of low ash coal.

In the case of the 12,5 % ash coal, the yield increases as the size fraction becomes finer, which conforms to the expectation of an increase in the liberation of the finer particle size fractions

5.4.2. Thickener Underflow

The washability curves of the thickener underflow and its size fractions are presented in Fig. 5.10. In this sample, the curve of the -25 micron size fraction lies well above the curves of the other size fractions over the entire range of yields, indicating that the washability characteristics of this fraction are considerably poorer in comparison with the other size fractions for any product ash specification. The +106 micron fraction exhibits slightly better washability characteristics than the -106+25 micron fraction up to a yield of approximately 80 %. Above this yield the

+106 micron fraction is markedly better as a result of the lower ash content of this size fraction.

The yields of coal at 7,4 % ash and 12,5 % ash of the thickener underflow and its size fractions are also presented in Table 5.2. For this sample the trend is the same for both products: the yield decreases as the particle size fraction becomes finer, with a particularly sharp decrease in the yield from the -25 micron fraction.

5.4.3. Composite Samples

A comparison of the washability curves of the three composite samples is presented in Fig. 5.11. It can be seen that the washability curve of the composite thickener underflow sample is almost identical to that of the sample milled to 90 % finer than 150 micron. It is only in the region of very low ash coal that the thickener underflow exhibits slightly improved washability characteristics. The washability curve of the sample milled to 30 % finer than 150 micron lies above the curves of the other two samples, indicating that the washability characteristics of this sample are significantly poorer.

An examination of Table 5.2 shows the extent of the improvement of the washability characteristics of the sample milled to 90 % finer than 150 micron over the sample milled to 30 % finer than 150 micron. The yield of low ash coal increases from 53,2 to 63,0 % and the yield of 12,5 % ash coal increases from 79,7 to 85,7 %. This indicates, as expected, an increase in liberation on further size reduction of the original sample.

5.4.4. Interpretation of the Results

From Table 5.2 it can be seen that the thickener underflow exhibits a different trend to the two milled samples with respect to yield of coal of a particular ash content. The main difference is the yield of low ash coal from the coarse fraction of the different samples. For the milled samples, this yield is very much lower than the yield from the intermediate size fraction. For the thickener underflow sample, the yield of low ash coal from the coarse fraction is slightly higher than the yield for the intermediate size fraction. In fact the +106 micron size fraction of the thickener underflow exhibits the best washability characteristics of all the samples. This can be explained by the very low ash content of this sample relative to the other size fractions, as a result of the removal of coarse unliberated gangue particles when the thickener underflow was passed through the classifying cyclone on the plant. Thus this size fraction has effectively been prewashed prior to the washability analysis.

The marked concentration of material in the intermediate relative density range of the −25 micron size fraction of all the samples was noted in section 5.3. This was ascribed to a concentration into this fraction during size reduction of either a heavy coal component (such as inertinite), or a light middling material. The latter possibility would imply that the −25 micron size fraction is less liberated than the other size fractions.

From Figs. 5.8 to 5.10 and Table 5.2 it can be seen that the −25 micron size fraction of all the samples gives a significantly lower yield of low ash coal than the other size fractions. This can only be explained by a concentration of middling material into the −25 micron size fraction. If the concentration of a heavier coal component was the only reason for the preponderance of intermediate density material in the -25 micron size fraction, then the yield of coal of a particular grade would either increase or remain constant as the size fraction examined became finer. Thus it appears from these results that the -25 micron size fraction is the least liberated size fraction.

While initially a lesser degree of liberation in the finest size fraction appears to be a serious contradiction of liberation theory, further consideration suggests that it is certainly possible. It is widely accepted that on fracture, many coals separate from the associated higher ash bands and intergrown impurities along the bedding planes (Sanders and Brookes, 1986). MacGregor (1983), during a study on the cuttability of South African coals, observed that the amount of mineral present in a coal significantly affected the grindability of the coal: the higher the percentage of mineral present in the coal, the more easily grindable it became. Taking these considerations into account, the following reason for the apparent decrease in the degree of liberation of the -25 micron size fraction relative to the other size fractions may be postulated.

Consider a large piece of run-of-mine coal that consists of both pure coal, with no mineral inclusions, and coal in which there is a high percentage of extremely fine clay particles intimately associated with the coal matrix. When such a particle is broken during a size reduction process, it is very possible that the clean regions of the particle would tend to separate from the mineral impregnated regions along the bedding planes within the coal matrix. During further size reduction, these pieces of clean coal would tend to break into relatively coarse fragments due to their higher structural strength, with relatively little -25 micron material produced. The clay rich pieces of the original particle, with the matrix weakened by the clay intrusions, would tend to break into a large number of very fine fragments during further size reduction, of which a substantial portion would tend to report to the -25 micron fraction. Since many of the clay particles range from a few microns to sub-micron in size (Stach, 1975), the fine fragments formed from the mineral rich regions of the coal would still remain substantially unliberated.

Examination of petrographic photographs of the coarser size fractions of some of the samples indicated that there were a large number of particles that would correspond to the hypothetical particle discussed above, i.e. they contained regions of relatively clean coal and regions where there was a large concentration of ultrafine syngenetic mineral inclusions.

Petrographic photographs of typical particles are shown in Fig. 5.12(a and b). Fig. 5.12(a) shows a particle from the +150 micron size fraction of the sample milled to 30 % finer than 150 micron. This shows a large vitrinite particle (grey) with regions of clean coal and regions that contain a high concentration of fine clay intrusions (brown flecks). Fig. 5.12(b) shows particles from the -150+106 micron size fraction of the same sample. This shows a clean vitrinite particle (dark grey) alongside an inertinite particle (off-white to light grey). The inertinite particle contains a large number of clay intrusions (dark flecks) distributed evenly throughout the particle.

Due to the difficulty of carrying out petrographic examination of -25 micron material, the presence of a high proportion of fine middling particles in this fraction could not be visually confirmed. Despite this, the apparent decrease in the liberation of the -25 micron size fraction relative to the coarser fractions presents no logical

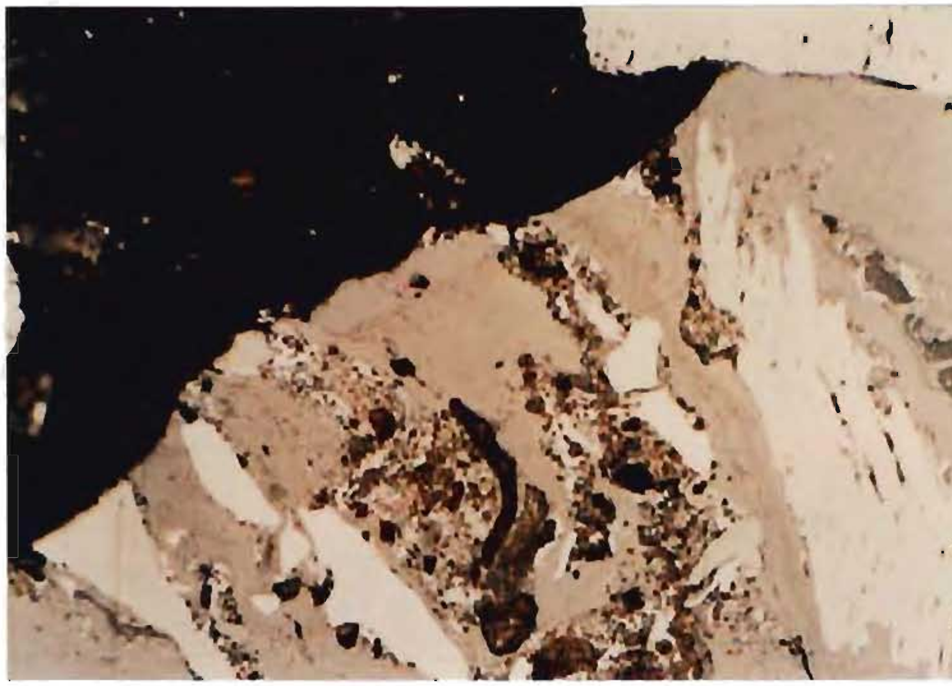

FIGURE 5.12(a) Petrographic photograph of particles in the +150 micron size fraction of the sample milled to 30 % finer than 150 micron.

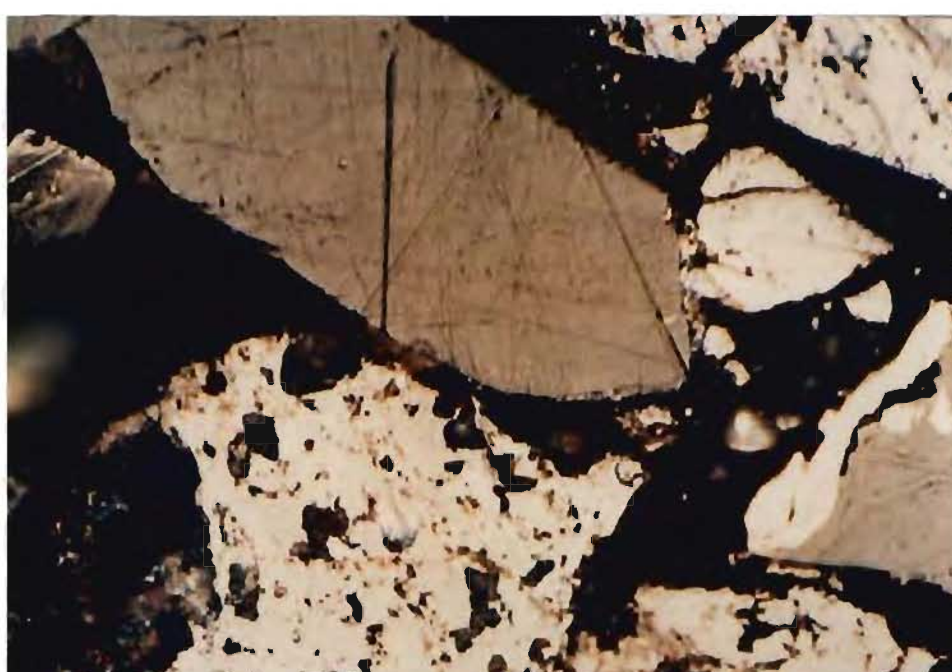

FIGURE 5.12(b) Petrographic photograph of particles in the -150+106 micron size fraction of the sample milled to 30 % finer than 150 micron.

difficulties with respect to conventional liberation theory if the factors discussed above are taken into account. This implies that during size reduction of complex heterogeneous material, such as this coal, the increase in the liberation of the overall sample could be accompanied by a decrease in the liberation of a particular fraction, in this particular case the finest fraction.

5.5. Petrographic Analysis

This section presents the results of petrographic analyses of the samples, some of the sample size fractions and some of the relative density fractions of the size fractions. All the analyses were performed by Falcon Research Laboratories.

It should be remembered that the accuracy of the petrographic analysis of a coal sample becomes limited if the sample is too fine. In this work considerable difficulty was experienced in the analysis of -25 micron material. Thus where petrographic analysis data of this size fraction is presented, these values can only be considered as estimates, particularly with respect to the distinction between reactive and non reactive inertinite. The distinction between vitrinite and non- vitrinite in this size fraction should be reasonably reliable.

All the petrographic analyses presented in this section, maceral or microlithotype, are on the basis of the ratio of the volume of a particular organic species to the total volume of organic material in the sample, expressed as a percentage.

5.5.1. Petrographic Characterization of the Coal

The Witbank No 2 seam coal mined by the Greenside Colliery is classified as a High Volatile Bituminous B blend coking coal. The average rank, vitrinite content and percent reactives are presented in Fig. 5.13. Maceral analyses of the samples milled to 30 % and 90 % finer than 150 micron and of the thickener underflow, are presented in Table 5.3.

TABLE 5.3

Maceral analyses of the samples milled to 30 % and 90 % finer than 150 micron and of the thickener underflow.

Sample	Vitrinite (%)	Exinite (%)	Inertinite Reactive (%)	Inertinite Non-reactive (%)	Total Reactive (%)
30% −150µm	25,5	2,4	18,5	53,5	46,4
90% −150µm	29,8	4,2	12,0	54,0	46,0
Thickener Underflow	31,3	1,6	14,4	52,7	47,3

The two milled samples were subsamples of the same original run-of-mine material, so the maceral analyses of these two samples should be the same. In Table 5.3 it can be seen that the analyses show a small discrepancy with respect to the amount of vitrinite and reactive inertinite in the two samples. However the percent reactives in both samples is almost identical. The analysis of the thickener underflow is very similar to that of the other two samples. In the light of the small discrepancy between the two milled samples, the differences in the maceral distribution of the thickener underflow can be regarded as insignificant. Thus for practical purposes the maceral distribution in all three samples can be considered to be the same.

FIGURE 5.13 The average rank analysis of the -10+6 mm coal sample in relation to reactive/inert organic composition.

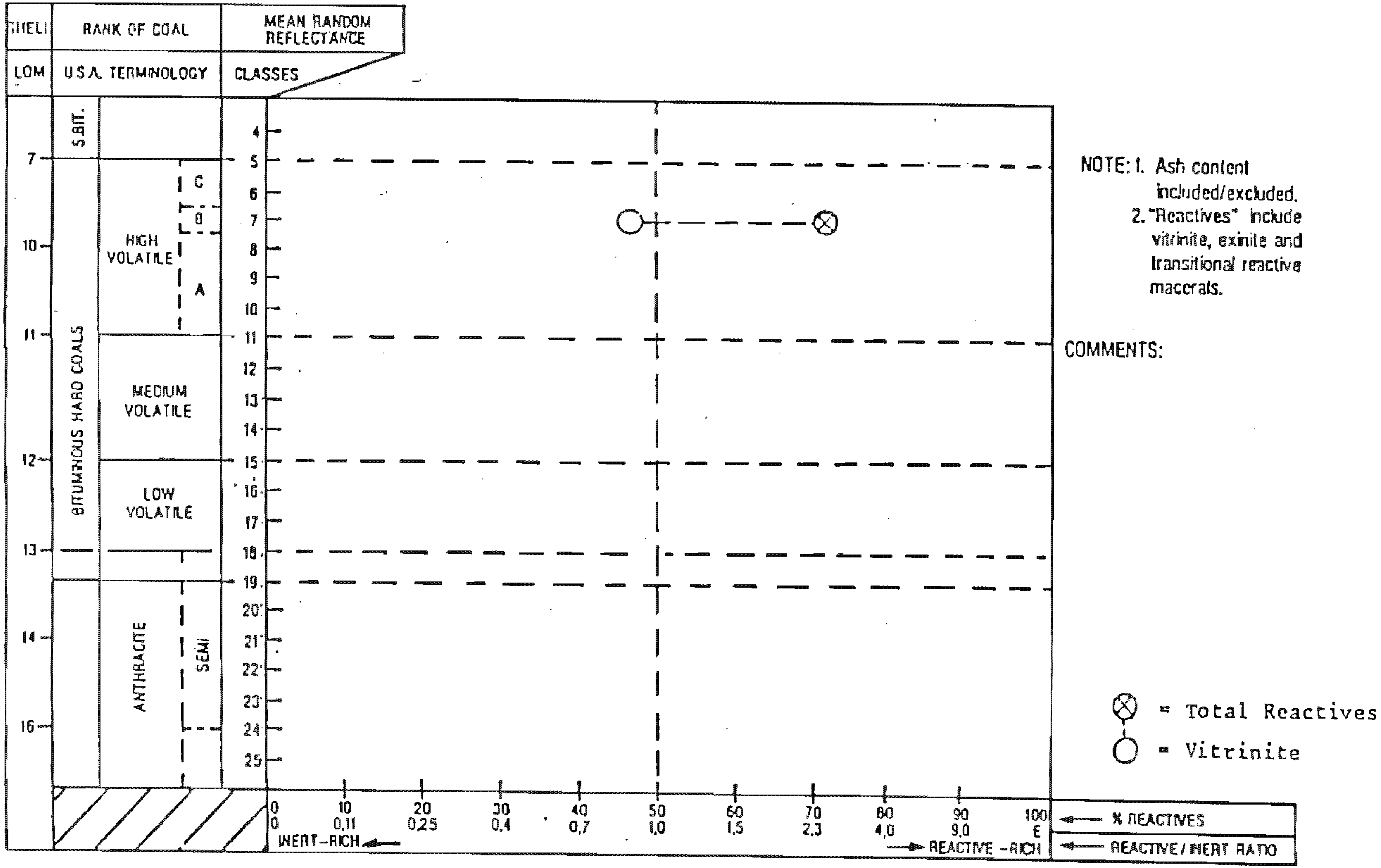

The minerals present in the coal were predominantly clays, which formed about 80 % of the inorganic material by volume. These existed mostly as very small particles finely distributed within the coal matrix (see Fig. 5.12). The balance of the minerals consisted mainly of carbonates. Pyrite formed only about 3 % of the minerals present.

5.5.2. Petrographic Analysis of the Size Fractions

The results of the petrographic analyses carried out on the size fractions of the two milled samples and on the thickener underflow are presented in Appendix E. For petrographic analysis, the two milled samples were split into five size fractions, namely +150, -150+106, -106+53, -53+25 and -25 micron. Since no marked differences were observed between the analyses of the three intermediate size fractions of the two milled samples, the thickener underflow was split into only three size fractions, namely +106, -106+25 and -25 micron.

The results of the analyses of the three samples are presented graphically in Fig. 5.14 by size fraction. The data in Fig. 5.14 have been presented as though they were continuous in order to facilitate comparison of the maceral distribution of the size fractions of the three samples.

From Fig. 5.14 it can be seen that there is no marked variation in the maceral distribution of the size fractions above 25 micron in any of the samples. However all three samples exhibit a decrease in the vitrinite content of the -25 micron fraction compared to the other size fractions, with a corresponding increase in the inertinite content. This decrease is most marked in the thickener underflow,

FIGURE 5.14 The maceral content of the three samples by size fraction.

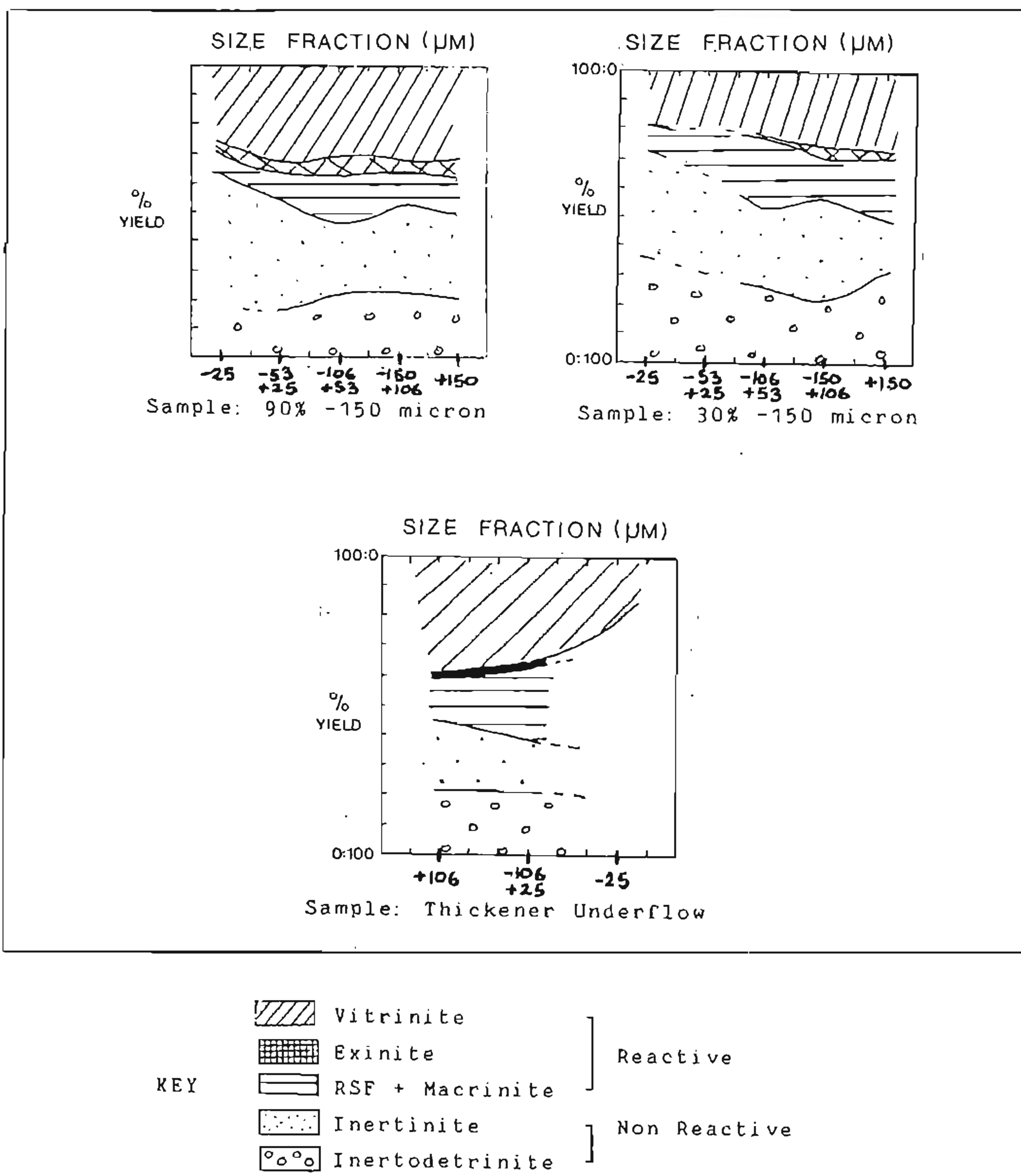

where the vitrinite content of the -25 micron fraction is about half of that of the other size fractions.

The concentration of inertinite into the finest size fraction during size reduction has also been observed by Birtek and King (1986) in an investigation of the liberation characteristics of a number of South African coals. It was found that this phenomenom generally occurred.

It was argued above (section 5.4.4.) that the concentration of intermediate relative density material into the -25 micron fraction as observed in Figs. 5.3 to 5.6 is due to the concentration of fine middling particles into this fraction. However the results of the petrographic analysis of the size fractions of the three samples indicates that there is also a concentration of inertinite into the -25 micron fraction. Thus the concentration of intermediate relative density material into the -25 micron size fraction is the result of both a concentration of middling material and inertinite into this size fraction.

5.5.3. Petrographic Washability Characteristics

As described in section 2.3.3.3., petrographic washability analysis determines the maceral distribution with respect to relative density for a particular sample. For this investigation petrographic washability analyses were carried out on the samples milled to 30 % and 90 % finer than 150 micron and on the thickener underflow. The two milled samples were split into four size fractions, namely -150+106, -106+53, -53+25 and -25 micron. The thickener underflow was split into three size fractions, namely +106, -106+25 and -25 micron. Each of these size fractions was split into five relative density fractions by heavy liquid separation, and a petrographic analysis was performed on each of the relative density fractions.

The detailed results of these analyses are presented in Appendix F. Maceral analyses were performed on all the samples. In addition microlithotype analyses were performed on the relative density fractions of the sample milled to 30 % finer than 150 micron and on the thickener underflow. While the microlithotype data of these samples are not discussed in this thesis, the data are included in Appendix F for completeness.

Figs. 5.15, 5.16 and 5.17 present the petrographic washability curves of the size fractions of the samples milled to 30 % and 90 % finer than 150 micron, and of the thickener underflow, respectively. The maceral content is plotted against the relative density for each of the size fractions. Although the data were obtained by analysing each individual relative density fraction, the data are presented as though they were continuous for ease of comparison.

The petrographic washability curves in Figs. 5.15 to 5.17 can be used to assess the degree of liberation of the organic constituents obtained during size reduction. The degree of group maceral liberation is indicated by the sharpness of the separation between the lighter coal component (vitrinite, R.D. 1,3 to 1,35) and the heavier coal components (inertinite, which includes reactive semifusinite and macrinite).

5.5.3.1. Milled Samples

As may be seen from Fig 5.15, which shows the petrographic washability of the size fractions of the sample milled to 30 % finer than 150 micron, there is a clear increase in the

FIGURE 5.15 Petrographic washability curves of the sample milled to 30 % finer than 150 micron by size fraction.

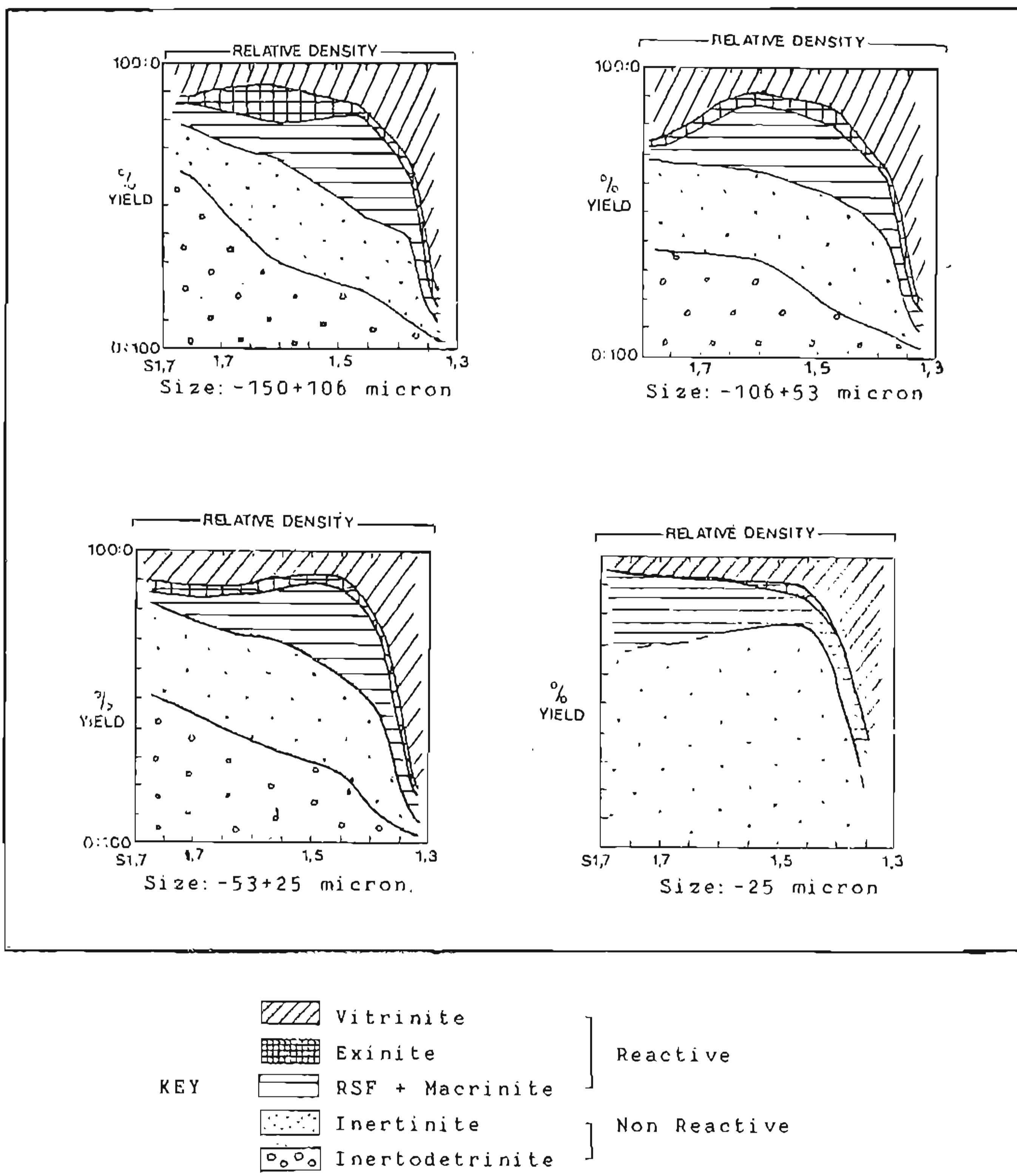

FIGURE 5.16 Petrographic washability curves of the sample milled to 90 % finer than 150 micron by size fraction.

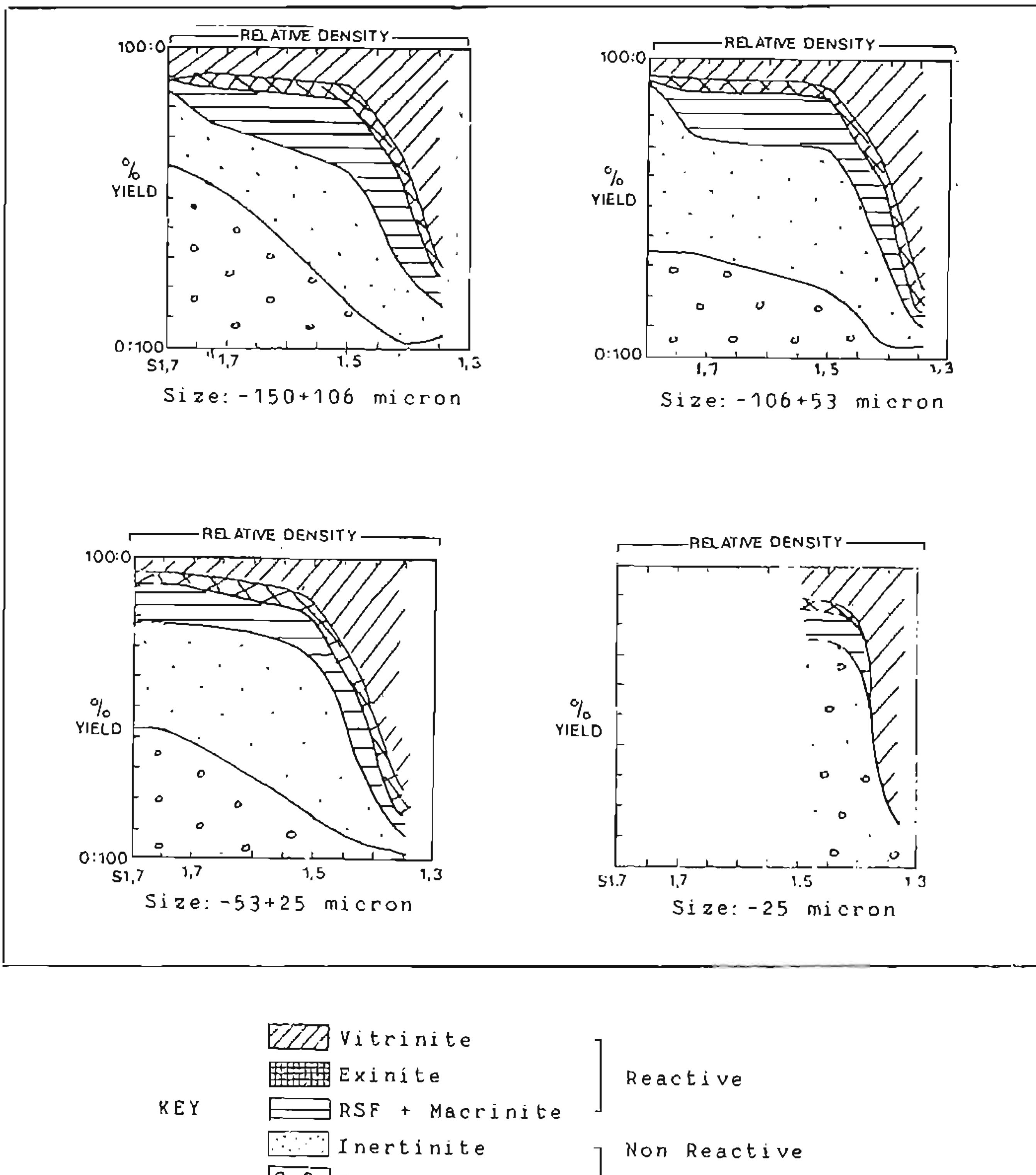

FIGURE 5.17 Petrographic washability curves of the thickener underflow sample by size fraction.

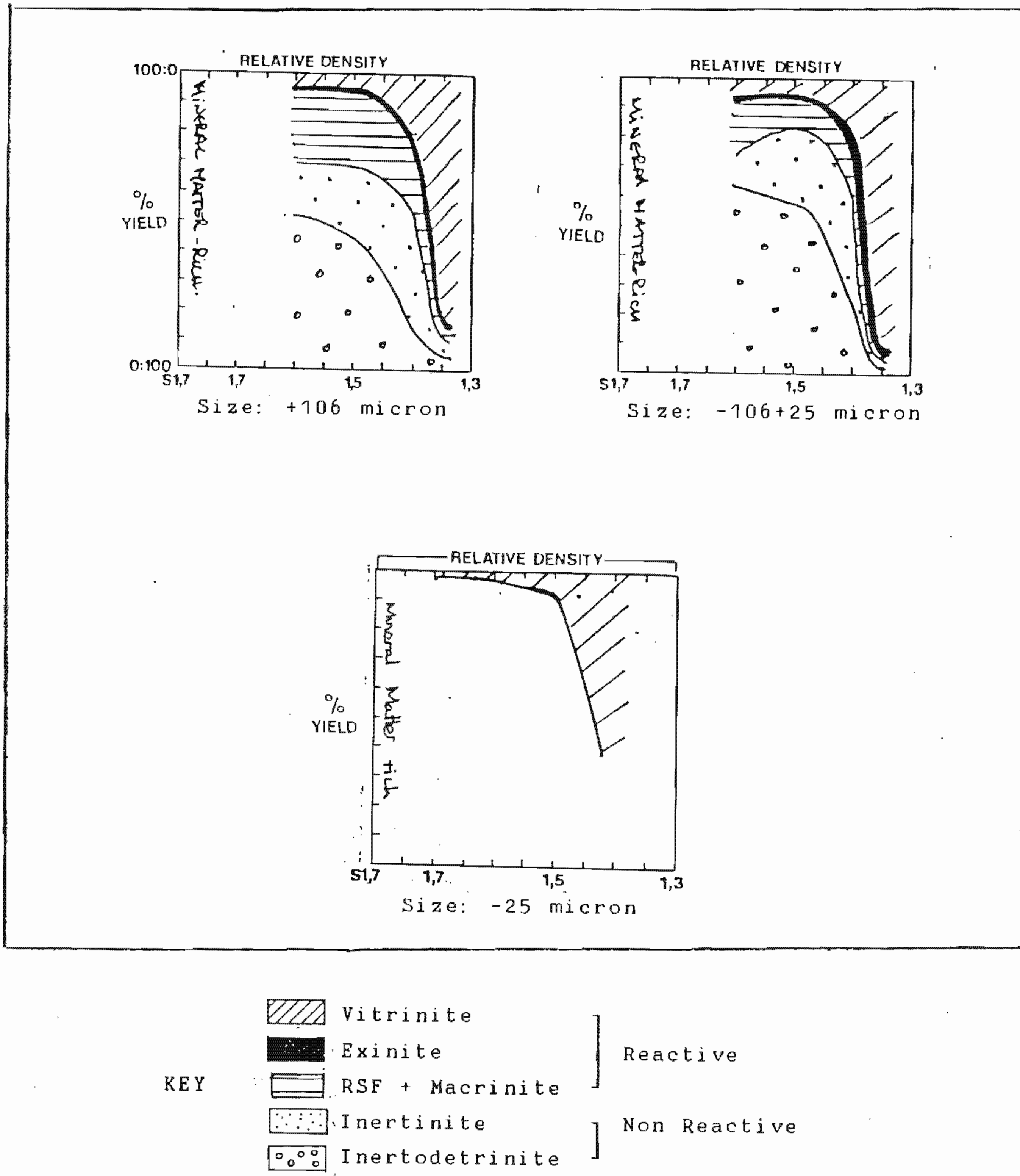

liberation of vitrinite relative to the more dense inertinite macerals as the average particle size decreases. The vitrinite content of the floats at relative density 1,35 is very high in all the size fractions, but as the average particle size decreases there is a significant decrease in the amount of vitrinite present in the higher relative density fractions.

It can also be seen that the exinite macerals, which have a relative density between 1,1 and 1,2, show no tendency to concentrate in any particular density fraction, but remain associated with the other macerals over the entire relative density range.

The petrographic washability curves of the size fractions of the sample milled to 90 % finer than 150 micron, shown in Fig. 5.16, exhibit very much the same trend as that observed in Fig. 5.15. However, in this sample the amount of vitrinite present in the high relative density fractions of the coarse size fractions has decreased as a result of the further size reduction of the sample. Also the separation of the vitrinite in the -25 micron fraction is very sharp, indicating that there is very good maceral liberation in this size fraction. Once again the exinite macerals remain substantially unliberated, despite the lower average particle size of the sample.

5.5.3.2. Thickener Underflow

The petrographic washability curves for the three size fractions of the thickener underflow sample are presented in Fig. 5.17. Unfortunately problems were experienced in the analysis of the -25 micron fraction, so the curve that has been presented for this size fraction is of little value. However in the other two size fractions it can be seen that the vitrinite liberation is very good, with a small but clear increase in the sharpness of the vitrinite separation of the -106+25 micron size fraction relative to the +106 fraction. In both size fractions there is very little vitrinite present in the relative density fractions above 1,35.

As observed in the milled samples, the exinite macerals remain substantially unliberated.

5.5.3.3. Discussion

In the different size fractions of all the samples, the degree of liberation of the vitrinite is relatively high, and it improves as the size fraction becomes finer. The separation of the vitrinite in the thickener undeflow sample is particularly good, probably due to the relative fineness of this sample.

The very good vitrinite separation in the -25 micron material indicates that although this size fraction contains significantly less vitrinite than the coarser size fractions (see section 5.5.2), the vitrinite that is present is very well liberated. The fact that most of the vitrinite reports to the Floats 1,35 relative density fraction suggests that there is relatively little mineral associated with the vitrinite. Thus, as suggested in section 5.5.2., the middling particles that are concentrated into the -25 micron size fraction consist predominantly of intimate associations of inertinite and clay.

The concentration of inertinite into the -25 micron size fraction is an apparent contradiction of the breakage behaviour that is predicted by the physical properties of the inertinite and vitrinite group macerals. Inertinite is tougher than vitrinite, and it would therefore be expected that the vitrinite would be more likely to concentrate into the −25 micron fraction. However, if the minerals are predominantly associated with the inertinite macerals, this would substantially reduce the strength of these macerals during size reduction. The relatively clean vitrinite would therefore be stronger than the inertinite-mineral association.

The exinite macerals remain substantially unliberated in the size fractions of all the samples. This is probably due to the fact that the exinite macerals are much tougher than the other maceral groups, and they tend to increase the strength of the coal bands in which they are associated (Falcon, 1984).

5.6. Quantitative Assessment of Liberation

5.6.1. Introduction

As discussed in section 2.3.3.4., float and sink analysis data can be presented in the form of an M-curve. The cumulative percent yield is plotted against the product of cumulative percent yield and cumulative ash content, this product being termed ash per hundred units of feed (Dell, 1957).

In this form, the data can be used to quantify the degree of liberation of a particular sample. The method used was that proposed by Birtek (1980) and used by Birtek and King (1984, 1986) in a study of the liberation characteristics of a number of South African coals.

The M-curve data for the size fractions of the two milled samples and of the thickener underflow is presented in

Appendix D. Each set of data was fitted to a function of the form (Birtek and King, 1984):

$$Y = A.X^{B}.e^{CX} + MX \qquad (5.3)$$

Where: Y = Ash per 100 units of feed (0 to 1)
X = Yield (0 to 1)
A,B,C,M = Function parameters (by nonlinear regression).

Least squares best estimates of the parameters A, B, C and M were obtained by nonlinear regression analysis of the experimental data. The function parameters and the sum of the error squared for each set of data are presented in Table 5.4. The data and fitted curves of the samples milled to 30 % and 90 % finer than 150 micron and of the thickener underflow are presented in Figs. 5.18, 5.19 and 5.20 by size fraction, respectively. A comparison of the M-curves of the three composite samples is presented in Fig. 5.21.

It can be seen in Table 5.4 and in Figs. 5.18 to 5.20 that equation (5.3) generally fits the data very well. For two of the samples (-25 micron fraction of the 30 % sample and the +106 micron fraction of the T/U sample) a relatively high error was obtained. This is due to the nature of the function, which overestimates the Y values in the low yield region when the ash content decreases very sharply in the high yield region. However, an examination of Figs. 5.18 to 5.20 indicates that even in the worst cases, Equation (5.3) fits the data adequately.

FIGURE 5.18 M-Curves of the sample milled to 30 % finer than 150 micron by size fraction.

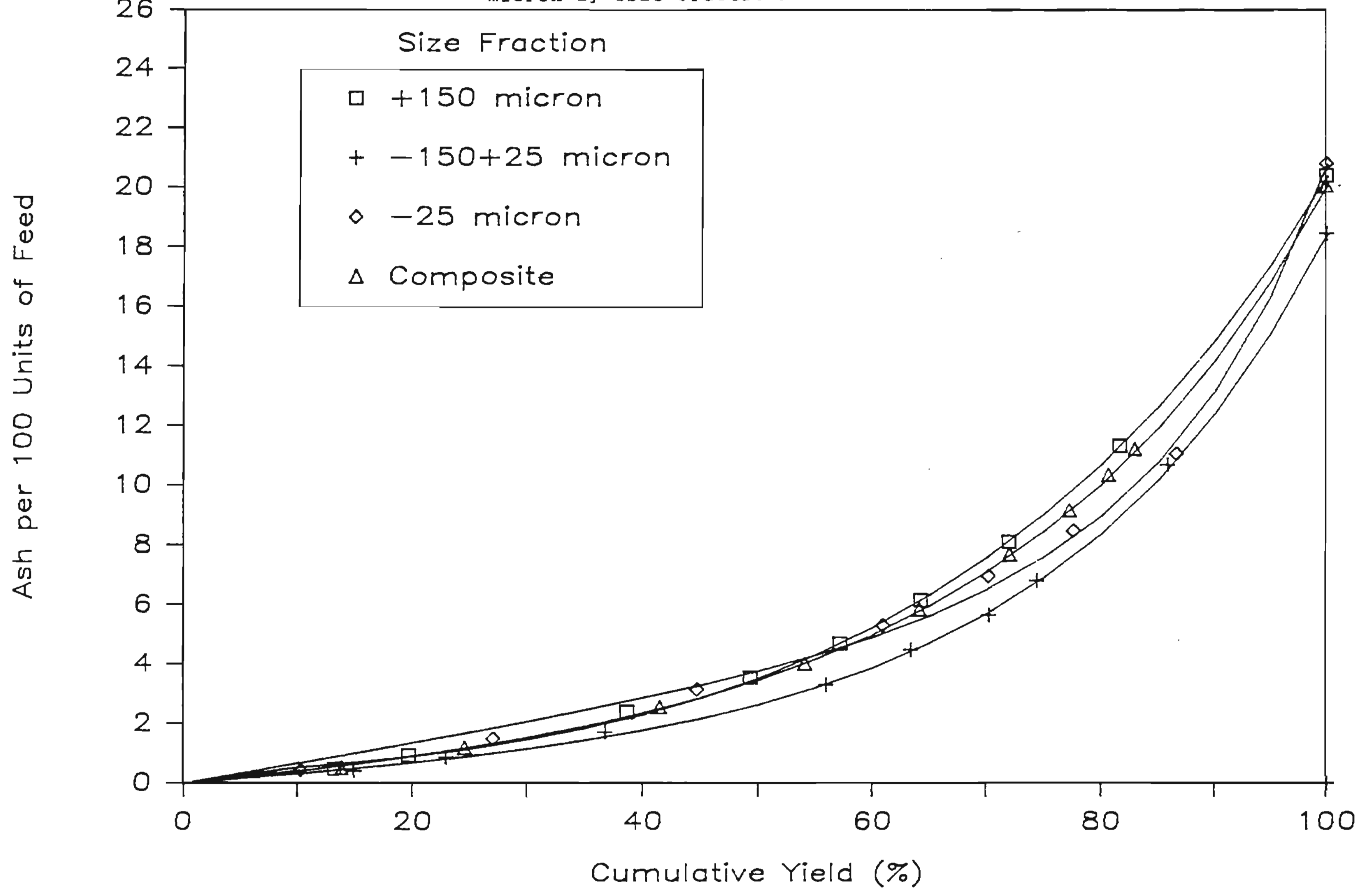

FIGURE 5.19 M-Curves of the sample milled to 90 % finer than 150 micron by size fraction.

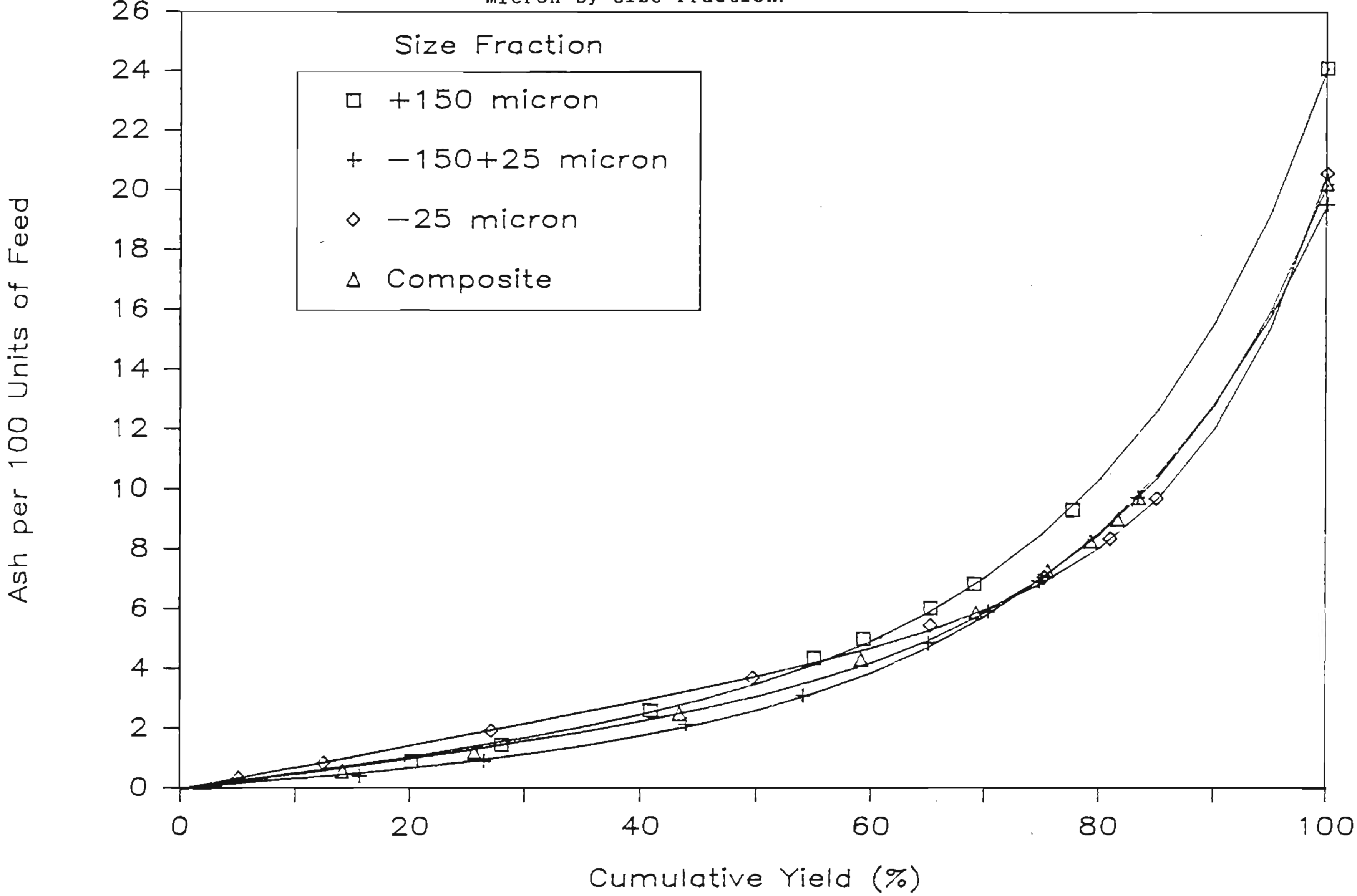

FIGURE 5.20 M-Curves of the thickener underflow sample by size fraction.

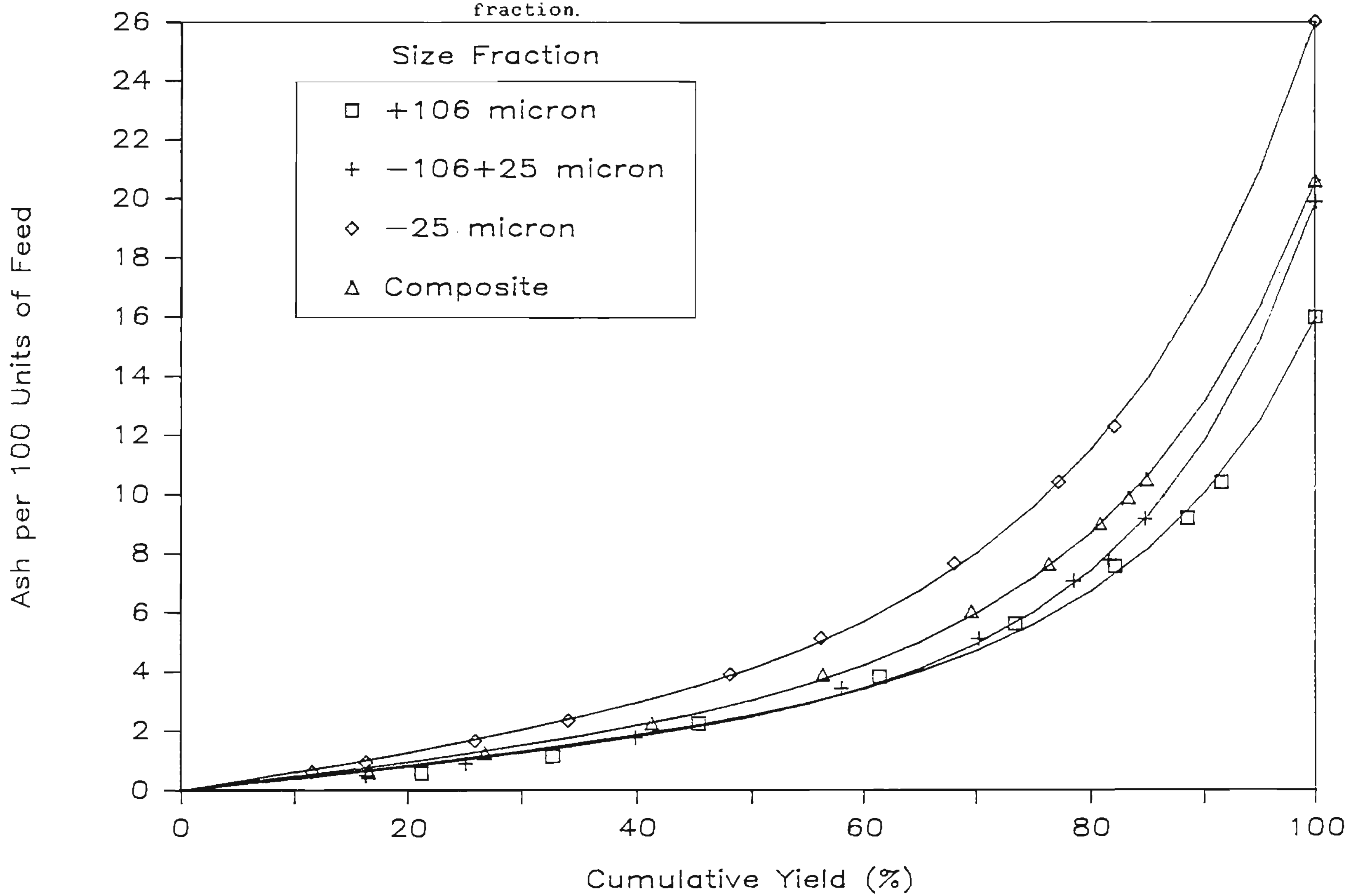

FIGURE 5.21 A comparison of the M-Curves of the three composite samples.

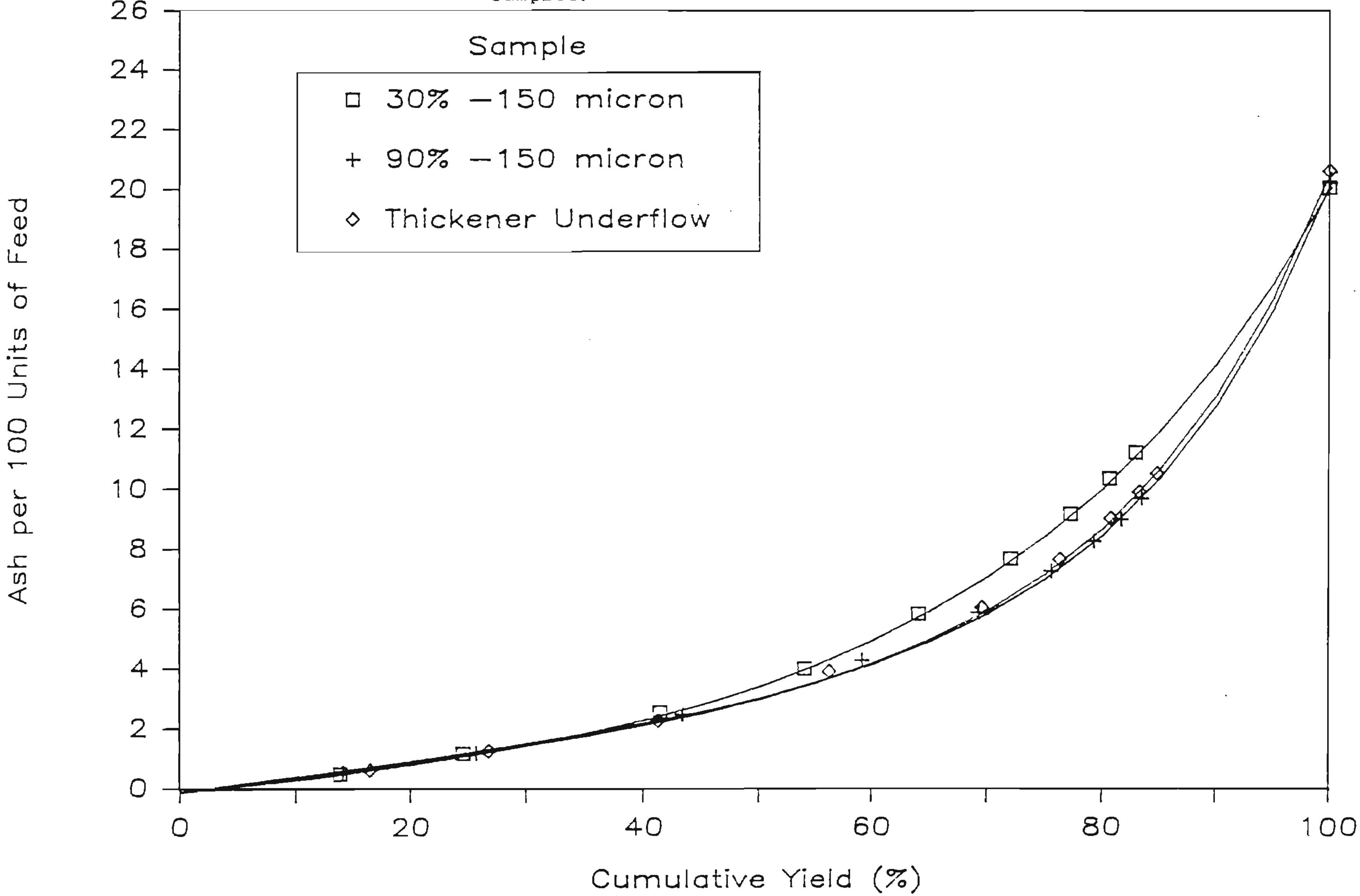

TABLE 5.4

Curve fit parameters for Equation (5.3) for the samples milled to 30 % and 90 % finer than 150 micron, and for the thickener underflow, by size fraction.

Sample	Size Fraction (micron)	A ($\times 10^3$)	B ($\times 10$)	C	M ($\times 10^2$)	Error² ($\times 10^6$)
30 %	+150	31,14	5,671	2,082	-4,921	9,07
less	-150+ 25	4,002	6,531	3,713	2,101	7,20
than	- 25	0,2378	2,753	6,382	6,656	70,91
150 µm	Composite	9,447	9,391	2,907	2,793	2,22
90 %	+150	1,392	2,898	4,954	4,349	15,24
less	-150+ 25	2,894	4,145	4,108	1,914	6,41
than	- 25	0,1028	16,42	7,161	7,336	4,66
150 µm	Composite	0,6926	4,466	5,411	4,704	12,01
Thick-	+106	0,4406	3,924	5,585	4,056	69,20
ener	-106+ 25	0,3156	2,203	6,231	3,846	16,47
Under-	- 25	2,339	8,169	4,455	5,848	9,54
flow	Composite	0,9808	4,524	5,111	4,314	10,93

The slope of the M-curve gives the instantaneous grade: differentiating equation (5.3) gives:

$$\text{Ash content} = \frac{dY}{dX} = A.e^{CX}\ (C.X^{B} + B.X^{B-1}) + M \qquad (5.4)$$

At $X = 0$:

$$\frac{dY}{dX} = M \qquad (5.5)$$

Therefore the function parameter M is the lowest ash content of coal concentrate, and represents a limiting value for any coal particle. In Table 5.4 it can be seen that the values of M vary between 1,9 and 7,3 percent. The negative value of M for the +150 micron size fraction of the sample milled to 30 % finer than 150 micron, while no problem mathematically, is clearly physically impossible. It was decided not to force the parameter M to be positive in the curve fitting routine, as the best possible curve fit was required for the liberation efficiency calculations.

As expected from the results already presented in this chapter, the values of M for the -25 micron size fraction of each of the samples is considerably higher than the values for the other size fractions, indicating that the particles in this size fraction have a considerably higher minimum ash content than the coarser size fractions.

5.6.2. Liberation Efficiency of the Samples

The liberation efficiencies of the three samples were calculated using the method described in section 2.3.3.4. These values are presented in Table 5.5 by size fraction. For purposes of comparison, the ash content and the yield of low ash coal (7,4 % ash; cf Table 5.2) have also been included.

In Table 5.5 it can be seen that, as expected, the liberation efficiency of the composite sample milled to 90 % finer than 150 micron is greater than that of the composite sample milled to 30 % finer than 150 micron. However the increase in the liberation efficiency is only 7,03 percent, despite the substantial decrease in the mean particle size of the sample. The liberation efficiencies of the thickener underflow and the sample milled to 90 % finer than 150 micron are almost exactly the same.

The liberation efficiencies of the size fractions of the three samples do not follow any clear trend. In the sample milled to 30 % finer than 150 micron, the liberation efficiency of the coarse size fraction is the lowest. The liberation efficiencies of the intermediate and -25 micron size fractions are very close, with the former slightly higher. The size fractions of the thickener underflow follow the same trend. In the sample milled to 90 % finer than 150 micron, however, the coarse size fraction has the highest liberation efficiency. The liberation efficiencies of the intermediate and -25 micron fractions are again very similar, with the former slightly higher.

In each of the samples, the liberation efficiencies of the -25 micron size fractions are higher than expected in the light of the poor washability characteristics exhibited by these fractions.

TABLE 5.5

Liberation Efficiency, ash content and yield of low ash coal (L.A.C., 7,4 % ash) of the samples milled to 30% and 90% finer than 150 micron, and of the thickener underflow, by size fraction.

Sample	Size Fraction (micron)	Liberation Efficiency (%)	Ash Content (%)	L.A.C. Yield (%)
30 % less than 150 µm	+150	55,20	20,4	50,6
	-150+ 25	61,74	16,8	65,8
	- 25	60,14	20,8	47,6
	Composite	56,91	20,1	53,2
90 % less than 150 µm	+150	67,62	24,1	51,1
	-150+ 25	64,42	19,5	64,3
	- 25	63,06	20,6	49,5
	Composite	64,00	20,2	63,0
Thickener Underflow	+106	59,29	16,0	71,5
	-106+ 25	69,75	19,9	70,3
	- 25	66,69	26,0	41,8
	Composite	64,63	20,6	62,5

5.6.3. Discussion

The definition of liberation used in the analysis of most mineral systems was discussed in section 2.3.1. This was the definition first proposed by Gaudin (1939), in which the degree of liberation of a certain mineral was defined as the percentage of that mineral occurring as free particles in relation to the total of that mineral occuring in free and locked forms. In section 2.3.1. it was pointed out that according to this definition, the degree of liberation of most South African coals would be zero, even after considerable size reduction.

For coal, where a product of a specific grade is required, a sample with no liberation by Gaudin's definition could give a very high yield of saleable product. Thus the analysis in this section is an attempt to compare the samples by their degree of "partial liberation". However this does not take into account the nature of the liberation that is occurring.

Two samples of coal could both be 50 % partially liberated, with the one sample containing 50 % ash-free coal and 50 % unliberated particles, while the other sample contains 100 % partially liberated particles. The yield of a particular product from each of these samples could be very different, particularly in the production of L.A.C.

This effect is apparent when the liberation efficiencies of the -25 micron size fractions are examined. The relatively high liberation efficiency of the -25 micron size fraction of each of the samples appears to contradict the relatively poor washability characteristics exhibited in each case by this size fraction. However an examination of Figs 5.8 to 5.10 and Table 5.2 shows that it is only in the production of low ash coal that the -25 micron samples exhibit poor washability characteristics. For a coal product of 12,5 % ash, very high yields are possible. Thus the −25 micron fraction contains relatively few heavy middling particles, a large proportion of light middlings and free ash, and very few clean coal particles.

The comparison of the liberation efficiencies of the samples is further complicated by the influence of the feed ash of each of the samples. If two samples have a liberation efficiency of 50 %, the first with a feed ash of 20 % and the second with a feed ash of 30 %, the yield of coal of a particular grade will again be very different. Thus for a comparison of the liberation efficiencies of two samples to be meaningful, their feed ash must be about the same.

It can be concluded that quantifying the liberation of a sample by size fraction using this method yields little useful information. It can however be used to quantify the degree of liberation as the mean particle size of the sample is reduced.

5.7. Ash Content as a Function of Relative Density

As discussed in section 2.3.3.5, if coal was considered to consist of a single coal component and an ash component, the relationship between ash content and the inverse of relative density would be linear. However it has been shown (Panopoulos and King, 1983; Birtek and King, 1984, 1986) that South African coals typically show a relationship between ash and relative density that is best fitted by two straight lines. This is best explained by considering the coal particle as a three component system, consisting of one ash component and two coal components. This can be accounted for by the presence of significant amounts of both vitrinite and inertinite in many South African coals.

Since Greenside No 2 seam coal typically consists of an ash to/vitrinite to inertinite ratio of 15:25:60 (volume basis), it can be expected that the relationship between ash and inverse relative density for this coal will also be well represented by two straight lines.

The data and fitted lines of the samples milled to 30 % and 90 % finer than 150 micron and of the thickener underflow are presented in Figs. 5.22, 5.23 and 5.24 by size fraction, respectively. A comparison of the three composite samples is presented in Fig. 5.25.

The linear regression coefficients for each of the samples and the predicted relative densities of the different coal, ash and mineral fractions (see equations 2.3, 2.4 and 2.5 in section 2.3.3.5.) are presented in Tables 5.6 and 5.7 by size fraction, respectively. The predicted relative density of the mineral matter was calculated using a mineral matter to ash ratio of 1,16 (Savage, 1967).

5.7.3. Discussion

From an examination of Figs. 5.22 to 5.24, it is apparent that the data can be well represented by two straight lines. The correlation coefficients, presented in Table 5.6, are in most cases very high.

In order to explain the scatter of some of the data, it is necessary to point out that a point on the graph represents the ash content of material that contains particles with a range of relative densities. Conversion of the discrete data to continuous data by taking the arithmetic mean of the relative density range could lead to error where the density interval is large, or where the distribution of particle densities in a particular range is uneven.

FIGURE 5.22 The ash content as a function of the inverse of relative density for the sample milled to 30 % finer than 150 micron by size fraction.

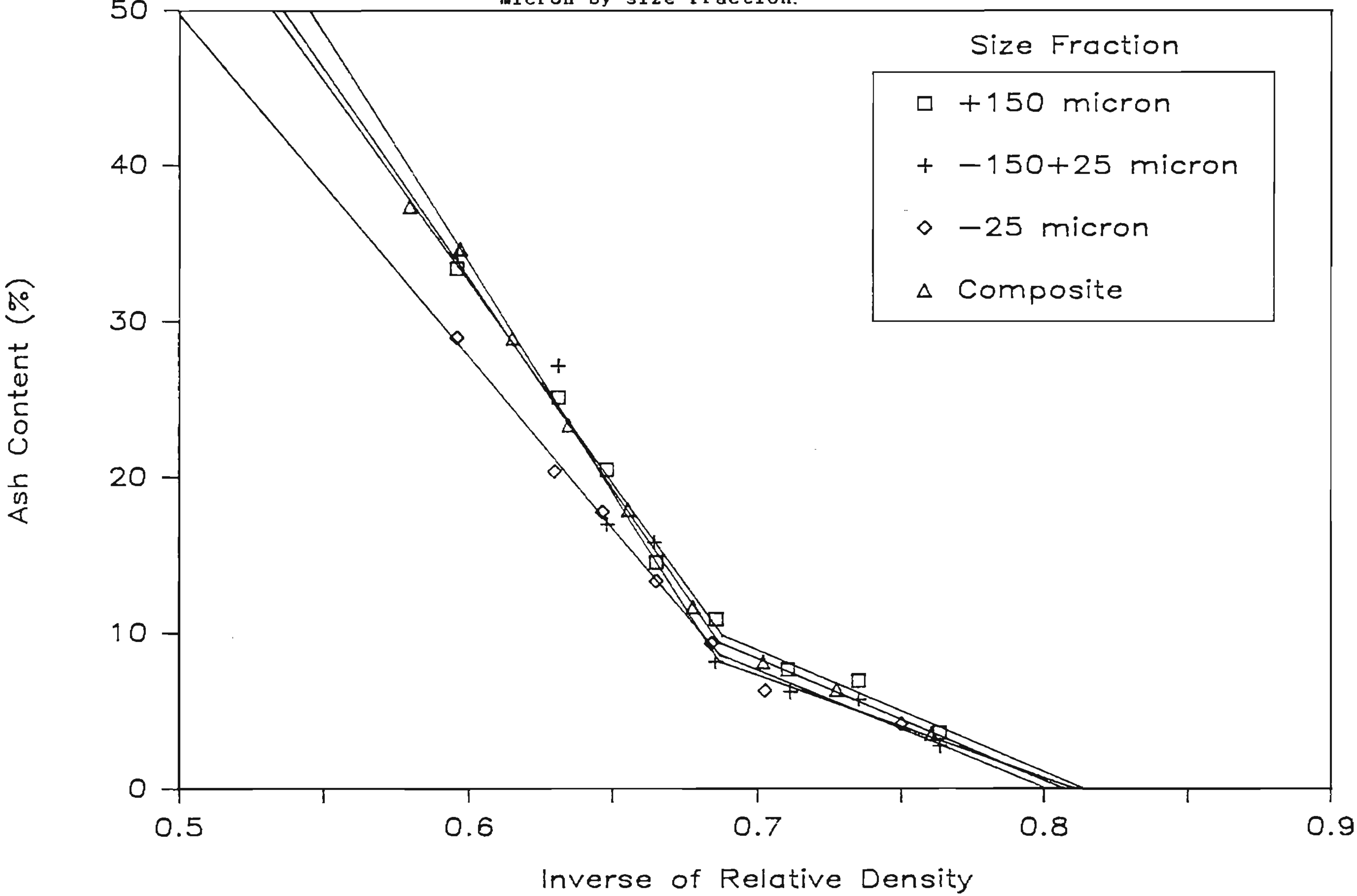

FIGURE 5.23 The ash content as a function of the inverse of relative density for the sample milled to 90 % finer than 150 micron by size fraction.

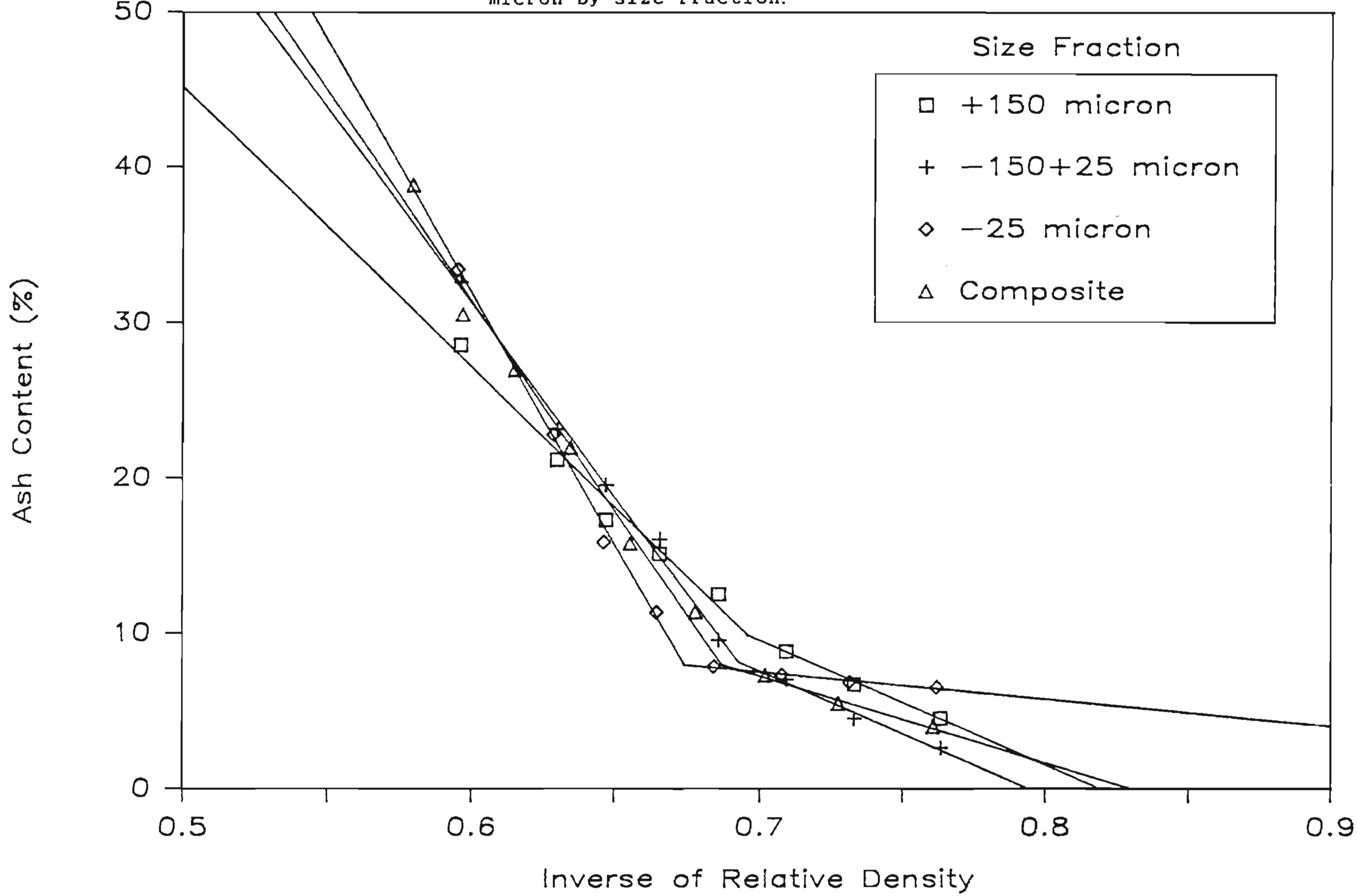

FIGURE 5.24 The ash content as a function of the inverse of relative density for the thickener underflow sample by size fraction.

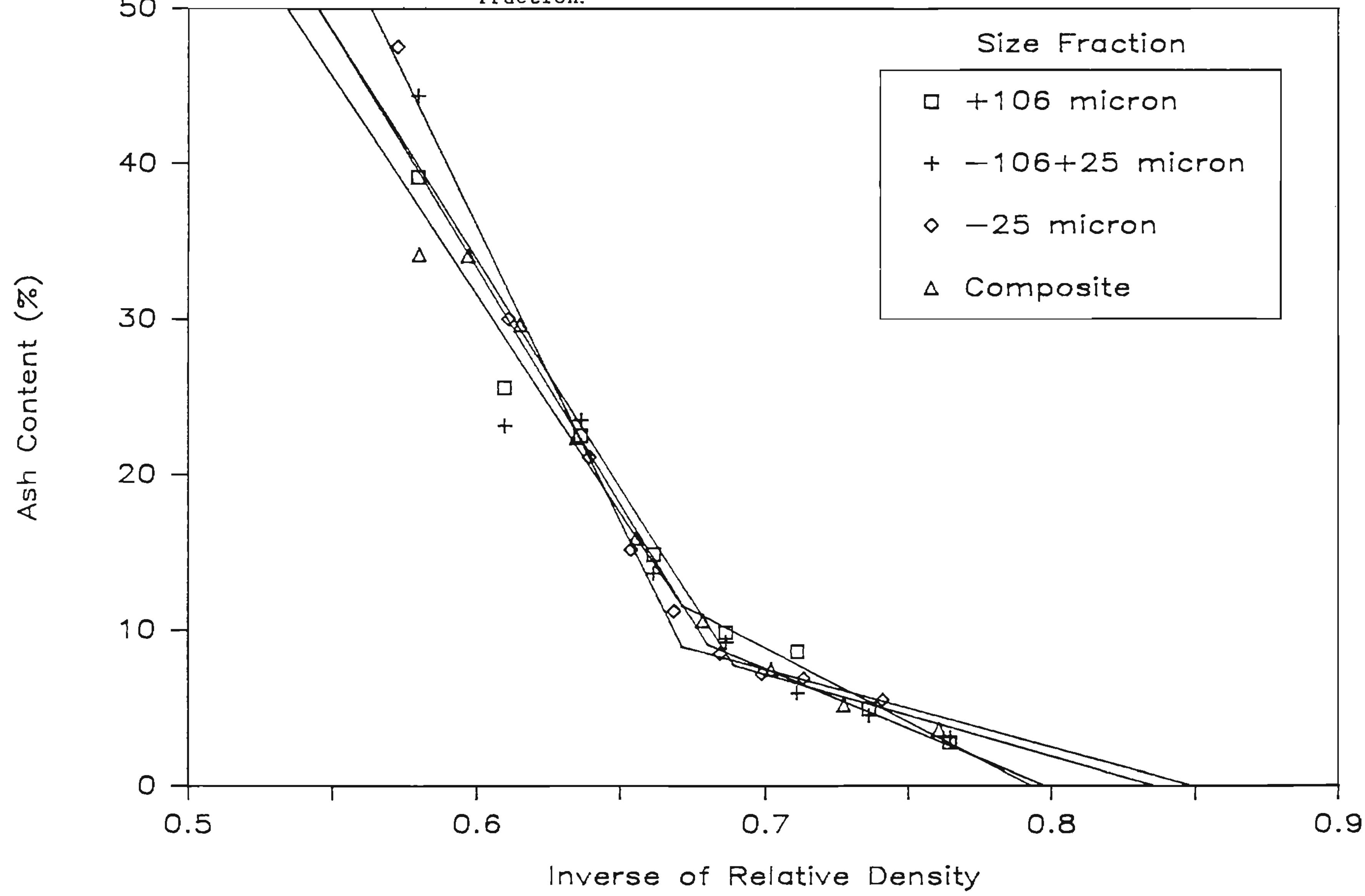

FIGURE 5.25 A comparison of the relationship between ash content and the inverse of relative density of the three composite samples.

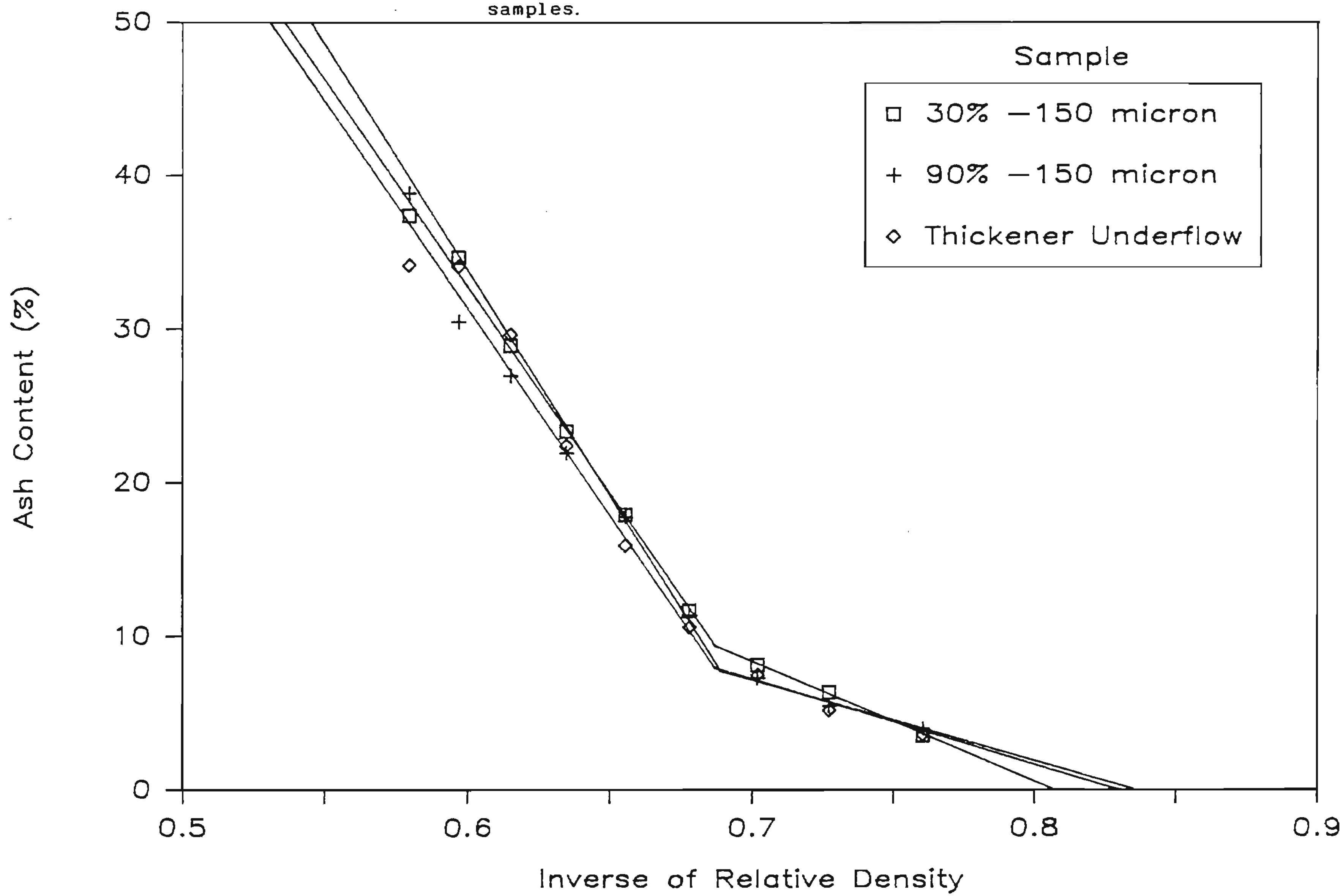

TABLE 5.6

Linear regression coefficients for the Inverse of relative density vs percent ash data. Each set of data is represented by two straight lines, one in the low ash region of the graph and one in the high ash region of the graph.

Low Ash Region				
Sample	Size Fraction (micron)	Intercept	Slope	Correlation Coefficient
30 % less than 150 µm	+150	63,5	-78,0	-0,949
	-150+ 25	53,4	-65,9	-0,972
	- 25	60,3	-75,3	-0,964
	Composite	63,5	-78,7	-0,998
90 % less than 150 µm	+150	65,4	-79,9	-0,998
	-150+ 25	64,3	-81,0	-0,988
	- 25	19,6	-17,3	-0,984
	Composite	46,3	-55,8	-0,990
Thickener Underflow	+106	75,8	-95,6	-0,984
	-106+ 25	60,9	-76,2	-0,970
	- 25	42,6	-50,2	-0,980
	Composite	44,0	-52,6	-0,978

High Ash Region				
Sample	Size Fraction (micron)	Intercept	Slope	Correlation Coefficient
30 % less than 150 µm	+150	187,3	-257,9	-0,997
	-150+ 25	211,0	-295,3	-0,981
	- 25	159,5	-219,7	-0,998
	Composite	194,0	-268,6	-0,998
90 % less than 150 µm	+150	135,4	-180,5	-0,989
	-150+ 25	180,8	-249,0	-0,997
	- 25	226,6	-324,6	-0,998
	Composite	193,7	-270,4	-0,992
Thickener Underflow	+106	199,6	-280,0	-0,975
	-106+ 25	215,9	-304,3	-0,942
	- 25	262,8	-378,1	-0,997
	Composite	209,6	-293,0	-0,993

TABLE 5.7

Predicted relative density of the light coal fraction(Sg_{lc}), the heavy coal fraction (Sg_{hc}), the ash (Sg_{a}) and the mineral matter (Sg_{m}). Sg_{m} was calculated by assuming a mineral to ash ratio of 1,16 (Savage,1967).

Sample	Size Fraction (micron)	Sg_{lc}	Sg_{hc}	Sg_{a}	Sg_{m}
	+150	1,228	1,377	2,953	2,551
30 % less	-150+ 25	1,233	1,400	2,661	2,367
than 150 µm	- 25	1,248	1,377	3,690	2,996
	Composite	1,240	1,385	2,857	2,493
	+150	1,221	1,333	5,099	3,669
90 % less	-150+ 25	1,260	1,377	3,082	2,632
than 150 µm	- 25	0,883	1,432	2,564	2,311
	Composite	1,205	1,396	2,886	2,516
	+106	1,261	1,403	2,811	2,470
Thickener	-106+ 25	1,252	1,409	2,626	2,346
Underflow	- 25	1,177	1,439	2,322	2,141
	Composite	1,196	1,398	2,673	2,357

The slope of the high ash line will be strongly influenced by the ash content at the highest relative density. However it is not possible to plot this as the density of the fraction is unknown. This can explain the difference in the slope of the high ash line of some of the size fractions. It is probably incorrect to interpret the differences in the slope of the high ash line as indicating a change in the relative density of the mineral matter for a particular size fraction.

In Table 5.7 it can be seen that the values predicted for the relative densities of the light and heavy coal fractions correspond closely in most cases with the relative densities of the macerals vitrinite and inertinite. The relative density of the mineral fraction generally falls well within the expected range, considering that the coal is predominantly clay, with some carbonates and quartz present.

CHAPTER 6

CONCLUSIONS

This chapter gives a summary of the main conclusions that can be drawn from the results of this investigation.

6.1. New Float and Sink Technique

A new apparatus and technique have been developed for the float and sink analysis of fines, to replace the present tedious and sometimes inaccurate methods of analysis. The method is rapid and accurate, and requires only a small amount of sample. Its application is not limited to coal, but its use should extend to all float and sink separations of material down to a few micron in size.

6.2. Liberation Characteristics of Greenside No 2 Seam Coal

The new device and method were used to determine the liberation characteristics of two samples of Greenside coal. The liberation behaviour of the thickener underflow sample (naturally arising fines) corresponded closely to that of the milled samples, despite the significant difference in their respective size, and size versus ash, distributions.

While an increase in the milling time resulted in an increase in the liberation of the milled samples, the change was quite small. None of the samples exhibited a high degree of liberation; even the finest samples contained a high proportion of middling material. Thus despite the fact that both the sample milled to 90 % finer than 150 micron and the thickener underflow sample show a potential yield of

63 % low ash coal, the high proportion of middling material present indicates that efficient and selective separation of a low ash product would be extremely difficult by a process such as flotation.

In the size fractions of the three samples, the distribution of the various inorganic and organic components was relatively similar, except in the finest fraction. The distribution of the various coal components in the -25 micron size fraction was in each case markedly different to that of the other size fractions. This fraction exhibited a concentration of both ash and inertinite, with a corresponding decrease in the concentration of vitrinite. The -25 micron fraction also exhibited significantly poorer washability characteristics, indicating that in each case this was the least liberated size fraction.

This can be explained by the tendency of the fine clay inclusions to be associated with the inertinite. These inclusions would tend to weaken the coal matrix, resulting in the formation of very fine particles during size reduction. These particles tend to report to the finest size fraction. The cleaner vitrinite particles, less weakened by mineral inclusions, form larger fragments. Despite the fine size of the inertinite fragments that are formed, the particles remain substantially unliberated due to the extremely fine size of the associated clay.

Maceral liberation was good in all the samples, particularly in the -25 micron size fraction. This indicates that selective separation of the different coal macerals for specific technological applications is possible provided a suitable technique can be found.

The definition of liberation efficiency employed in this thesis is useful for evaluating the change in liberation as a particular sample is reduced in size. However it is of limited use in comparing two different samples, or size fractions of a sample, for two reasons:

(a) The ash content of the two samples must be very similar for the comparison to be meaningful.

(b) The liberation efficiency is effectively a measure of the "partial liberation" of the sample. This does not take into account the type of liberation that has occured, and therefore can be of little help in assessing the beneficiation potential of the coal.

The relationship between ash and relative density can be well represented by two straight lines, indicating that this coal can be well modelled as a three component system, i.e. a light coal component, a heavy coal component and an ash or mineral component. The predicted relative densities of the two coal components were very reasonable, corresponding closely to the relative density of vitrinite and inertinite. Most of the predicted mineral relative densities were between 2,3 and 2,6, which is the relative density range of the clay minerals, the predominant mineral in the coal.

From this investigation it is clear that appreciable liberation will only be achieved by grinding significantly finer than the coal investigated in this thesis, which consisted of the naturally arising fines discard and coal milled to a similar degree of fineness. This implies that in order to produce a low ash product, further milling of the naturally arising fines would be required.

REFERENCES

ANON, "Sixty one years of mining and still a winner", S. A. Mining World, pp 36 - 46, May 1985.

BIRTEK, N. "Application of release analysis to the beneficiation of a coalmanite ore", Third Balkan Mineral Processing Conference, Belgrade, 1980. Referred to in Birtek and King (1984) op cit.

BIRTEK, N. AND KING, R.P. "Distribution of ash in fine coal from several South African Collieries", Johannesburg, Department of Metallurgy at the University of the Witwatersrand, Report CSPCOAL 5, 1984.

BIRTEK, N. AND KING, R.P. "Distribution of ash in fine coal from several South African Collieries", Johannesburg, Department of Metallurgy at the University of the Witwatersrand, Report CSPCOAL 14, 1986.

DAWSON, M.F. "Coal flotation - Tests on Newcastle Platberg Colliery fines discard", MINTEK Tech. Memo., Aug. 1983.

DELL, C.C. "Determination of flotation washability data", J. Inst. Fuel, vol. 30, pp 523 - 526, 1957.

DMEA (Department of Mineral and Energy Affairs). "South African Discard and Duff Coal National Inventory - 1985", Government Printer, Pretoria, 1987.

FALCON, R.M.S. "Coal in South Africa, Part II: The application of petrography to the characterisation of coal", Mineral Sci. Engng, vol. 10, pp 28 - 52, Jan. 1978(a).

FALCON, R.M.S. "Coal in South Africa, Part III: The fundamental approach to the characterisation and rationalisation of South African coals", Mineral Sci. Engng, vol. 10, pp 130 - 153, April 1978(b).

FALCON, L.M. AND FALCON, R.M.S. "The application of petrology to certain beneficiation techniques on S.A. coals", International Congress of Applied Metallurgy, Pretoria, 1982.

FALCON, L.M. AND FALCON, R.M.S. "Fundamental factors affecting the efficiency of fine coal beneficiation - the petrographic/mineralogical composition of coal", Proc. MINTEK 50, Randburg, 1984.

FICKLING, R.S. "An investigation into the froth flotation of four South African Coals", M.Sc Thesis, University of Cape Town, 1986.

FOURIE, P.J.F., VAN DER WALT, P.J. AND FALCON, L.M. "The beneficiation of fine coal by dense - medium cyclone", J. S. Afr. Inst. Min. Metall., vol. 80, pp 357 - 361, Oct. 1980.

GAIGHER, J.L. "The mineral matter in some South African coals", Fuel Research Institute, Report No. 45, 1980.

GAUDIN, A.M. Principles of Mineral Dressing, McGraw-Hill, London, 1939.

HALL, P.E. "The specific gravity investigation of coal samples: Further studies and a new technique", J. Chem. Metall. Min. Soc. S. Afr., pp 263 - 269, Feb. 1934.

HORSFALL, D.W. "The treatment of fine coal", Chemsa, pp 124 - 129, July 1976.

HORSFALL, D.W. "Coal - key to energy: a personal viewpoint", Rhodesian Science Journal, Feb., 1977.

HORSFALL, D.W. "A general review of coal preparation in South Africa", J. S. Afr. Inst. Min. Metall., pp 257 - 268, Aug., 1980.

INTERNATIONAL ORGANIZATION FOR STANDARDIZATION. "Coal cleaning tests - determination of float and sink characteristics of coal and combustible shale", Technical Committee 27, Subcommittee 1, N176E, 1981.

KING, R.P. "A quantitative model for mineral liberation", J. S. Afr. Inst. Min. Metall., pp 170 - 172, Oct. 1975.

KING, R.P. "A model for the quantitative estimation of mineral liberation by grinding", Int. J. Miner. Process., vol. 6, pp 207 - 220, 1979.

KING, R.P. CSP Progress Report, May 1982.

KING, R.P. AND JUCKES, A.H. "Cleaning of fine coal by dense - medium hydrocyclone", Department of Metallurgy, University of the Witwatersrand, Report CSPCOAL1, Jun. 1983.

KLIMPEL, R.R. "A preliminary model of liberation from a binary system", Powder Tech., vol. 34, pp 121 - 130, 1983.

MACGREGOR, I.M. "Preliminary results on the relationship of coal petrology to coal cuttability in some South African coals", ICAM 81, Proceedings of the First International Congress on Applied Mineralogy, The Geological Society of South Africa, pp 117 - 128, 1983.

MEHLISS, A.T.M. "Operating and developing coal mines in the Republic of South Africa", The Minerals Bureau of South Africa, Directory 2, 1985.

PANOPOULOS, G. AND KING, R.P. "The effect of particle size distribution on coal flotation", The South African Institute of Mining and Metallurgy, Colloquium on Floatation, MINTEK, Randburg, Sept. 1983.

PANOPOULOS, G., KING, R.P. AND JUCKES, A.H "The effect of particle size distribution on coal flotation", J. S. Afr. Inst. Min. Metall., pp 141 -151, May, 1986.

PERRY, R.H. AND CHILTON, C.H. "Chemical Engineers' Handbook", 5th ed., McGraw-Hill, 1973.

SANDERS, G.J. AND BROOKES, G.F. "Preparation of the `Gondwana' Coals. 1. Washability Characteristics", Coal Preparation, vol. 3, pp 105 - 132, 1986.

SAVAGE, W.H. "The mineral matter content of South African Coals", S. Afr. Chemical Processing, pp 177 - 181, Dec. - Jan., 1967 - 1968.

STACH, E. "Stach's Textbook of Coal Petrology", 2nd Ed., Gebruder Borntraeger, pp 124, 1975.

WIEGEL, R.L. AND LI, K. "A random model for mineral liberation by size reduction", Trans. A.I.M.E. 238, pp 179 - 189, 1967.

APPENDIX A

PARTITION CURVE DATA FOR THE COMPARISON OF THE TWO FLOAT AND SINK TECHNIQUES

Table A.1

Partition curve data of Sample 1 (Figure 3.5) obtained independently using two different float and sink techniques: a double column gravitational technique (Prof. King, University of the Witwatersrand), and the new technique.

Mean Relative Density	Overflow		Underflow		Reconst -ituted Feed	Partition Factor (%)
	Fract. Yield (%)	Yield	Fract. Yield (%)	Yield		
	Double Column Float and Sink Technique					
-	22,94	12,33	5,86	2,71	15,04	81,97
1,319	8,38	4,50	2,24	1,03	5,54	81,32
1,359	7,52	4,04	2,45	1,14	5,18	78,08
1,398	6,89	3,70	2,32	1,07	4,78	77,51
1,440	16,63	8,94	7,43	3,44	12,38	72,24
1,480	13,53	7,27	7,12	3,29	10,57	68,82
1,519	9,67	5,20	8,28	3,83	9,02	57,59
1,561	5,88	3,16	6,23	2,88	6,04	52,30
1,602	4,19	2,25	6,04	2,79	5,04	44,65
1,640	1,74	0,94	4,02	1,86	2,79	33,50
1,679	0,78	0,42	3,08	1,43	1,85	22,77
S1,679	1,84	0,99	44,92	20,77	21,76	4,55
Whole	100,00	53,75	100,00	46,25	100,00	-
	New Float and Sink Technique					
F1,264	0,76	0,41	0,17	0,08	0,49	83,70
1,303	26,89	14,45	7,85	3,63	18,08	79,90
1,374	17,84	9,59	4,73	2,19	11,78	81,40
1,431	19,53	10,50	7,71	3,57	14,07	74,60
1,483	16,67	8,96	11,06	5,12	14,08	63,60
1,533	8,56	4,60	8,01	3,70	8,30	55,40
1,587	5,25	2,82	6,62	3,06	5,88	48,00
1,656	2,52	1,35	8,18	3,78	5,13	26,30
S1,694	1,98	1,06	45,67	21,12	22,18	4,80
Whole	100,00	53,75	100,00	46,25	100,00	-

Table A.2

Partition curve data of Sample 2 (Figure 3.6) obtained independently using two different float and sink techniques: a double column gravitational technique (Prof. King, University of the Witwatersrand), and the new technique.

Mean Relative Density	Overflow Fract. Yield (%)	Overflow Yield	Underflow Fract. Yield (%)	Underflow Yield	Reconst -ituted Feed	Partition Factor (%)
Double Column Float and Sink Technique						
-	13,08	7,05	4,58	2,11	9,16	76,96
1,319	18,71	10,08	6,49	2,99	13,08	77,10
1,361	7,56	4,07	3,39	1,57	5,64	72,24
1,399	9,18	4,95	4,24	1,96	6,91	71,66
1,436	14,89	8,02	7,34	3,39	11,41	70,32
1,479	17,01	9,16	10,37	4,78	13,95	65,71
1,522	7,97	4,30	7,38	3,40	7,70	55,80
1,561	4,91	2,65	9,04	4,17	6,82	38,84
1,601	2,31	1,24	3,95	1,82	3,06	40,56
1,637	1,85	1,00	3,47	1,60	2,60	38,42
1,676	0,49	0,26	3,28	1,51	1,78	14,88
S1,676	2,04	1,10	36,46	16,81	17,91	6,14
Whole	100,00	53,89	100,00	46,11	100,00	-
New Float and Sink Technique						
F1,302	10,70	5,77	2,81	1,30	7,07	81,60
1,327	21,17	11,41	6,04	2,79	14,20	80,35
1,377	17,37	9,36	5,97	2,75	12,11	77,30
1,427	14,83	7,99	8,73	4,03	12,02	66,50
1,469	10,23	5,51	7,54	3,48	8,99	61,30
1,511	12,42	6,69	9,58	4,42	11,11	60,20
1,558	6,60	3,56	8,06	3,72	7,28	48,90
1,609	3,16	1,70	6,90	3,18	4,88	34,80
S1,637	3,52	1,90	44,37	20,46	22,36	8,50
Whole	100,00	53,89	100,00	46,11	100,00	-

Table A.3

Partition curve data of Sample 3 (Figure 3.7) obtained independently using two different float and sink techniques: a double column gravitational technique (Prof. King, University of the Witwatersrand). and the new technique.

Mean Relative Density	Overflow Fract. Yield (%)	Overflow Yield	Underflow Fract. Yield (%)	Underflow Yield	Reconst -ituted Feed	Partition Factor (%)
Double Column Float and Sink Technique						
-	9,41	4,95	0,18	0,09	5,04	98,26
1,333	28,26	14,87	6,29	2,98	17,85	83,30
1,394	12,37	6,51	7,81	3,70	10,21	63,77
1,436	13,73	7,22	6,18	2,93	10,15	71,16
1,475	15,59	8,20	8,14	3,86	12,26	68,02
1,516	9,52	4,85	9,14	4,33	9,18	52,85
1,555	5,20	2,73	10,25	4,86	7,59	36,03
1,595	2,20	1,16	6,51	3,09	4,24	27,25
1,639	1,10	0,58	5,44	2,58	3,15	18,31
1,680	0,59	0,31	2,82	1,33	1,64	18,78
S1,680	2,34	1,23	37,25	17,65	18,89	6,53
Whole	100,00	52,61	100,00	47,39	100,00	-
New Float and Sink Technique						
F1,341	30,30	15,94	0,71	0,34	16,28	97,90
1,357	7,81	4,11	4,45	2,11	6,22	66,10
1,393	10,64	5,60	6,37	3,02	8,62	65,00
1,437	18,69	9,83	6,48	3,07	12,90	76,20
1,478	11,56	6,08	8,96	4,25	10,33	58,90
1,514	8,22	4,32	9,22	4,37	8,69	49,70
1,552	4,85	2,55	7,02	3,33	5,88	43,40
S1,571	7,93	4,17	56,79	26,91	31,08	13,40
Whole	100,00	52,61	100,00	47,39	100,00	-

APPENDIX B

SIZE DISTRIBUTION DATA

TABLE B.1

The size distribution of the four samples.

Screen Size (μm)	Cumulative Weight of Sample less than a Particular Screen Size (%)			
	30% -150 μm	60% -150 μm	90% -150 μm	Thickener Underflow
250	39,5	88,1	100,0	81,5
150	29,5	63,2	92,3	72,4
106	23,2	51,5	71,9	63,7
75	18,4	42,5	58,2	54,8
53	15,0	35,2	47,2	47,2
38	12,9	29,9	41,9	41,7
25	9,9	23,8	32,0	34,9

TABLE B.2

The ash content of the size fractions of the four samples.

Size Fraction (μm)	Ash Content (%)			
	30% -150 μm	60% -150 μm	90% -150 μm	Thickener Underflow
+250	22,7	26,3		16,3
-250+150	19,1	24,0	24,1	17,6
-150+106	19,3	21,0	28,3	17,3
-106+ 75	19,0	20,3	20,5	18,6
- 75+ 53	19,1	19,8	20,0	19,3
- 53+ 38	18,7	19,4	18,1	20,9
- 38+ 25	19,1	19,3	19,1	22,6
- 25	23,3	22,7	22,1	26,0
Composite	21,7	22,4	22.6	21,0

APPENDIX C

DENSITY DISTRIBUTION DATA

TABLE C.1

Percent floats in each relative density interval of the size fractions of the sample milled to 30 % finer than 150 micron.

	Size Fraction (micron)						
Relative Density	+150	-150 +106	-106 +75	-75 +53	-53 +38	-38 +25	-25
Floats 1,35	17,7	17,0	16,1	16,2	15,3	13,0	4,8
1,35-1,40	7,7	13,8	13,2	12,3	14,6	14,2	8,6
1,40-1,45	16,4	15,6	16,3	17,7	16,1	16,1	13,4
1,45-1,50	12,3	17,2	13,2	13,0	13,0	15,1	20,4
1,50-1,55	8,1	4,8	7,6	6,8	8,0	9,1	17,2
1,55-1,60	5,0	3,8	5,6	6,3	6,3	5,7	9,2
1,60-1,65	4,4	6,4	5,3	4,9	5,1	3,9	4,4
1,65-1,70	3,9	4,0	3,5	3,4	3,0	2,9	2,3
1,70-1,75	3,2	1,7	2,5	2,2	1,1	2,0	1,8
Sinks 1,75	21,3	15,7	16,7	17,2	17,5	18,0	17,9

TABLE C.2

Percent floats in each relative density interval of the size fractions of the sample milled to 60 % finer than 150 micron.

	Size Fraction (micron)						
Relative Density	+150	-150 +106	-106 +75	-75 +53	-53 +38	-38 +25	-25
Floats 1,35	14,8	14,0	15,2	14,2	16,4	11,5	3,7
1,35-1,40	11,3	14,5	14,3	14,3	9,6	12,7	9,6
1,40-1,45	15,1	13,8	14,3	13,7	14,0	16,5	13,3
1,45-1,50	12,7	11,7	12,3	11,3	16,9	15,5	21,5
1,50-1,55	6,4	9,1	9,0	10,3	8,4	9,1	16,1
1,55-1,60	5,4	6,9	6,2	6,1	6,5	5,6	10,3
1,60-1,65	4,3	3,7	4,3	4,0	3,7	3,5	4,0
1,65-1,70	3,1	2,2	3,1	3,0	2,3	2,4	2,3
1,70-1,75	1,9	2,3	1,9	2,4	2,1	1,8	1,7
Sinks 1,75	25,0	21,8	19,4	20,1	20,1	21,4	19,0

TABLE C.3

Percent floats in each relative density interval of the size fractions of the sample milled to 90 % finer than 150 micron.

Relative Density	Size Fraction (micron)						
	+150	-150 +106	-106 +75	-75 +53	-53 +38	-38 +25	-25
Floats 1,35	16,2	17,2	16,5	17,0	17,3	13,1	5,8
1,35-1,40	15,2	13,0	13,2	14,1	13,5	15,4	9,1
1,40-1,45	14,4	14,9	17,3	15,2	16,4	17,6	18,3
1,45-1,50	10,6	12,9	11,8	13,6	13,7	14,1	21,7
1,50-1,55	6,9	6,4	8,7	8,1	8,0	9,2	13,6
1,55-1,60	4,4	5,2	5,6	5,9	5,6	4,7	6,6
1,60-1,65	3,6	5,4	4,1	4,1	3,3	3,8	3,1
1,65-1,70	3,0	4,0	3,0	2,4	2,5	2,6	3,0
1,70-1,75	1,8	2,0	2,1	2,2	2,3	2,0	2,0
Sinks 1,75	23,9	19,0	17,7	17,4	17,4	17,5	16,8

TABLE C.4

Percent floats in each relative density interval of the size fractions of the thickener underflow sample.

Relative Density	Size Fraction (micron)		
	+106	-106 +25	-25
Floats 1,35	24,8	18,6	5,2
1,35-1,40	12,3	11,6	8,1
1,40-1,45	13,7	15,7	13,0
1,45-1,50	14,6	16,6	16,0
1,50-1,55	9,6	10,8	15,2
1,55-1,60	6,6	4,9	12,7
1,60-1,65	4,6	2,4	5,5
1,65-1,70	2,9	1,8	2,0
1,70-1,75	1,7	1,5	1,3
Sinks 1,75	9,2	16,1	21,0

APPENDIX D

WASHABILITY DATA

TABLE D.1

Washability data for the +150 micron size fraction of the sample milled to 30% minus 150 micron.

Relative Density	Yield (%)	Cum. Yield (%)	Cum. Ash Content (%)	Ash Content (%)	Ash per 100 Units of Feed
Floats 1,28	0,0	0,0	-	-	-
1,280-1,340	13,27	13,27	3,62	3,62	0,48
1,340-1,381	6,45	19,72	4,72	6,98	0,93
1,381-1,434	18,99	38,71	6,17	7,68	2,39
1,434-1,482	10,65	49,36	7,19	10,90	3,55
1,482-1,524	7,84	57,20	8,20	14,56	4,69
1,524-1,562	7,11	64,31	9,56	20,50	6,15
1,562-1,606	7,77	72,08	11,24	25,14	8,10
1,606-1,750	9,63	81,71	13,85	33,39	11,32
Sinks 1,75	18,29	100,00	20,40	49,66	20,40

TABLE D.2

Washability data for the -150+25 micron size fraction of the sample milled to 30 % finer than 150 micron.

Relative Density	Yield (%)	Cum. Yield (%)	Cum. Ash Content (%)	Ash Content (%)	Ash per 100 Units of Feed
Floats 1,28	0,0	0,0	-	-	-
1,280-1,340	14,97	14,97	2,74	2,74	0,41
1,340-1,381	7,98	22,95	3,79	5,76	0,87
1,381-1,431	13,81	36,76	4,71	6,24	1,73
1,431-1,486	19,17	55,93	5,90	8,18	3,30
1,486-1,524	7,45	63,38	7,07	15,85	4,48
1,524-1,562	6,86	70,24	8,04	17,00	5,65
1,562-1,606	4,24	74,48	9,13	27,19	6,80
1,606-1,750	11,34	85,82	12,45	34,26	10,69
Sinks 1,75	14,18	100,00	18,46	54,83	18,46

TABLE D.3

Washability data for the -25 micron size fraction of the sample milled to 30 % finer than 150 micron.

Relative Density	Yield (%)	Cum. Yield (%)	Cum. Ash Content (%)	Ash Content (%)	Ash per 100 Units of Feed
Floats 1,28	0,0	0,0	-	-	-
1,280-1,387	10,30	10,30	4,17	4,17	0,43
1,387-1,441	16,78	27,08	5,50	6,32	1,49
1,441-1,482	17,63	44,71	7,02	9,35	3,14
1,482-1,524	16,23	60,90	8,70	13,33	5,30
1,524-1,569	9,29	70,23	9,90	17,77	6,95
1,569-1,606	7,40	77,63	10,91	20,39	8,47
1,606-1,750	8,97	86,60	12,77	28,95	11,06
Sinks 1,75	13,40	100,00	20,80	72,70	20,80

TABLE D.4

Washability data of the sample milled to 30 % finer than 150 micron (reconstituted from the size fraction data).

Relative Density	Yield (%)	Cum. Yield (%)	Cum. Ash Content (%)	Ash Content (%)	Ash per 100 Units of Feed
Floats 1,28	0,0	0,0	-	-	-
1,28-1,35	13,9	13,9	3,54	3,54	0,49
1,35-1,40	10,7	24,6	4,78	6,39	1,18
1,40-1,45	16,9	41,5	6,15	8,14	2,55
1,45-1,50	12,6	54,1	7,44	11,69	4,02
1,50-1,55	10,1	64,2	9,09	17,93	5,84
1,55-1,60	7,9	72,1	10,65	23,33	7,68
1,60-1,65	5,2	77,3	11,88	28,93	9,18
1,65-1,70	3,4	80,7	12,84	34,67	10,36
1,70-1,75	2,3	83,0	13,52	37,38	11,22
Sinks 1,75	17,0	100,0	20,06	52,05	20,06

TABLE D.5

Washability data for the +150 micron size fraction of the sample milled to 90 % finer than 150 micron.

Relative Density	Yield (%)	Cum. Yield (%)	Cum. Ash Content (%)	Ash Content (%)	Ash per 100 Units of Feed
Floats 1,28	0,0	0,0	-	-	-
1,280-1,340	20,16	20,16	4,51	4,51	0,91
1,340-1,389	7,89	28,05	5,13	6,71	1,44
1,389-1,431	12,89	40,94	6,30	8,85	2,58
1,431-1,485	14,15	55,09	7,90	12,53	4,35
1,485-1,520	4,28	59,37	8,42	15,11	5,00
1,520-1,570	5,95	65,32	9,23	17,31	6,03
1,570-1,604	3,82	69,14	9,89	21,18	6,84
1,604-1,750	8,61	77,75	11,96	28,58	9,30
Sinks 1,75	22,25	100,00	24,10	66,52	24,10

TABLE D.6

Washability data for the -150+25 micron size fraction of the sample milled to 90 % finer than 150 micron.

Relative Density	Yield (%)	Cum. Yield (%)	Cum. Ash Content (%)	Ash Content (%)	Ash per 100 Units of Feed
Floats 1,28	0,0	0,0	-	-	-
1,280-1,340	15,62	15,62	2,62	2,62	0,41
1,340-1,389	10,84	26,46	3,40	4,52	0,90
1,389-1,431	17,42	43,88	4,85	7,05	2,13
1,431-1,485	10,14	54,02	5,74	9,59	3,10
1,485-1,520	11,03	65,05	7,49	16,06	4,87
1,520-1,570	5,31	70,36	8,40	19,55	5,91
1,570-1,604	4,46	74,82	9,28	23,16	6,94
1,604-1,750	8,54	83,36	11,67	32,61	9,73
Sinks 1,75	16,64	100,00	19,54	58,97	19,54

TABLE D.7

Washability data for the -25 micron size fraction of the sample milled to 90 % finer than 150 micron.

Relative Density	Yield (%)	Cum. Yield (%)	Cum. Ash Content (%)	Ash Content (%)	Ash per 100 Units of Feed
Floats 1,28	0,0	0,0	-	-	-
1,280-1,345	5,06	5,06	6,52	6,52	0,33
1,345-1,390	7,45	12,51	6,71	6,84	0,84
1,390-1,437	14,62	27,13	7,04	7,32	1,91
1,437-1,486	22,55	49,68	7,41	7,86	3,68
1,486-1,524	15,60	65,28	8,35	11.34	5,45
1,524-1,570	9,99	75,27	9,35	15,88	7,04
1,570-1,610	5,73	81,00	10,30	22.78	8,34
1,610-1,750	4,01	85,01	11,39	33,41	9,68
Sinks 1,75	14,99	100,00	20,57	72,63	20,57

TABLE D.8

Washability data of the sample milled to 90 % finer than 150 micron (reconstituted from the size fraction data).

Relative Density	Yield (%)	Cum. Yield (%)	Cum. Ash Content (%)	Ash Content (%)	Ash per 100 Units of Feed
Floats 1,28	0,0	0,0	-	-	-
1,28-1,35	14,1	14,1	4,00	4.00	0,56
1,35-1,40	11,6	25,7	4,66	5,47	1,20
1,40-1,45	17,7	43,4	5,74	7,31	2,49
1,45-1,50	15,8	59,2	7,25	11,39	4,29
1,50-1,55	10,1	69,3	8,50	15,78	5,89
1,55-1,60	6,3	75,6	9,62	21,94	7,27
1,60-1,65	3,7	79,3	10,43	26,98	8.27
1,65-1,70	2,4	81,7	11,02	30,51	9.00
1,70-1,75	1,8	83,5	11,62	38,85	9.70
Sinks 1,75	16,5	100,0	20,23	63,68	20,23

TABLE D.9

Washability data for the +106 micron size fraction of the thickener underflow sample.

Relative Density	Yield (%)	Cum. Yield (%)	Cum. Ash Content (%)	Ash Content (%)	Ash per 100 Units of Feed
Floats 1,28	0,0	0,0	-	-	-
1,280-1,336	21,18	21,18	2,79	2,79	0,59
1,336-1,381	11,50	32,68	3,55	4,95	1,16
1,381-1,432	12,65	45,33	4,97	8.64	2,25
1,432-1,483	16,06	61,39	6,25	9,86	3,84
1,483-1,540	12,08	73,47	7,67	14,89	5,64
1,540-1,603	8,64	82,11	9,23	22,5	7,58
1,603-1,677	6,38	88,49	10,41	25,60	9,21
1,677-1,774	3,06	91,55	11,37	39,13	10,41
Sinks 1,774	8,45	100,00	16,00	60,34	16,00

TABLE D.10

Washability data for the -106+25 micron size fraction of the thickener underflow sample.

Relative Density	Yield (%)	Cum. Yield (%)	Cum. Ash Content (%)	Ash Content (%)	Ash per 100 Units of Feed
Floats 1,28	0,0	0,0	-	-	-
1,280-1,336	16,25	16,25	3,08	3,08	0,50
1,336-1,381	8,77	25,02	3,58	4,51	0,90
1,381-1,432	14,84	39,86	4,47	5,97	1,78
1,432-1,483	18,05	57,91	5,96	9,25	3,45
1,483-1,540	12,28	70,19	7,31	13,68	5,13
1,540-1,603	8,29	78,48	9.02	23,50	7,08
1,603-1,677	3,06	81,54	9,55	23,14	7,79
1,677-1,774	3,16	84,70	10,85	44,39	9,19
Sinks 1,774	15,30	100,00	19,90	69,41	19,90

TABLE D.11

Washability data for the -25 micron size fraction of the thickener underflow sample.

Relative Density	Yield (%)	Cum. Yield (%)	Cum. Ash Content (%)	Ash Content (%)	Ash per 100 Units of Feed
Floats 1,31	0,0	0,0	-	-	-
1,310-1,390	11,50	11,50	5,5	5,50	0,63
1,390-1,414	4,53	16,03	5,90	6,91	0,95
1,414-1,449	9,91	25,94	6,40	7,21	1,66
1,449-1,474	8,06	34,00	6,90	8,51	2,35
1.474-1,518	14,06	48,06	8,17	11.24	3.92
1,518-1,541	8,05	56,11	9,18	15,21	5,14
1,541-1,588	11,96	68,07	11,28	21,13	7,67
1,588-1,684	9,14	77,21	13,50	30,03	10,42
1,684-1,810	4,82	82,03	15,50	47,54	12,30
Sinks 1,810	17,97	100,00	26,00	73.93	26,00

TABLE D.12

Washability data of the thickener underflow sample (reconstituted from the size fraction data).

Relative Density	Yield (%)	Cum. Yield (%)	Cum. Ash Content (%)	Ash Content (%)	Ash per 100 Units of Feed
Floats 1,28	0,0	0.0	-	-	-
1,28-1,35	16,2	16,2	3,60	3,60	0,58
1,35-1,40	10,6	26,8	4,23	5,19	1.13
1,40-1,45	14,0	40,8	5,35	7,49	2.18
1,45-1,50	15,6	56,4	6,81	10,63	3,84
1,50-1,55	11,9	68,3	8,40	15,94	5,74
1,55-1,60	8.2	76.5	9,90	22,39	7,57
1,60-1,65	4,3	80,8	10,95	29,63	8,85
1,65-1,70	2,3	83.1	11,59	34,07	9,63
1,70-1,75	1,5	84,6	11,99	34,15	10,14
Sinks 1.75	15,3	100.0	20,58	68,21	20,58

APPENDIX E

PETROGRAPHIC ANALYSIS DATA OF THE SIZE FRACTIONS

TABLE E.1

The maceral content of the size fractions of the sample milled to 30 % finer than 150 micron.

Size Fraction (micron)	Vitrinite (%)	Exinite (%)	Inertinite Reactive (%)	Inertinite Non-reactive (%)	Total Reactive (%)
+150	27,0	3,0	20,0	50,0	50,0
-150+106	26.0	3.0	14,0	57,0	43.0
-106+ 53	22.0	1.0	21.0	56.0	44,0
- 53+ 25	----	---	----	----	----
- 25	20,0	0,0	7.0	73.0	27,0

TABLE E.2

The maceral content of the size fractions of the sample milled to 90 % finer than 150 micron.

Size Fraction (micron)	Vitrinite (%)	Exinite (%)	Inertinite Reactive (%)	Inertinite Non-reactive (%)	Total Reactive (%)
+150	30.7	8.3	11.3	49.7	50.3
-150+106	32.4	3.3	13.0	51.3	48.7
-106+ 53	30.4	6.0	18.3	45.3	54.7
- 53+ 25	32.6	2.7	11.0	53.7	46.3
- 25	26.0	3.0	7.0	64.0	36.0

TABLE E.3

The maceral content of the size fractions of the thickener underflow sample.

Size Fraction (micron)	Vitrinite (%)	Exinite (%)	Inertinite Reactive (%)	Inertinite Non-reactive (%)	Total Reactive (%)
+106	39,0	1,7	14,3	45,0	55,0
-106+ 25	35,0	1,5	23,5	40,0	60,0
- 25	20,0	0,0	0,0	80,0	20,0

APPENDIX F

PETROGRAPHIC WASHABILITY ANALYSIS DATA

TABLE F.1

Maceral analysis of the relative density fractions of the -150+106 micron size fraction of the sample milled to 30 % finer than 150 micron.

Relative Density	Vitrinite (%)	Exinite (%)	Inertinite Reactive (%)	Inertinite Non-reactive (%)	Total Reactive (%)
S1,70	12,0	2,0	7,3	78.7	21.3
1,51-1,70	8,3	3,6	24,3	63,7	36,3
1,43-1,51	16,0	2,6	33,6	47,8	52,2
1,35-1,43	35,6	3,6	21,6	39,2	60,8
F1,35	79.3	4,3	4,9	11.5	88,5

TABLE F.2

Microlithotype analysis of the relative density fractions of the -150+106 micron size fraction of the sample milled to 30 % finer than 150 micron.

Relative Density	Vitrites (%)	Inter-mediates (%)	Inertites (%)	Carbo-minerites (%)	Liptites (%)
S1,70	1,0	3,5	34,5	59,0	2,0
1,51-1,70	3,0	9,5	82,5	4,5	0,5
1,43-1,51	4,0	18,5	74,5	0,5	2,5
1,35-1,43	13,5	41.0	45,5	0,0	0,0
F1,35	67,5	27.5	3,0	0,0	2,5

TABLE F.3

Maceral analysis of the relative density fractions of the -106+53 micron size fraction of the sample milled to 30 % finer than 150 micron.

Relative Density	Vitrinite (%)	Exinite (%)	Inertinite Reactive (%)	Inertinite Non-reactive (%)	Total Reactive (%)
S1,70	20,3	5,3	6,9	67,4	32,6
1,50-1,70	11,6	4,3	21,6	62,4	37,6
1,43-1,50	16,0	5,0	22,3	56,6	43,3
1,35-1,43	34,0	3,6	21,6	40,7	59,3
F1,35	78,3	3,6	7,9	10,0	90,0

TABLE F.4

Microlithotype analysis of the relative density fractions of the -106+53 micron size fraction of the sample milled to 30 % finer than 150 micron.

Relative Density	Vitrites (%)	Inter-mediates (%)	Inertites (%)	Carbo-minerites (%)	Liptites (%)
S1,70	4,5	7,0	46,5	42,0	0,0
1,50-1,70	3,0	16,0	76,5	3,0	1,5
1,43-1,50	10,0	13,0	72,0	1,0	4,0
1,35-1,43	16,5	31,5	47,5	0,0	4,5
F1,35	65,7	22,0	5,3	0,0	7,0

TABLE F.5

Maceral analysis of the relative density fractions of the -53+25 micron size fraction of the sample milled to 30 % finer than 150 micron.

Relative Density	Vitrinite (%)	Exinite (%)	Inertinite Reactive (%)	Inertinite Non-reactive (%)	Total Reactive (%)
S1,70	11,0	3,0	6,0	80,0	20,0
1,51-1,70	11,5	3,5	14,5	70,5	29,5
1,43-1,51	9,2	2,8	28,6	58,4	41,6
1,36-1,43	26,8	3,2	25,6	44,4	55,6
F1,36	79,3	2,0	9,6	9,0	91,0

TABLE F.6

Microlithotype analysis of the relative density fractions of the -53+25 micron size fraction of the sample milled to 30 % finer than 150 micron.

Relative Density	Vitrites (%)	Inter-mediates (%)	Inertites (%)	Carbo-minerites (%)	Liptites (%)
S1,70	3,5	2,5	32,5	61,5	0,0
1,51-1,70	3,0	7,0	87,0	0,0	3,0
1,43-1,51	3,0	12,5	83,0	0,5	1,0
1,36-1,43	10,5	19,0	68,0	0,0	2,5
F1,36	79,0	14,5	5,0	0,0	1,5

TABLE F.7

Maceral analysis of the relative density fractions of the -25 micron size fraction of the sample milled to 30 % finer than 150 micron (estimates).

Relative Density	Vitrinite (%)	Exinite (%)	Inertinite Reactive (%)	Inertinite Non-reactive (%)	Total Reactive (%)
S1,70	5	0	0	95	5
1,50-1,70	7	0	20	73	27
1,43-1,50	10	3	10	77	23
1,35-1,43	34	0	10	56	44
F1,36	—	-	--	--	—

TABLE F.8

Microlithotype analysis of the relative density fractions of the -25 micron size fraction of the sample milled to 30 % finer than 150 micron (estimates).

Relative Density	Vitrites (%)	Inter-mediates (%)	Inertites (%)	Carbo-minerites (%)	Liptites (%)
S1,70	5	0	25	70	0
1,50-1,70	5	0	90	5	0
1,43-1,50	7	0	91	2	0
1,35-1,43	26	0	73	1	0
F1,35	--	-	--	-	0

TABLE F.9

Maceral analysis of the relative density fractions of the -150+106 micron size fraction of the sample milled to 90 % finer than 150 micron.

Relative Density	Vitrinite (%)	Exinite (%)	Inertinite Reactive (%)	Inertinite Non-reactive (%)	Total Reactive (%)
S1,77	11,0	0,0	4,2	84,8	15,2
1,51-1,77	8,4	5,2	11,4	75,0	25,0
1,43-1,51	12,0	5,6	24,0	58,4	41,6
1,35-1,43	35,8	6,2	27,0	31,0	69,0
F1,35	72,0	5,4	7,8	14,8	85,2

TABLE F.10

Maceral analysis of the relative density fractions of the -106+53 micron size fraction of the sample milled to 90 % finer than 150 micron.

Relative Density	Vitrinite (%)	Exinite (%)	Inertinite Reactive (%)	Inertinite Non-reactive (%)	Total Reactive (%)
S1,70	5,8	2,0	0,0	92,2	7,8
1,50-1,70	6,2	4,4	14,1	75,3	24,7
1,43-1,50	9,7	3,2	17,9	69,2	30,8
1,35-1,43	36,0	6,6	22,1	35,3	64,7
F1,35	76,1	8,0	5,0	10,9	89,1

TABLE F.11

Maceral analysis of the relative density fractions of the -53+25 micron size fraction of the sample milled to 90 % finer than 150 micron.

Relative Density	Vitrinite (%)	Exinite (%)	Inertinite Reactive (%)	Inertinite Non-reactive (%)	Total Reactive (%)
S1,71	---	---	---	---	---
1,50-1,71	5,0	4,0	13,3	77,7	22,3
1,43-1,50	14,5	6,0	13,5	66,0	34,0
1,35-1,43	43,1	9,3	17,7	29,9	70,1
F1,35	76,4	8,5	6,9	8,2	91,8

TABLE F.12

Maceral analysis of the relative density fractions of the -25 micron size fraction of the sample milled to 90 % finer than 150 micron (estimates).

Relative Density	Vitrinite (%)	Exinite (%)	Inertinite Reactive (%)	Inertinite Non-reactive (%)	Total Reactive (%)
S1,70	---	---	---	---	---
1,50-1,70	---	---	---	---	---
1,43-1,50	---	---	---	---	---
1,36-1,43	14,3	2,2	10,7	72,8	27,2
F1.36	84,8	0,0	0,0	15,2	84,8

TABLE F.13

Maceral analysis of the relative density fractions of the -106 micron size fraction of the thickener underflow sample.

Relative Density	Vitrinite (%)	Exinite (%)	Inertinite Reactive (%)	Inertinite Non-reactive (%)	Total Reactive (%)
S1,78	0,0	0,0	0,0	0,0	0,0
1,50-1,78	5,3	0,7	25,7	68,3	31,7
1,42-1,50	6,7	1,0	24,0	68,3	31,7
1,35-1,42	22,0	2,0	24,7	51,3	48,7
F1,35	82,0	1,3	4,7	12,0	88,0

TABLE F.14

Microlithotype analysis of the relative density fractions of the +106 micron size fraction of the thickener underflow sample.

Relative Density	Vitrites (%)	Inter-mediates (%)	Inertites (%)	Carbo-minerites (%)	Liptites (%)
S1,78	0,7	2,0	11,0	86,3	0,0
1,50-1,78	3,3	1,3	92.1	3,3	0,0
1,42-1,50	2,7	7,7	88,7	0,3	0,6
1,35-1,42	9,7	32,0	57,3	0,7	0,3
F1,35	75,7	17,0	6.0	0,0	1,3

TABLE F.15

Maceral analysis of the relative density fractions of the -106+25 micron size fraction of the thickener underflow sample.

Relative Density	Vitrinite (%)	Exinite (%)	Inertinite Reactive (%)	Inertinite Non-reactive (%)	Total Reactive (%)
S1,78	0,0	0,0	0,0	0,0	0,0
1,50-1,78	5,0	2,0	19,0	74,0	26,0
1,43-1,50	7,0	0,5	11,5	81,4	19,0
1,35-1,43	20,5	4,0	16,0	59,5	40,5
F1,35	89,5	3,0	0.5	7,0	93,0

TABLE F.16

Microlithotype analysis of the relative density fractions of the -106+25 micron size fraction of the thickener underflow sample.

Relative Density	Vitrites (%)	Intermediates (%)	Inertites (%)	Carbominerites (%)	Liptites (%)
S1,78	0,5	0,0	2,5	97,0	0,0
1,50-1,78	3,5	3,5	88,0	4,5	0,5
1,43-1,50	3,0	4,0	93,0	0,0	0,0
1,35-1,43	20,0	19,0	60,0	0,0	1,0
F1,35	85,0	11,5	3,0	0,0	0,5

TABLE F.17

Maceral analysis of the relative density fractions of the -25 micron size fraction of the thickener underflow sample (estimates).

Relative Density	Vitrinite (%)	Exinite (%)	Inertinite Reactive (%)	Inertinite Non-reactive (%)	Total Reactive (%)
S1,77	0	0	0	0	0
1,50-1,77	3	0	0	97	3
1,43-1,50	7	0	0	93	7
F1,43	61	0	0	39	61

APPENDIX G

DERIVATION OF THE RELATIONSHIP BETWEEN ASH CONTENT AND RELATIVE DENSITY

$$Ash(\%) = \frac{(100/Sg) - (100/Sg_c)}{(1/Sg_a) - (1/Sg_c)}$$

Where Sg = relative density of a particle
Sg_c = relative density of coal
Sg_a = relative density of ash

Let Ash(%) = A

Cross multiplication of equation (1) yields:

$$A/Sg_a - A/Sg_c = 100/Sg - 100/Sg_c$$

Therefore:

$$\frac{Sg_c.A - Sg_a.A}{Sg_c.Sg_a} = \frac{100.Sg_c - 100.Sg}{Sg.Sg_c}$$

Cross multiply:

$$A(Sg.Sg_c^{2} - Sg.Sg_c.Sg_a) = 100.Sg_a.Sg_c^{2} - 100.Sg.Sg_c.Sg_a$$

Therefore:

$$Ash(\%) = \frac{100.Sg_a.Sg_c - 100.Sg.Sg_a}{Sg.Sg_c - Sg.Sg_a}$$

Therefore:

$$Ash(\%) = \frac{(100.Sg_a.Sg_c/(Sg_c - Sg_a))}{Sg} - \frac{100.Sg_a}{Sg_c - Sg_a}$$

Or:

$$Ash(\%) = P*Sg^{-1} + Q$$

where:

$$P = \frac{100.Sg_a.Sg_c}{Sg_c - Sg_a} \quad \text{and} \quad Q = -\frac{100.Sg_a}{Sg_c - Sg_a}$$

These equations can be rearranged to give:

$$Sg_c = \frac{P(Q-100)}{100.Q} - \frac{P}{100}$$

and

$$Sg_s = \frac{Q.Sg_c}{Q - 100}$$

APPENDIX H

"A NEW METHOD FOR THE RAPID FLOAT-SINK ANALYSIS OF COAL FINES", BY J-P. FRANZIDIS AND M.C. HARRIS. REPRINT OF A PAPER APPEARING IN THE J. S. AFR. INST. MIN. METALL.

J. S. Afr. Inst. Min. Metall., vol. 86, no. 10.
Oct. 1986. pp. 409-414.

A new method for the rapid float–sink analysis of coal fines

by J-P. FRANZIDIS* and M.C. HARRIS†

SYNOPSIS

Float-sink analysis has wide application in the coal laboratory. This paper evaluates the established methods used for the float-sink analysis of fine coal, and then describes a new method and apparatus that can be used for material down to a few micrometres in size. The method is rapid and accurate, and requires only a small amount of sample. The results presented show close agreement with the float-sink analyses obtained by the more classical technique using separating columns. The new centrifugal method reduces the time required for the analysis by a factor of ten.

SAMEVATTING

Gravitasie skeiding analises het 'n wye toepassing in die steenkool laboratorium. Hierdie referaat evalueer bestaande gravitasie skeiding analise tegnieke vir fyn steenkool en beskryf dan 'n nuwe metode en apparaat wat vir partikel groottes van slegs 'n paar mikrometers gebruik kan word. Die metode is vinnig en akkuraat en benodig slegs 'n klein hoeveelheid monster. Resultate, wat goed ooreenstem met dié verkry in die meer klassieke skeidingskolomtegniek, word ingesluit. Die nuwe sentrifugale metode het gely tot die reduksie in analise tyd met 'n faktor van tien.

Introduction

Float-sink analysis is a widely used technique in the coal laboratory. It finds application, firstly, in the study of coal washability or liberation from ash and, secondly, in the determination of coal-washery performance through the use of partition curves and the data derived from them. However, while float-sink analysis of plus 0,5 mm material presents little difficulty, the established methods are tedious and tricky for fine coal. This is particularly true of coal smaller than 53 μm in size.

Existing Methods

The most common method for the float-sink analysis of fines involves the use of separating funnels in which particles are separated under gravity in a suitable heavy liquid. For samples containing very fine particles or a high proportion of near-gravity material, this technique becomes extremely time-consuming since a very long separating time is required. Also, the separation of coal particles finer than 53 μm by this method has been found to be impracticable[1].

Alternative methods aimed at speeding up the process rely on the use of a centrifuge. In the method recommended by the International Organization for Standardization (ISO)[2], a sample of coal (20 to 60 g) is placed in a centrifuge tube with liquid of the lowest density. After spinning, the floats are collected from the surface with a scoop, liquid of the next highest density is added to the sinks, and the process is repeated until the highest density is reached. A disadvantage of this method is the initial high loading of the tubes, which can result in a significant amount of entrained, and thus misplaced, material; moreover, it is difficult in practice to scoop all the floats from the surface accurately without leaving some material behind or causing some mixing with the sinks. The sequential treatment of a single sample can also lead to significant cumulative error as the sample being treated becomes smaller.

Another centrifugal method is that of Hall[3], in which a fine gauze tray is fitted inside the centrifuge tube, being suspended between the floats and the sinks by wires hung over the edge of the tube. This gauze is used to pull out the solid plug of floats after centrifuging. Problems with this method are that the gauze, during the centrifuging, tends to trap some sink material, which will report to the floats; and that, when the gauze is removed some of the float material is invariably left behind and is difficult to recover.

New Apparatus and Method

A new apparatus has been devised for speeding up the float-sink analysis of coal fines, and making it less prone to error. This apparatus, which is also designed to fit into a centrifuge tube, has been provisionally manufactured out of Perspex, although, as this is soluble in most organic liquids, a material such as polytetrafluoroethylene (PTFE) or stainless steel would be more suitable.

The heavy liquid used to date is zinc chloride. Its advantages are that it is very cheap, and does not give off toxic vapours like the more commonly used organic liquids such as bromoform or tetrabromoethane (TBE). A limitation is that the highest relative density that can be obtained is 1,8.

The device, shown in Fig. 1, fits inside a standard 100 ml PTFE centrifuge tube. It consists of a tapered

* Senior Lecturer.
† Student.
Both the above of the Department of Chemical Engineering, University of Cape Town, Rondebosch, 7700 Cape Province.
 SA ISSN 0038-223X/$3.00 + 0.00. Paper received 23rd July, 1985.

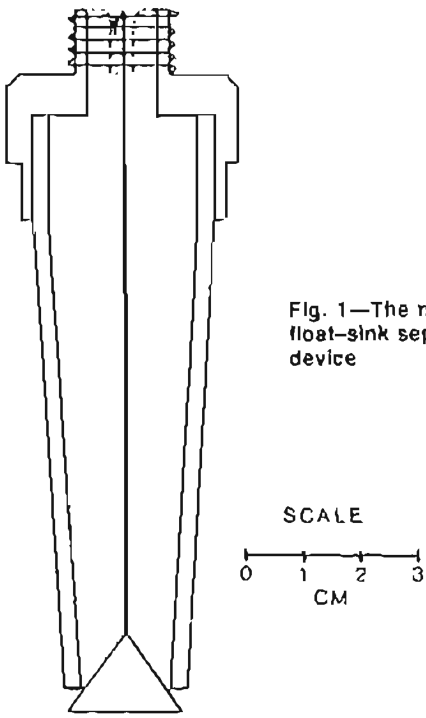

Fig. 1—The new float–sink separating device

tube, with the bottom sealed by a conical plug. This plug is connected via a rod to a spring at the top of the device. When sufficient downward force acts on the plug (as occurs during centrifuging), the spring is compressed, opening the bottom of the tube.

The use of the new apparatus is illustrated in Fig. 2. Unlike the ISO method, in which a single sample is treated sequentially, the new method uses separate samples at each relative density, obtaining cumulative data directly.

The procedure can be broken down into four stages.

A Approximately 2 g of dry coal is accurately weighed into a 30 ml sample bottle. The sample bottle has a conical bottom leading into a 4 mm glass tube, which is connected to a short piece of rubber tube. The rubber tube is clamped shut. A few millilitres of zinc chloride solution are added to the bottle, along with a few microlitres of a chemical dispersant known as Tween 20 (polyoxyethylene sorbitan monolaurate). After the bottle has been sealed, it is shaken until the coal is thoroughly wetted. The bottle is then placed in an ultrasonic bath for 5 minutes to aid in further dispersion. The lid of the sample bottle is removed, and any adhering coal is washed into the bottle with a few millilitres of zinc chloride solution. The rubber tube of the sample bottle is then inserted into the top of the separating device, and the clamp is removed. A syringe is used to wash any remaining coal particles from the sample bottle into the device. The separating device is then filled to the required level with zinc chloride solution, as is the centrifuge tube.

B The device is inserted into a centrifuge tube, although the contents of the two remain isolated from each other. The tube is then spun in a centrifuge.

C During spinning, centrifugal force on the conical plug pulls it down, compressing the spring. This links the fluid in the separating device with that in the centrifuge tube, and enables sink material to enter the tube.

D When the centrifuge stops spinning, the spring causes the conical plug to seal the device again, isolating the float material from the sink material. Thus, the two fractions are separated by mere removal of the device from the centrifuge tube. The separation is achieved without any of the problems associated with the methods previously discussed.

It is important that a centrifuge with a swing-arm rotor should be used, so that the line of force acts down the centre of the tube. With the tube spinning at 4000 r/min, about 15 minutes are required for samples of material larger than 25 μm; samples of smaller material usually require between 1 and 2 hours of spinning time.

If material smaller than 53 μm is being analysed, the conical plug can be locked during the initial centrifuging, resulting in a provisional separation in the device. If this is not done, the fine coal slurry in the device would behave like a liquid with a higher relative density than the clear zinc chloride solution in the centrifuge tube. Thus, when the conical plug opened, mixing would result, causing some float material to report to the sinks. After a provisional separation has been obtained, the spring can be released, enabling the conical plug to open, and the tube can be re-centrifuged to give the final separation.

Reproducibility of Results

In order to establish the precision of the method, a number of replicate experiments were conducted on different size fractions of a sample consisting of a synthetic mixture of washed and waste coal from the Greenside Colliery. The float–sink analyses were carried out at relative densities of 1,4, 1,5, and 1,6. As can be seen from Table I, the method is extremely precise for the size ranges examined, the maximum standard deviation for four replicates being only 0,6 per cent. Also, a mass balance of the float and the sink material shows acceptably small and relatively constant losses in mass.

TABLE I
REPRODUCIBILITY OF THE NEW METHOD

Size fraction μm	Relative density	Number of replicates	Mean float %	Standard deviation	Average lost material %
−300 +106	1,6	4	56,3	0,2	0,9
−106 +75	1,6	2	59,1	0,3	2,8
−75 +38	1,6	4	59,9	0,3	2,5
−38 +20	1,5	4	49,8	0,6	2,1
−300 +106	1,4	4	34,5	0,4	2,4
−106 +75	1,4	2	34,8	0,2	2,4
−75 +38	1,4	4	31,1	0,5	2,5

To investigate the reproducibility of the method, samples of Greenside No. 2 seam coal were obtained from Professor R.P. King of the Department of Metallurgy at the University of the Witwatersrand. The samples consisted of cyclone underflow and overflow that had been taken during the operation of a pilot rig in which the dense-medium separation of fines was being investigated[4]. Partition-curve data were obtained by the new method for the cycloning of material between 90 and

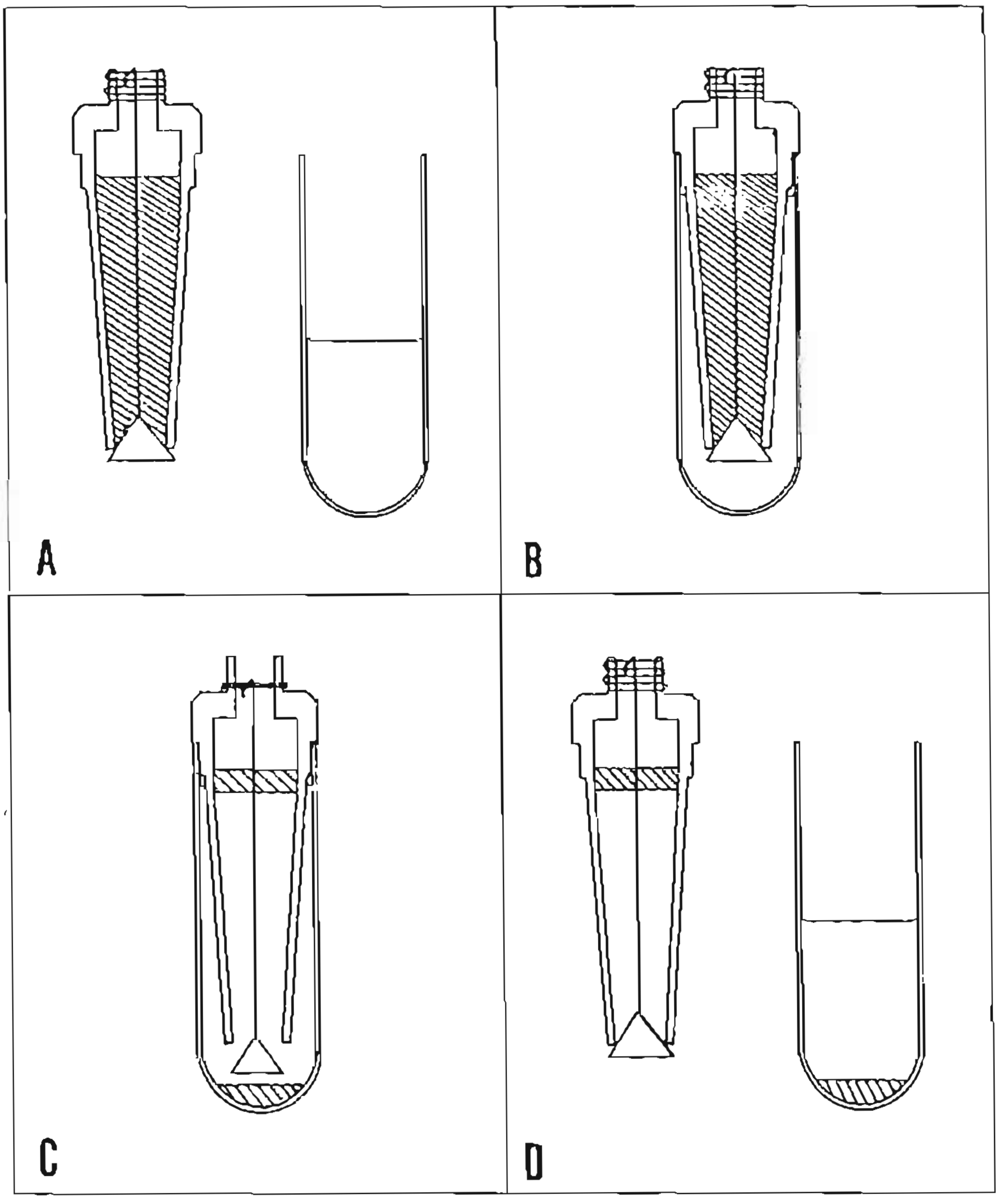

Fig. 2—Use of the new device

75 μm. The results were then compared with those of Professor King's research group, which had been obtained by use of the double-column gravitational separating technique illustrated in Fig. 3. This method is very accurate but extremely time-consuming. The top column acts as a 'rougher' and the lower column as a 'cleaner'. Sequential treatment of a single sample was used, with Certigrav as the heavy liquid.

Partition curves comparing the two sets of results are shown in Figs. 4 to 6. (The horizontal axes—labelled 'Mean Specific Gravity'—would be more accurately described by 'Mean Relative Density'.)

The following partition function used by King[4] was fitted to the results:

$$R(x) = b_1 + (b_4 - b_3)\frac{\exp(b_2 x) - 1}{\exp(b_2 x) + \exp(b_2) - 2},$$

where x = normalized relative density, S/S_c
S = relative density of particle
S_c = cut-point relative density (S at a partition factor of 0,5)
R = partition factor
b_2, b_3, and b_4 are function parameters.

TABLE II
CURVE-FITTING DATA FOR PARTITION CURVES 1, 2, AND 3

Item	New method	Funnel method	Combined data
Partition curve 1 (Fig. 4)			
S_c	1,563	1,57	1,57
$\Sigma(\text{error})^2$	42,30	21,32	73,56
$\frac{\Sigma(\text{error})^2}{\text{No. of points}}$	6.04	2,13	4,33
Partition curve 2 (Fig. 5)			
S_c	1,546	1,553	1,550
$\Sigma(\text{error})^2$	34,46	198,48	247,55
$\frac{\Sigma(\text{error})^2}{\text{No. of points}}$	4,96	19,85	14,56
Partition curve 3 (Fig. 6)			
S_c	1,519	1,523	1,523
$\Sigma(\text{error})^2$	121,09	187.17	386,43
$\frac{\Sigma(\text{error})^2}{\text{No. of points}}$	20,18	20,78	25,76

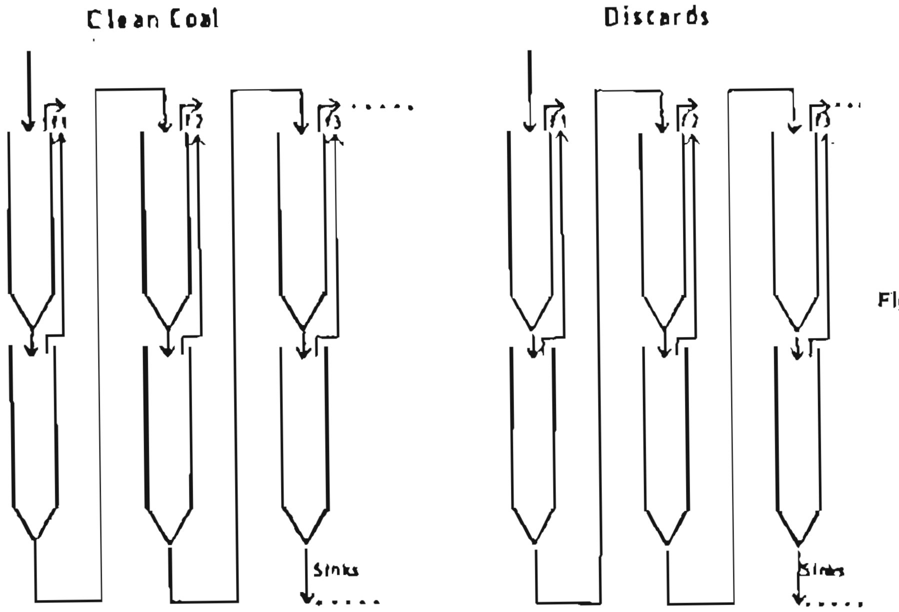

Fig. 3—Double-column method of float-sink analysis (from King and Juckes[4])

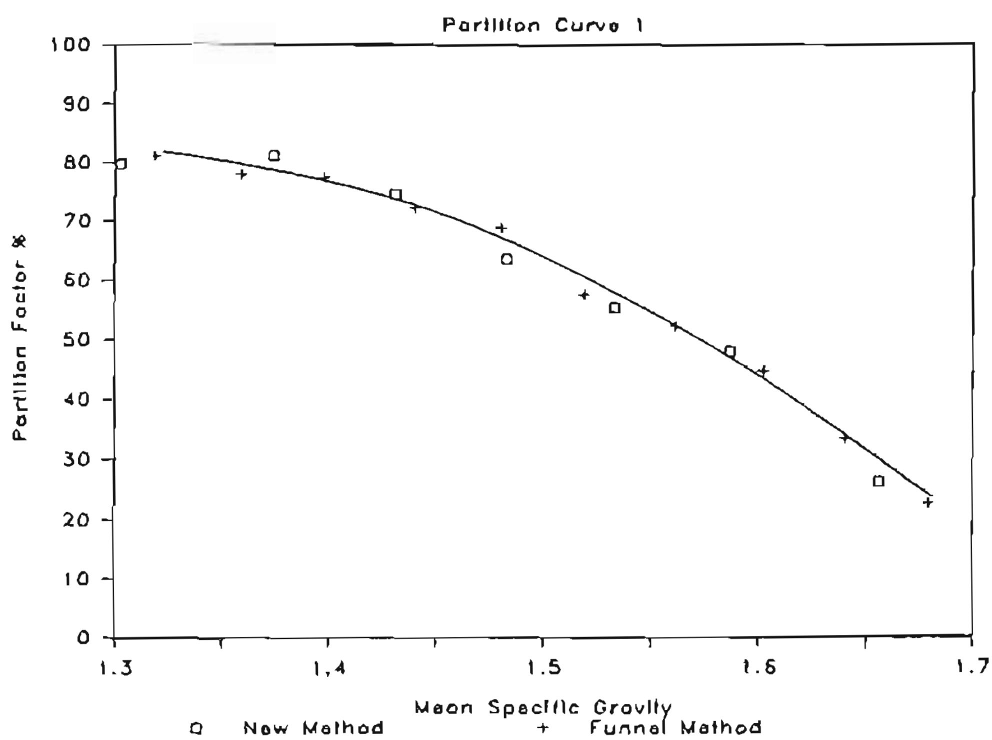

Fig. 4—Comparison of the results obtained from the new method with those from the double-column method, sample 1

Least-squares best estimates of the parameters S_c, b_2, b_3, and b_4 were obtained by non-linear regression analysis of the experimental data.

In each case, curves were fitted to the combined set of data, and to each set of data obtained by the two different methods. Table II presents the least-squares fit for each curve and the cut-point. As a different number of points was used to obtain each curve, the sum of error squared divided by the number of points is included for purposes of comparison.

A very good agreement between the two sets of data can be seen in Figs. 4 and 5. The poor fit apparent in Fig. 6 can be explained by the fact that there was insufficient material to obtain more points in the higher density range of the graph (see Fig. 6, graph A). Thus, the first two points have an exaggerated effect on the shape of the curve. Both sets of data exhibit a high degree of scatter, indicating possible inconsistencies in the coal sample, rather than problems in either of the float-sink methods. The high degree of scatter requires a large

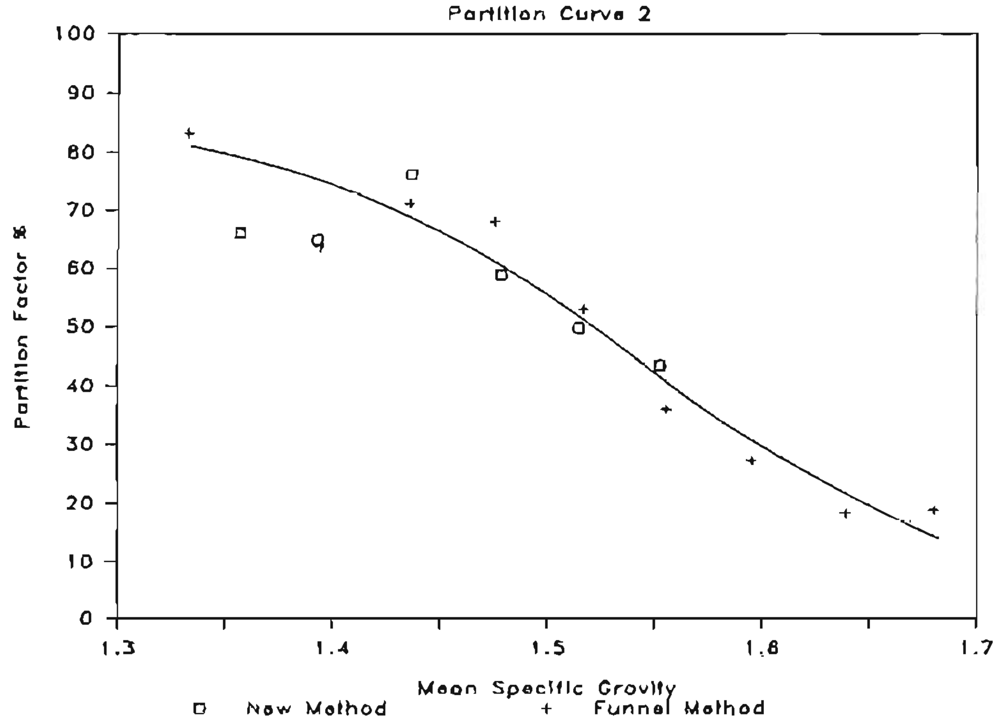

Fig. 5—Comparison of the results obtained from the new method with those from the double-column method, sample 2

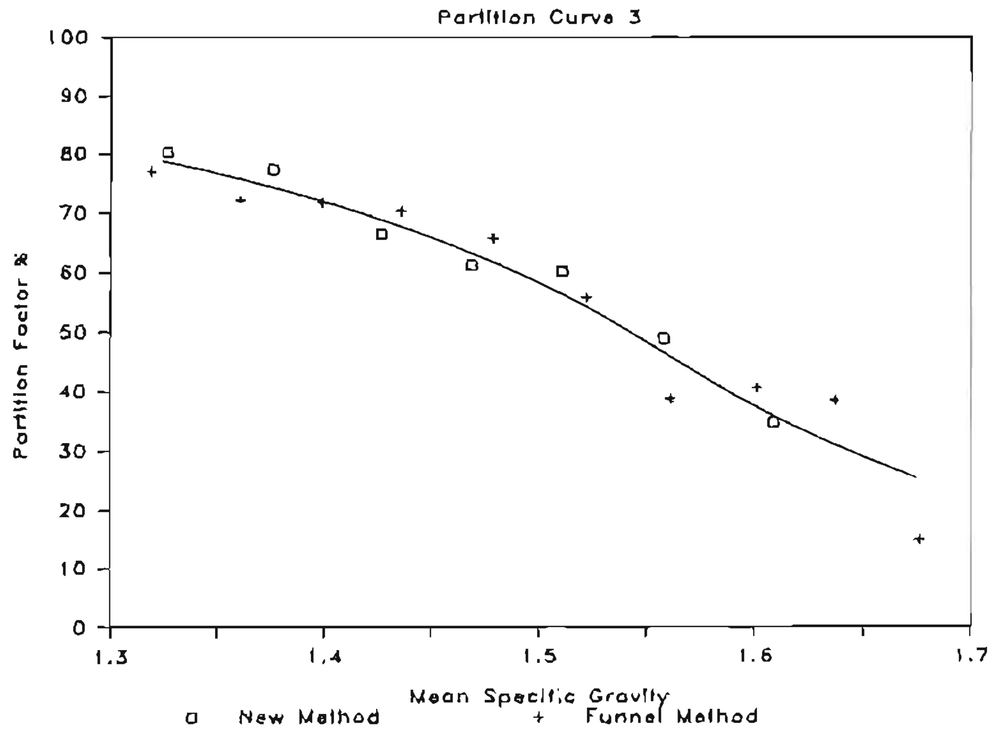

Fig. 6—Comparison of the results obtained from the new method with those from the double-column method, sample 3

number of points if the curve fitting is to be satisfactory. When the graph based on the combined data is compared with that based on the separating-funnel data, a much better agreement is apparent.

Conclusions

Float–sink analyses can be carried out very easily with the new apparatus, with none of the problems associated with other methods. The method has been shown to be reproducible, and its results correspond satisfactorily to the results obtained by the more traditional separating-funnel method.

On account of the difficulties associated with other methods, many collieries and coal laboratories do not carry out float–sink determinations on the minus 0,5 mm fines, despite the increasing proportion of this size fraction in run-of-mine material. The simplicity of the new separating device and method makes it possible for such analyses to be made quickly and accurately on a routine basis.

Although the apparatus was designed specifically for use in the beneficiation of fine coal, its application is not limited to coal, and it should prove a useful tool in all mineral-processing laboratories.

Acknowledgements

The authors are indebted to Mr A.M. Barker, Chief Technical Officer in the Department of Chemical Engineering at the University of Cape Town, who made the apparatus. The authors thank Professor R.P. King of the Department of Metallurgy at the University of the Witwatersrand for his advice and encouragement, and for providing the samples used in the testing of the new device along with the results of float–sink analyses performed in his laboratory. This research programme is being funded by the Foundation for Research Development of the C S I R.

References

1. King, R.P., and Juckes, A.H. Private communication.
2. International Organization for Standardization. *Coal cleaning tests—Determination of float and sink characteristics of coal and combustible shale*. Technical Committee 27, Subcommittee 1, N176E. 1981.
3. Hall, P.E. The specific gravity investigation of coal samples: Further studies and a new technique. *J. Chem. Metall. Min. Soc. S. Afr.*, Feb. 1934. pp. 263–269
4. King, R.P., and Juckes, A.H. Cleaning of fine coals by dense-medium hydrocyclone. Department of Metallurgy, University of the Witwatersrand, *Report* CSPCOAL1. Jun. 1983.

Flat rolling

The 4th International Steel Rolling Conference is to be held in Deauville (France) from 1st to 3rd June, 1987.

The Conference will provide an opportunity for specialists to make an appraisal of the status and trend of development of the process and operating technology of rolling on plate, and hot- and cold-strip mills. The scope of this event will extend to all stages of the process, starting from the hot slab ready for rolling down to the temper-mill for cold-reduced or hot-strip mill material. The metallurgy of continuous annealing will not be explored.

In the case of the plate/mill, heat treatment such as rapid cooling out of the rolling heat is clearly part of the process, although the handling of such topics should concentrate on the thermal and technological aspects of this particular process and on its consequences on the upstream and downstream operations, and not on the metallurgy; hot and cold levelling will, of course, be considered.

New mill strand and roll technology should be reviewed, and their effectiveness in controlling strip shape and easing the hot strip mill scheduling constraints appraised on the basis of theoretical and experimental work.

The influence on plant efficiency and product quality of the coupling of several stages of the process and of the processing of 'endless strip' in the cold-rolling plant should also be further analysed.

Mill computer control based on accurate mathematical models remains an essential area for research and development, while closed-loop control linked to recently introduced sensors and actuators, which has found new applications in the field of flat rolling, deserves the attention of the specialists.

Although it is not intended to include in the programme reheating furnaces, coating lines, nor product metallurgical developments *per se*, papers dealing with such topics as the following fall within the scope of the Conference:

- Influence of the product temperature level and homogeneity on mill control, mill performance, and product quality
- Optimum use of the technical features of the rolling plant in relationship to metallurgical and surface-finish requirements.

The design of production scheduling systems may also be considered in so far as the emphasis is placed on such desired impacts on plant operation and mill performance as

- Schedule free rolling on the hot-strip mill
- Hot charging and direct rolling
- Improved crown and flatness control of the hot-rolled strip.

Lastly, maintenance, which has such a direct influence on plant efficiency, should not be overlooked.

Further information can be obtained from

Secretariat
4th International Steel Rolling Conference
IRSID
B.P. 64
57210 Maizières-lès-Metz
France.
Téléphone: 87 80 21 11, télex: 860 253 IRSIDMZ,
Télécopieur: 87 80 61 86

Corrigenda

The following diagrams should replace the Figs. 4, 5, and 6 that appeared on pages 412 and 413 of the October 1986 issue. These relate to the paper entitled 'A new method for the rapid float-sink analysis of coal fines' by J-P. Franzidis and M.C. Harris

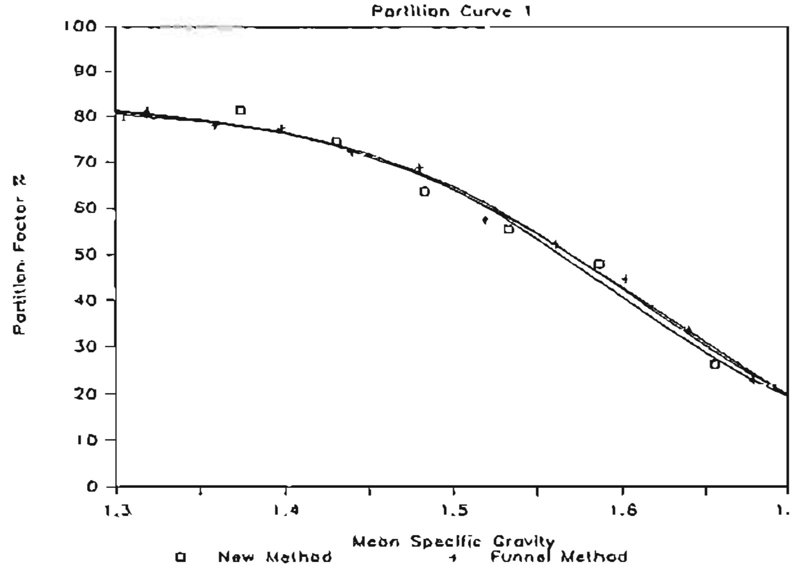

Fig. 4—Comparison of the results obtained from the new method with those from the double-column method, sample 1

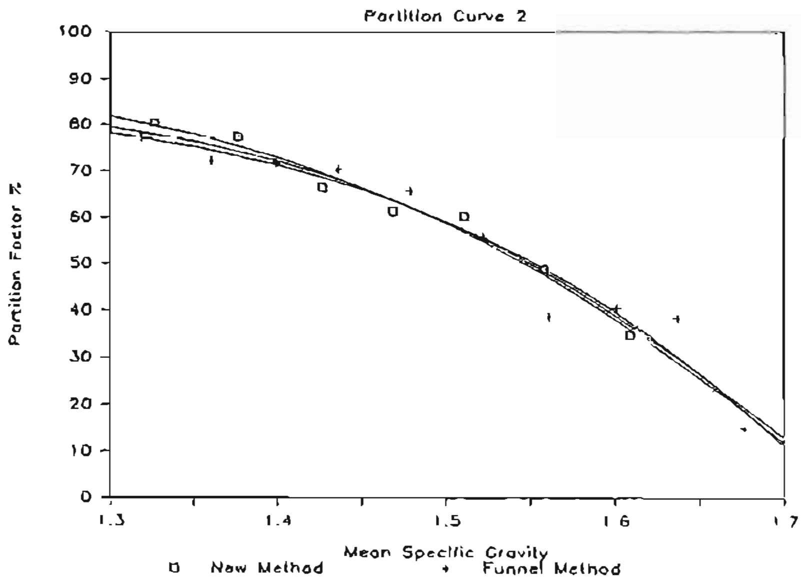

Fig. 5—Comparison of the results obtained from the new method with those from the double-column method, sample 2

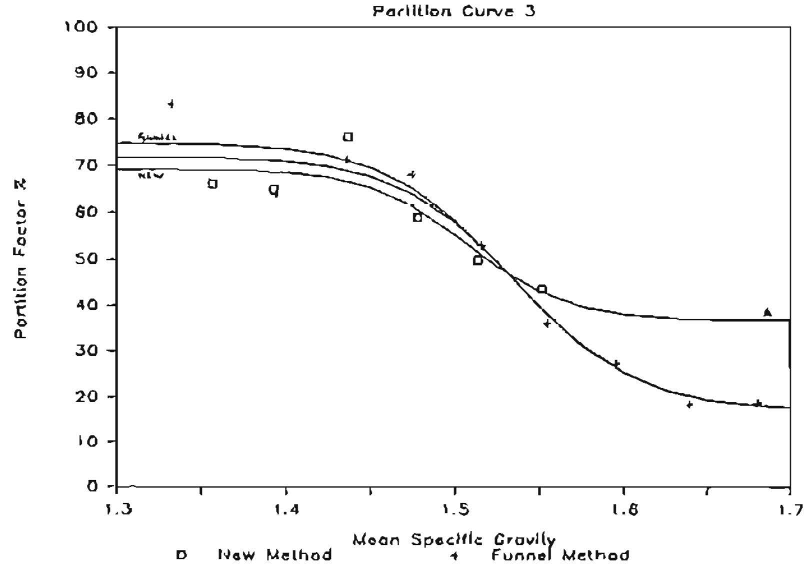

Fig. 6—Comparison of the results obtained from the new method with those from the double-column method, sample 3